Fundamental Investigation of Antimonides: A Synthetic, Structural and Reactivity Study

Mihaiela Emilia Ghesner

A thesis submitted in partial fulfilment of the requirements for the degree

Doctor of Natural Science (Dr. rer. nat.)

Faculty of Chemistry and Biology

University of Bremen

Bremen 2004

1. Referee: Prof. Dr. H. J. Breunig

2. Referee: Prof. Dr. G.-V. Röschenthaler

Date of doctoral examination: 23. January 2004

CONTENTS

Introduction 1

Aims of the present study 3

Results and Discussion 4

1. Primary and secondary stibanes 4

1.1. Introduction 4

1.2. Synthesis and characterization of $(C_6H_5)SbH_2$, $[2,4,6\text{-}(CH_3)_3C_6H_2]SbH_2$, $[2\text{-}(Me_2NCH_2)C_6H_4]SbH_2$, $(C_6H_5)_2SbH$ and $(^tBu_2Sb)_2$ 5

2. Mononuclear alkali metal diorganoantimonides 11

2.1. Introduction 11

2.2. Synthesis and characterization of $[(C_6H_5)_2SbLi\cdot(thf)_3]$ and $[(2,4,6\text{-}(CH_3)_3C_6H_2)_2SbLi\cdot(thf)_3]$ 12

2.3. Synthesis and characterization of $[2\text{-}(Me_2NCH_2)C_6H_4][(Me_3Si)_2CH]SbLi\cdot 2thf$, $[2\text{-}(Me_2NCH_2)C_6H_4][(Me_3Si)_2CH]SbNa\cdot tmeda$ and $[2\text{-}(Me_2NCH_2)C_6H_4][(Me_3Si)_2CH]SbK\cdot pmdeta$ 15

3. Zintl compounds containing the Sb_7^{3-} anion 20

3.1. Introduction 20

3.2. Synthesis and characterization of tris(tmeda-lithium)-, tris(pmdeta-sodium)- and tris(pmdeta-potassium)hepta-antimonide $[Sb_7Li_3\cdot(tmeda)_3]$, $[Sb_7Na_3\cdot(pmdeta)_3]$, $[Sb_7K_3\cdot(pmdeta)_3]$ 21

4. The cleavage of *cyclo*-$(^tBuSb)_4$ with alkali metals (Li, Na, and K) 26

4.1. Introduction 26

4.2. Synthesis and characterization of $[(^tBu_4Sb_3)][Li(tmeda)_2]$, $[(^tBu_4Sb_3)Na(tmeda)]$, $[(^tBu_4Sb_3)Na(tmeda)_2]$, $[(^tBu_4Sb_3)Na(pmdeta)]$, $[(^tBu_4Sb_3)K(pmdeta)]$, $[(^tBu_3Sb_2)K(pmdeta)]$, $[(^tBu_2Sb)K(pmdeta)]$ 27

5. 2-(3',5'-Dimethylphenyl)-5,7-dimethylstibindolyl potassium·pmdeta 44
5.1. Introduction 44
5.2. Synthesis and characterization of
2-(3',5'-dimethylphenyl)-5,7-dimethylstibindolyl potassium·pmdeta 44
6. Experimental Section 49
6.1. General Comments 49
6.2. Primary and secondary stibanes 51
6.3. Mononuclear alkali metal organoantimonides 54
6.4. Dinuclear alkali metal organoantimonides 57
6.5. Trinuclear alkali metal organoantimonides 58
6.6. Stibindolyl anion 61
6.7. Zintl compounds containing the Sb_7^{3-} anion 62
7. Summary 64
8. References 68
9. Appendix 74
9.1 Abbreviations 74
9.2. Details of crystal structure determination 76
CURRICULUM VITAE 107
Publications 108
Contribution to professional reports 109
Acknowledgements 110

Introduction

Antimonides are of interest to chemists not only because of the nature of their bonding but also because such structures can exhibit unusual stability and/or reactivity. Alkali diorganoantimonides, $R_2Sb^-M^+$ (M = alkali metal), for example, are important synthons and found use in the preparation of numerous antimony containing compounds, *i.e.*: homoleptic or heteroleptic triorganoantimony compounds, R_3Sb,[1,2] diorganoantimony hydrides, R_2SbH,[3] distibanes, R_2Sb-SbR_2,[4,5,6] compounds containing antimony(III)-main group element bonds, R_2Sb-ER'_2 (E = N[7], P[8], As[8], Ga[9], In[9]) and compounds with antimony(III)-transition metal bonds, R_2Sb-ML_n (ML_n = VCp_2[10], $Cu(PMe_3)_2$[3]). Despite the synthetic importance, very little work has been done to understand their structure. In fact, the only structurally characterized mononuclear alkali diorganoantimonides are $[Ph_2Sb][Li(12\text{-crown-}4)_2]$ $^1/_3$thf[4] and $[\{(Me_3Si)_2SbLi\cdot 1DME\}_\infty]$[11] (DME = 1,2-dimethoxyethan). Even less studied are the asymmetrically substituted mononuclear alkali diorganoantimonides, $RR'Sb^-M^+$ ($R \neq R'$). Such compounds are potential chiral reagents or catalysts for enantioselective syntheses.[12-16] The only known asymmetrical alkali metal diorganoantimonide, PhMeSbNa,[17-19] was reported without structural data as an intermediate in the preparation of asymmetrical tertiary stibanes.

As for the dianionic species of the type $RSb^{2-}M^+_2$ (R = organic group) the number of works are limited to a paper published in 1976 by *Issleib*, who postulated the formation of $Na_2[PhSb]$ from the reduction of *cyclo*-$(PhSb)_6$ with appropriate amounts of sodium in liquid ammonia.[20] However, no concrete evidences for the existence of a such species are provided.

It has been also shown by *Issleib*[15] and more recently by *Breunig*[20] that reactions of cyclic stibanes, *cyclo*-$(RSb)_n$ (R = Ph, ^{t}Bu), with alkali metals lead to the fragmentation of the antimony-ring with formation of anionic species containing antimony-antimony bonds (*A*). Such compounds are of interest not only from

structural point of view but also as building blocks for other interesting antimony compounds.

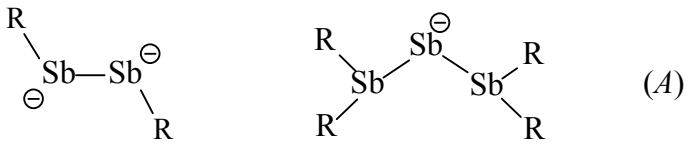

(*A*)

The antimonides are known also in solids such as intermetallic Zintl phases. The synthesis of Sb_7^{3-} has attracted much interest and several theoretical studies have been published, followed by experimental confirmations. The first crystal structure of a salt of this type, has been reported by *Corbett* and co-workers in 1976 with the Zintl compound Na_3Sb_7[21] (*B*).

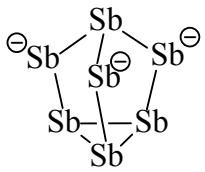

(*B*)

Some of these compounds which possess “glass-like” thermal conductivity, have the ability to vary the electronic properties with doping level. Also the relatively good electronic properties obtained in these semiconductor materials, make them interesting for thermoelectronic applications and also many other possible interesting properties that might lead to an entirely different range of applications from superconductivity to large band gap semiconductors.[22]

Aims of the present study

Important synthons for the synthesis of organoantimonides are the primary and secondary stibanes. Organoantimony hydrides have been synthesized before from the reaction of the corresponding organoantimonyhalides with $LiAlH_4$. Alternatively also other synthetic routs, like hydrolysis of the Sb-Si bond in compounds of the type $R_2SbSiMe_3$ and $RSb(SiMe_3)_2$, or hydrolysis of an diorganoantimonides have been used. One aim of this study was to synthesize known and novel organoantimony hydrides as intermediates for further transformations.

The number of reports mentioned in the literature on the synthesis and characterization of symmetric and asymmetric substituted diorganoantimonides, R^1R^2SbM ($R^1 = R^2$ or $R^1 \neq R^2$), are few and often these compounds are prepared and further used without being isolated which makes questionable their purity. In this work attempts were to be made for the synthesis, isolation, and structural characterization of diorganoantimonides both in solution and in solid state. Also metalation of primary stibanes, $RSbH_2$, was to be investigated. Such reactions are expected to allow access to the dianionic species $RSb^{2-}M^{+}_2$. However it is accepted that such compounds are very reactive and difficult to isolate if at all.

In two earlier reports the reactions of cyclic stibanes with alkali metals as a potential source of novel antimonides are mentioned. However from these attempts no clean products could be isolated and the mechanism of the cleavage of the antimony rings remains still ambiguous. As part of this study the ring cleavage of *cyclo*-(^{t}BuSb)$_4$ with alkali metals was to be reinvestigated and the mechanism of the ring cleavage to be elucidated.

Results and Discussion

1. Primary and secondary stibanes

1.1. Introduction

Since the synthesis of the first organoantimony hydrides in the early 1960s[23] numerous other examples of primary and secondary stibanes have been reported[24]. Research in this area was driven by the application of these compounds as reducing agents[12] or precursors for electronic materials[25,26], as well as by their implication as synthons for other interesting antimony containing compounds[27]. The hydrogen derivatives of the Group 15 elements are known to display decreased stabilities with increasing atomic number. Many hydrides of antimony, e.g., the monostibanes SbH_3,[28] $RSbH_2$ (R = CH_3, C_6H_5), and R_2SbH (R = CH_3, C_2H_5)[23] or the distibane Sb_2H_4,[29] decompose in minutes or hours at room temperature with autocatalysis to form dihydrogen and antimony or organoantimony compounds with Sb-Sb bonds. This instability is probably not a consequence of unusually weak antimony-hydrogen bonds ($E_{Sb\text{-}H}$ = 255 kJ mol^{-1},[30] $E_{Sb\text{-}C}$ = 215 kJ mol^{-1} [31]) but may be due to insufficient steric protection. Indeed, the substitution of one or two hydrogens in SbH_3 by bulkier organic group is already known to increase the stability of stibanes. For example, phenylstibane, $PhSbH_2$, decomposes at room temperature[32], whereas ^{t}BuCH$_2$SbH$_2$[25], Me$_3$SiCH$_2$SbH$_2$[26] and [(Me$_3$Si)$_2$CH]$_2$SbH[24] are colourless liquids which are stable for long periods under an inert atmosphere at ambient temperature. Under the protection of bulky organic groups, three crystalline antimony hydrides could be isolated as stable compounds and characterized by X-ray crystallography: Mes_2SbH (Mes = 2,4,6-$(CH_3)_3C_6H_2$,[3] $ArSbH_2$ (Ar = 2,6-[2,4,6-triisopropylphenyl]$_2$C$_6$H$_3$,[33] and R(H)Sb-Sb(H)R (R = [(CH$_3$)$_3$Si]$_2$CH)[34].

1.2. Synthesis and characterization of $(C_6H_5)SbH_2$, $[2,4,6\text{-}(CH_3)_3C_6H_2]SbH_2$, $[2\text{-}(Me_2NCH_2)C_6H_4]SbH_2$, $(C_6H_5)_2SbH$ and $(^tBu_2Sb)_2$

The primary arylstibanes $(C_6H_5)SbH_2$ (**1**), $[2,4,6\text{-}(CH_3)_3C_6H_2]SbH_2$ (**2**), $[2\text{-}(Me_2NCH_2)C_6H_4]SbH_2$ (**3**) were prepared in high yields (93 % **1**, 92 % **2**, 87 % **3**) by the reaction of the corresponding arylantimony dichlorides, $RSbCl_2$ (R = C_6H_5, 2,4,6-$(CH_3)_3C_6H_2$, 2-$(Me_2NCH_2)C_6H_4$) with $LiAlH_4$ in Et_2O at low temperature.

$$RSbCl_2 + 2LiAlH_4 \xrightarrow[-80\ ^oC]{Et_2O} RSbH_2 + 2LiCl + 2AlH_3$$

R = C_6H_5 **1**,
2,4,6-$(CH_3)_3C_6H_2$ **2**,
2-$(Me_2NCH_2)C_6H_4$ **3**

Similar to the synthesis of the primary stibanes, reaction of $(C_6H_5)_2SbCl$ with $LiAlH_4$ in 1:1 molar ratio in Et_2O at low temperature gives the secondary phenylstibane $(C_6H_5)_2SbH$ (**4**) in 92 % yield and high purity.

$$(C_6H_5)_2SbCl + LiAlH_4 \xrightarrow[-80\ ^oC]{Et_2O} \underset{\mathbf{4}}{(C_6H_5)_2SbH} + LiCl + AlH_3$$

The stibanes **1**[32,35,36] and **4**[5,32,35, 37,38] were reported earlier as colourless liquids at room temperature and the yields of these reactions are usually lower than those reported in this work. All primary and secondary stibanes reported here are prepared as light and air sensitive colourless liquids, which solidify at low temperatures. **1 - 4** are soluble in petroleum ether, toluene, diethyl ether and other common organic solvents. They are unstable at room temperature but can be stored for weeks at –30 °C in an inert atmosphere. The only exception is **1**, which can be stored only for few days even at –30 °C and under inert atmosphere. **1 - 4** were characterized by mass spectrometry and NMR (^1H, ^{13}C) and IR spectroscopy. The ^1H- and ^{13}C-NMR spectra

of **1** - **4** in C_6D_6 at 20 °C contain the expected signals corresponding to structures with the antimony atom in pyramidal environments.

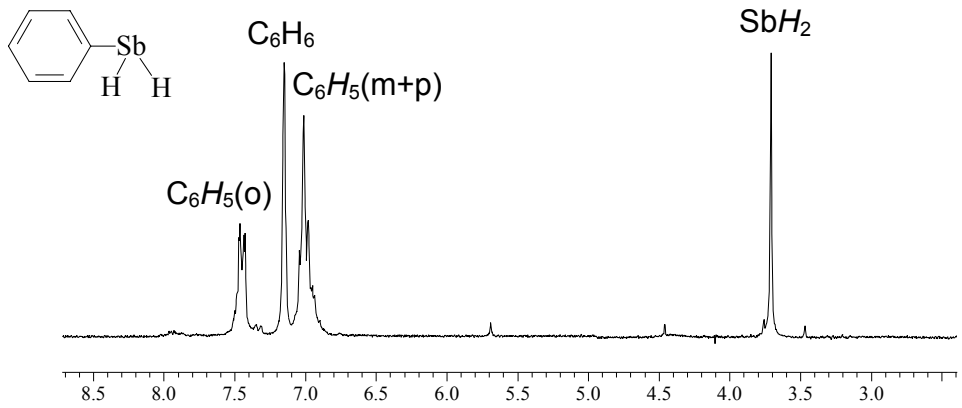

Figure 1. ^{1}H-NMR (C_6D_6, 200 MHz) spectrum of $(C_6H_5)SbH_2$ (**1**).

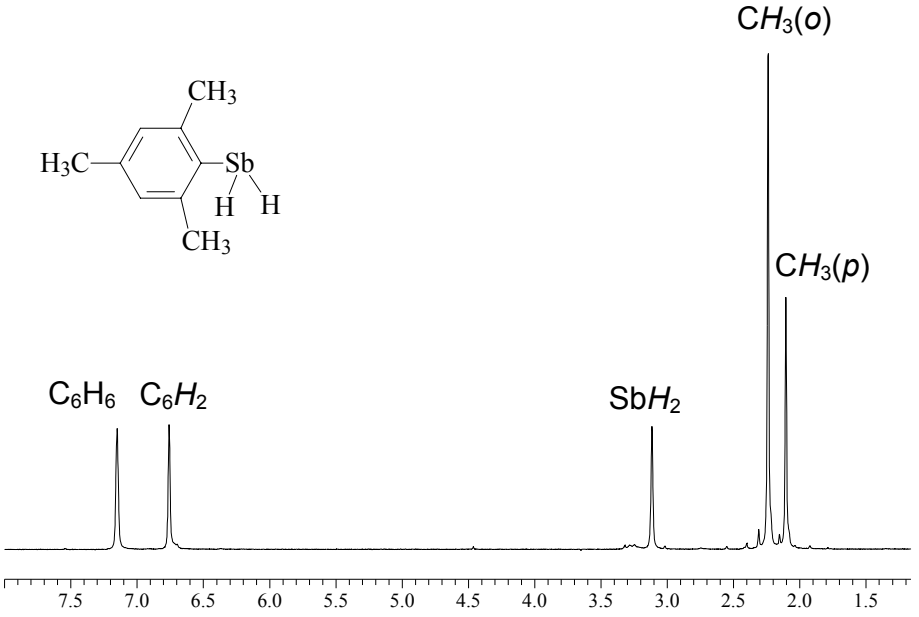

Figure 2. ^{1}H-NMR (C_6D_6, 200 MHz) spectrum of $[2,4,6\text{-}(CH_3)_3C_6H_2]SbH_2$ (**2**).

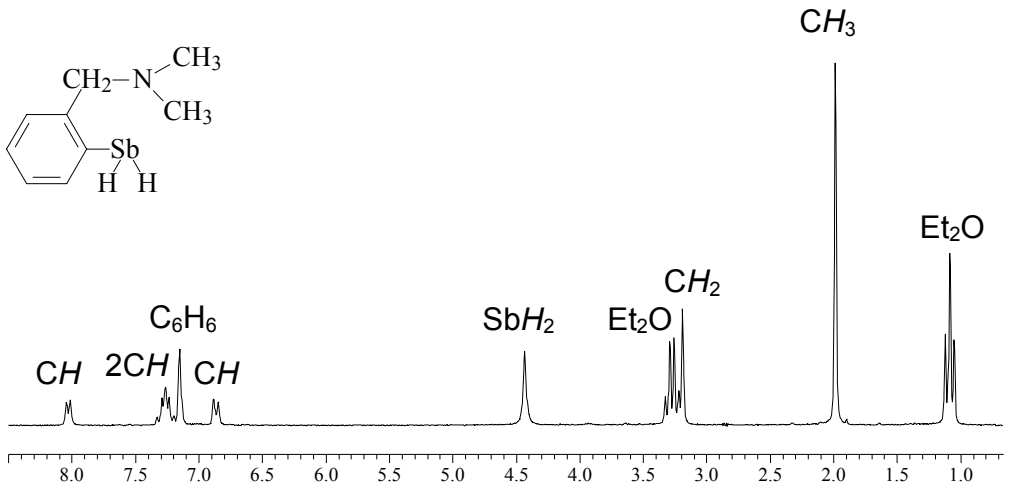

Figure 3. ^{1}H-NMR (C_6D_6, 200 MHz) spectrum of a solution containing [2-(Me_2NCH_2)C_6H_4]SbH_2 (**3**) and Et_2O.

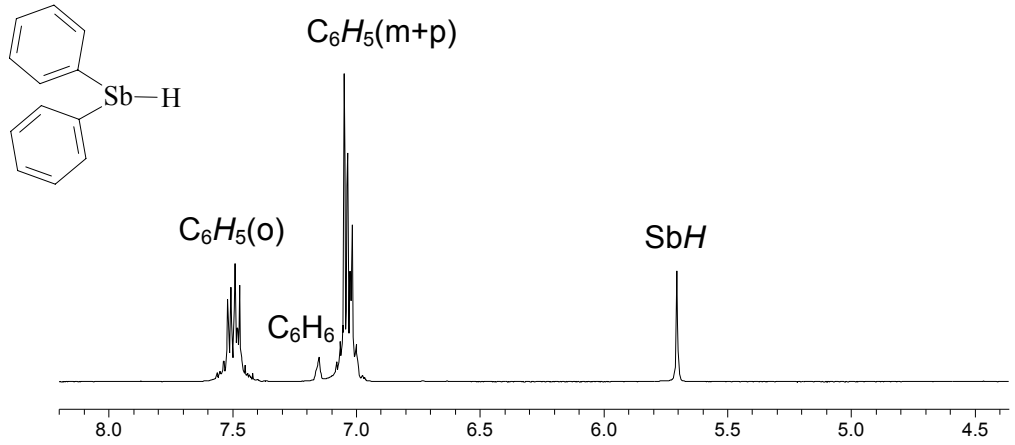

Figure 4. ^{1}H-NMR (C_6D_6, 200 MHz) spectrum of $(C_6H_5)_2SbH$ (**4**).

Clear evidence for the presence of the hydrogen atoms bonded to antimony in **1** - **4** comes from the observation of singlet signals in the range 3.11-5.70 ppm in the ^{1}H-NMR spectra, with the lowest field shift corresponding to the secondary stibane **4** (Table 1). This pattern of the spectra is suggestive for no coupling between the hydrogen atoms bonded to antimony and those belonging to the aromatic rings. The ^{1}H-NMR spectra of **1** - **4** are given in the Figures 1-4.

The mass spectra contain molecular ions only in the case of **2**. The IR stretching frequencies of the Sb-H bonds are within the expected range. The frequencies of the Sb-H bands are observed at 1791 cm^{-1} in **1**, 1863 cm^{-1} in **2**, 1806 cm^{-1} in **3** and 1819 cm^{-1} in **4**. These values compare well with those found for $ArSbH_2$ (Ar = C_6H_3-2,6-$Trip_2$; Trip = C_6H_2-2,4,6-*i*-Pr_3)[33] 1875 cm^{-1}, $(Me_3Si)_2CHSbH_2$[34] 1860 cm^{-1}, $Me_3CCH_2)_2SbH$[25] 1840 cm^{-1}, and $(Me_3SiCH_2)_2SbH$[26] 1835 cm^{-1} respectively. Selected spectroscopic features for **1** - **4** are presented in Table 1.

Table 1. Selected spectroscopic data for the arylstibanes **1** - **4**.

Compound	**1**	**2**	**3**	**4**
IR $\nu_{(Sb-H)}$ (cm^{-1})	1791	1863	1806	1819
^{1}H-NMR SbH_2/SbH (ppm)	3.70	3.11	4.43	5.70

Single crystals for X-ray diffraction studies could be obtained only in the case of **2**. The structure of **2** consists of discrete $MesSbH_2$ molecules, as illustrated in Figure 5. Selected bond lengths and bond angles are given in Table 2. Since the hydrogen atoms bonded to antimony were not located, values for the H-Sb-H and C-Sb-H bond angles remain unknown. However, it is evident from the NMR and IR spectra and also from the observation of the molecular ion in the mass spectra that the antimony atom is in the pyramidal environment of one mesityl group and two hydrogen atoms. A pyramidal geometry around the antimony atom was found in the crystal of $ArSbH_2$ [Ar = C_6H_3-2,6-(C_6H_2-2,4,6-*i*-$Pr_3)_2$][33] for which the hydrogens atoms bonded to antimony were located. The structure of this stibane is however subject to disorder.

Table 2. Selected interatomic distances (pm) and angles (º) in **2**.

[2,4,6-$(CH_3)_3C_6H_2$]SbH_2 (**2**)			
Sb-C(1)	215.4	Sb-C(1)-C(2)	124.84
C-C	133.0 – 152.7	Sb-C(1)-C(6)	116.25

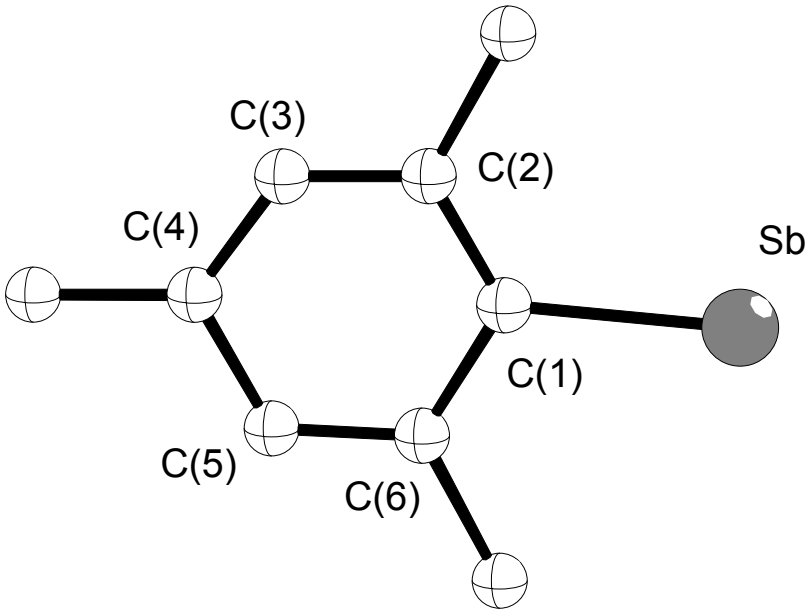

Figure 5. Structure and atom numbering scheme for **2**.

The Sb-C bond length (215.40 pm) in **2** lies in the usual range and is close to the value of 217.00 pm seen in $ArSbH_2$ [Ar = C_6H_3-2,6-(C_6H_2-2,4,6-*i*-Pr_3)$_2$][33].
An interesting feature of **2** is the crystallization of MesSb units into parallel layers. An illustration of this phenomenon is shown in Figure 6. The distance between layers is 362.40 pm.

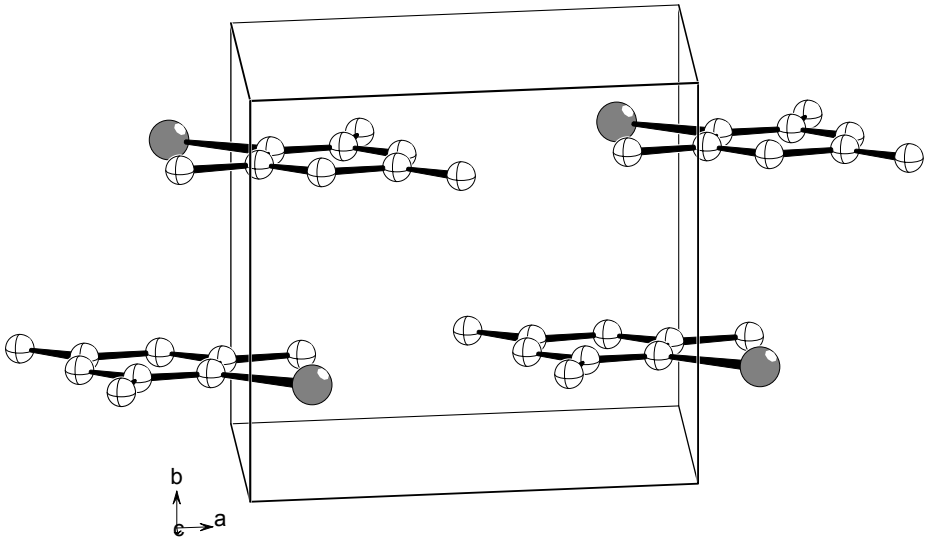

Figure 6. Diagram illustrating stacking of MesSb moieties in the crystal of **2**.

Attempts to synthesize the secondary alkylstibanes ^{t}Bu$_2$SbH by adding ^{t}Bu$_2$SbCl to LiAlH$_4$ at –80 °C, followed by work up of the reaction product at –30 °C resulted in the isolation of the know distibane ^{t}Bu$_2$Sb-Sb^{t}Bu$_2$ (**5**) as the only crystalline product.

$$2\,{}^t\mathrm{Bu_2SbCl} + 2\,\mathrm{LiAlH_4} \xrightarrow[\substack{-2\,\mathrm{LiCl}\\ -2\,\mathrm{AlH_3}\\ -\mathrm{H_2}}]{-80\ ^{\circ}\mathrm{C}} {}^t\mathrm{Bu_2Sb\text{-}Sb}{}^t\mathrm{Bu_2}$$

5

The synthesis of **5** was achieved in 83 % yield and high purity. The reverse procedure (*i.e.* addition of LiAlH$_4$ to ^{t}Bu$_2$SbCl) gives the desired antimony hydride, ^{t}Bu$_2$SbH[39]. Previously reported methods for the preparation of **5** [39,40] are more complicated and we found it difficult to obtain a pure product.

2. Mononuclear alkali metal diorganoantimonides

2.1. Introduction

Alkali diorganoantimonides, $R_2Sb^-M^+$ (M = Li, Na, K), are important synthons and found use in the preparation of numerous antimony containing compounds, *i.e.*: homoleptic or heteroleptic triorganoantimony compounds, R_3Sb,[1,2] diorganoantimony hydrides, R_2SbH,[3] distibanes, $R_2Sb\text{-}SbR_2$,[4,5,6] compounds containing antimony(III)-main group metal bonds, $R_2Sb\text{-}ER'_2$ (E = N[7], P[8], As[8], Ga[9], In[9]) and compounds with antimony(III)-transition metal bonds, $R_2Sb\text{-}ML_n$ (ML_n = VCp_2[10], $Cu(PMe_3)_2$[3]). Despite the synthetic importance, very little work has been done to understand their structure. In fact, the only structurally characterized mononuclear alkali diorganoantimonides are $[Ph_2Sb][Li(12\text{-crown-}4)_2]$ $^1/_3$thf[4] and $[\{(Me_3Si)_2SbLi\cdot 1DME\}_\infty]$[11] (DME = 1,2-dimethoxyethan). The structure of $[Ph_2Sb][Li(12\text{-crown-}4)_2]\cdot{}^1/_3$thf consist of well separated $[Ph_2Sb]^-$ and $[Li(12\text{-crown-}4)_2]^+$ ions , while in the structure of $[\{(Me_3Si)_2SbLi\cdot 1DME\}_\infty]$ dimethoxyethane-coordinated lithium atoms alternate with $Sb(SiMe_3)_2$ groups giving infinite chains of tetrahedrally coordinated lithium and antimony atoms. For the synthesis of mononuclear alkali diorganoantimonides the reduction of triorganoantimony compounds and diorganoantimony halides with alkali metals and the reaction of diorganoantimony hydrides with organolithium reagents have been proved to be particularily useful. The color of the solutions obtained from these reactions range from orange to deep red. They are extremely reactive towards oxygen and moisture. Less studied are the asymmetrically substituted mononuclear alkali diorganoantimonides, $RR'Sb^-M^+$ ($R \neq R'$). Such compounds are potential chiral reagents or catalysts for enantioselective syntheses.[12-16] The only known asymmetrical alkali metal diorganoantimonide, PhMeSbNa,[17-19] was reported without structural data as an intermediate in the preparation of asymmetrical tertiary stibanes.

Diaryl lithium antimonides

2.2. Synthesis and characterization of $[(C_6H_5)_2SbLi\cdot(thf)_3]$ and $[(2,4,6\text{-}(CH_3)_3C_6H_2)_2SbLi\cdot(thf)_3]$

Reactions of the secondary arylstibanes $(C_6H_5)_2SbH$ or $(2,4,6\text{-}(CH_3)_3C_6H_2)_2SbH$ in thf with one equivalent *n*-butyllithium at -70 °C give the solvated lithium antimonides $[(C_6H_5)_2SbLi\cdot(thf)_3]$ (**6**), respectively $[(2,4,6\text{-}(CH_3)_3C_6H_2)_2SbLi\cdot(thf)_3]$ (**7**).

$$R_2SbH + {}^{n}BuLi + 3thf \xrightarrow[-\,70\,^{o}C]{thf} R_2SbLi\cdot(thf)_3 + BuH$$

$R = C_6H_5$ (**6**)

$R = 2,4,6\text{-}(CH_3)_3C_6H_2$ (**7**)

6 and **7** are air and water sensitive both in solution and solid state. Red crystals of **6** and **7** were obtained by cooling concentrated solutions in tetrahydrofuran at -28 °C. Crystals of these diorganoantimonides decompose above 29 °C (**6**) or 36 °C (**7**) to a black material. The molecular and crystal structures of **6** and **7** were determined by X-ray diffraction analysis (Figure 7 and 8). Selected bond lengths and angles are given in Table 3. The crystals of **6** and **7** consist of discrete molecules. By contrast, the phosphide analogue of **6**, $[\{Ph_2PLi\cdot 2thf\}_\infty]$ forms polymer chains in the crystal, which are built up by alternating diphenylphosphide and $Li(thf)_2$ units.[41] The crystal structure determination of **7** reveals the existence of two crystallographically independent molecules with similar bond lengths and angles. The Sb atoms in **6** and **7** are in trigonal-pyramidal environments (Σ(angles at Sb) ≈ 289° in **6** and 304° in **7**), while the lithium atoms are four coordinate by an antimony and three oxygen atoms of three thf ligands in a tetrahedral environment. A trigonal-pyramidal coordination of the pnicogen-center exists also in metaldiorganoarsenides and phosphides [4,42]. In contrast the nitrogen atom in metalamides usually adopts a trigonal planar geometry.[43]

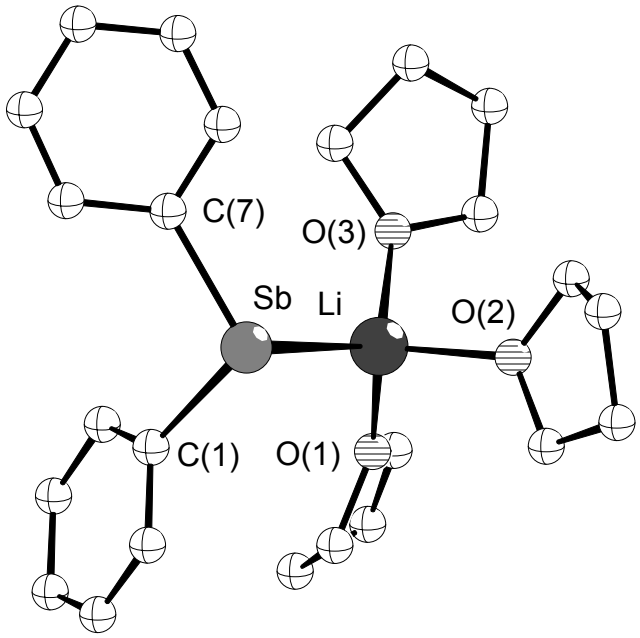

Figure 7. Structure and atom numbering scheme for **6**.

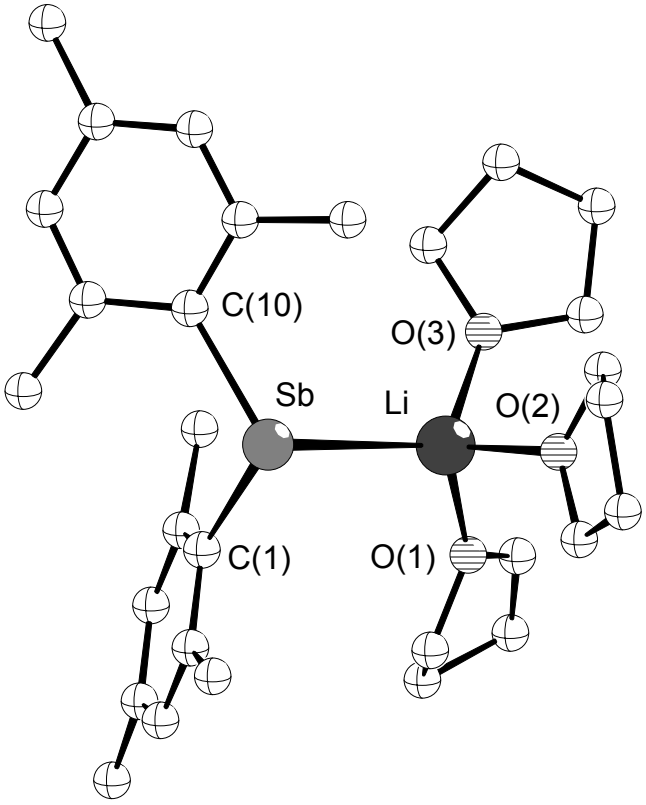

Figure 8. Structure and atom numbering scheme for **7**.

The Sb-Li bond lengths (288.10 pm in **6** and 293.70 pm in **7**) correspond to the sum of the covalent radii of these elements (293 pm). Comparable Sb-Li bond lengths have been found in $[\{(Me_3Si)_2SbLi\cdot DME\}_\infty]$[11] (293.30 pm) and in the Zintl compounds $[Sb_7Li_3\cdot 6HNMe_2]$[44] (292 pm) and $[Sb_7Li_3(tmeda)_3]$ toluene[44] (289 pm) [tmeda = $(Me_2NCH_2)_2$].

The structures of $[Ph_2Sb][Li(12\text{-crown-}4)_2]$ $^1/_3$thf[4], $[Ph_2As][Li(12\text{-crown-}4)_2]$ thf[45], and $[Ph_2P][Li(12\text{-crown-}4)_2]$[4] consist of well separated ions which is suggestive for the ionic nature of the pnicogen-lithium bond in this compounds. In contrary, in the structure of the lithium amide $[Li(12\text{-crown-}4)NPh_2]$[4] there is a strong Li-N bond leaving the nitrogen atom in a trigonal planar environment.

Table 3. Selected interatomic distances (pm) and angles (º) in **6** and **7**. For **7** there are two independent molecules in the asymmetric unit (the values for the second molecule are given in brackets).

$[Ph_2SbLi\cdot(thf)_3]$ (**6**)			
Sb-Li	288.10	C(1)-Sb(1)-C(1)	100.58
Sb(1)-C(1)	215.60	C(7)-Sb-Li	96.96
Sb(1)-C(7)	216.00	C(1)-Sb-Li	91.77
Li(1)-O(1)	195.30	Sb-Li-O(1)	115.24
Li(1)-O(2)	191.50	Sb-Li-O(2)	114.68
Li(1)-O(3)	193.60	Sb-Li-O(3)	114.20
		O(1)-Li-O(2)	103.70
C(7)-Sb-Li-O(3)	13.43	O(2)-Li-O(3)	105.33
C(7)-Sb-Li-O(2)	108.29	O(1)-Li-O(3)	102.30
C(7)-Sb-Li-O(1)	131.42	C(1)-Sb-Li-O(1)	30.54
C(1)-Sb-Li-O(3)	87.45	C(1)-Sb-Li-O(2)	150.83
$[(2,4,6\text{-}(CH_3)_3C_6H_2)_2SbLi\cdot(thf)_3]$ (**7**)			
Sb-Li	294.40 (289.40)	C(1)-Sb-C(10)	103.95 (105.10)
Sb-C(10)	218.10 (217.30)	Li-Sb-C(10)	92.13 (109.27)

Sb-C(1)	219.00 (218.00)	Li-Sb-C(1)	110.69 (89.84)
Li-O(1)	196.20 (191.00)	O(1)-Li-O(2)	103.48 (102.75)
Li-O(2)	193.20 (198.60)	O(3)-Li-O(2)	98.68 (100.92)
Li-O(3)	194.50 (198.00)	O(3)-Li-Sb(1)	112.32 (107.51)
C(1)-Sb-Li-O(2)	112.03	O(1)-Li-Sb	120.49 (117.99)
		O(2)-Li-Sb	109.88 (121.98)
C(1)-Sb-Li-O(3)	139.19	C(1)-Sb-Li-O(1)	8.00
C(10)-Sb-Li-O(1)	97.78	C(10)-Sb-Li-O(2)	142.19
C(10)-Sb-Li-O(3)	33.41		

Asymmetrically substituted alkali metal diorganoantimonides

2.3. Synthesis and characterization of [2-(Me$_2$NCH$_2$)C$_6$H$_4$][(Me$_3$Si)$_2$CH]-SbLi·2thf, [2-(Me$_2$NCH$_2$)C$_6$H$_4$][(Me$_3$Si)$_2$CH]SbNa·tmeda and [2-(Me$_2$NCH$_2$)C$_6$H$_4$][(Me$_3$Si)$_2$CH]SbK·pmdeta

The chiral racemic alkylarylantimonide [2-(Me$_2$NCH$_2$)C$_6$H$_4$][(Me$_3$Si)$_2$CH]SbLi·2thf (**8**) forms by metalation of [2-(Me$_2$NCH$_2$)C$_6$H$_4$][(Me$_3$Si)$_2$CH]SbH with *n*-BuLi in thf.

$$[2\text{-}(Me_2NCH_2)C_6H_4][(Me_3Si)_2CH]SbH \xrightarrow[^{n}BuH]{+\ n\text{-BuLi} + 2thf} [2\text{-}(Me_2NCH_2)C_6H_4][(Me_3Si)_2CH]SbLi{\cdot}2thf \quad (\mathbf{8})$$

Treatment of [2-(Me$_2$NCH$_2$)C$_6$H$_4$][(Me$_3$Si)$_2$CH]SbH with K in liquid ammonia and addition of pmdeta gives [2-(Me$_2$NCH$_2$)C$_6$H$_4$][(Me$_3$Si)$_2$CH]SbK·pmdeta (**10**).

$$[2\text{-}(Me_2NCH_2)C_6H_4][(Me_3Si)_2CH]SbH \xrightarrow[-\ H_2]{+\ K + pmdeta\ /\ NH_3\ (l)} [2\text{-}(Me_2NCH_2)C_6H_4][(Me_3Si)_2CH]SbK{\cdot}pmdeta \quad (\mathbf{10})$$

Transmetalation of (**8**) with sodium *tert*-butoxide in the presence of tmeda leads to [2-(Me_2NCH_2)C_6H_4][($Me_3Si)_2$CH]SbNa·tmeda (**9**).

$$[2\text{-}(Me_2NCH_2)C_6H_4][(Me_3Si)_2CH]SbLi\cdot 2thf + NaO^tBu \xrightarrow[-\ 2thf]{Et_2O\ /\ tmeda} [2\text{-}(Me_2NCH_2)C_6H_4][(Me_3Si)_2CH]SbNa\cdot tmeda \quad (\mathbf{9})$$

Closely related to **8**, **9**, and **10** are the phosphorus analogues [2-(Me_2NCH_2)C_6H_4][($Me_3Si)_2$CH]PLi·2thf, [2-(Me_2NCH_2)C_6H_4][($Me_3Si)_2$CH]--PNa·tmeda, and [2-(Me_2NCH_2)C_6H_4][($Me_3Si)_2$CH]PK·pmdeta.[46]

The antimonides **8**, **9**, and **10** are air- and moisture-sensitive solids that decompose at room temperature but can be stored for a long time in an inert atmosphere at –30 ºC. They are slightly soluble in petroleum ether or hexane and readily soluble in tetrahydrofuran and aromatic hydrocarbons. The hydrolysis of **8**, **9** and **10** gives the hydride [2-(Me_2NCH_2)C_6H_4][($Me_3Si)_2$CH]SbH.

The antimony centers in **8**, **9**, and **10** are effectively protected by the bis(trimethylsilyl)methyl and the 2-(*N*,*N*-dimethylaminomethyl)phenyl substituents which combine bulkiness with the potential for supplemental Lewis base interaction.

^{1}H-NMR spectra of **8**, **9**, and **10** at 20 °C contain singlet signals for the $SiMe_3$ and the NMe_2 groups and two doublets (**8**) or a broad signal (**9** and **10**) for the CH_2 protons. These data suggest that M-Sb (M = Li, Na) bond scission, inversion at nitrogen and rotation around the Sb-C bond of the alkyl substituent takes place in solutions of **8** - **9**. These processes probably do not involve loss of chirality at the antimony centers because the non-equivalence of the CH_2 protons is preserved. A similar spectral pattern was also observed in the case of the analogous phosphorus compounds.[46]

Although the solid state structure of **10** was not determined it is probable that its structure is similar to that of **8** and **9** and of the phosphide analogues [2-(Me_2NCH_2)C_6H_4][($Me_3Si)_2$CH]PK·pmdeta[46]. In the case of **9** also ^{1}H-NMR spectra at low temperatures were recorded. Cooling a solution of **9** in CD_5CD_3 to temperatures below –85 °C leads to a freezing of the dynamic process. At this

temperature the spectra contain two signals which indicate the non-equivalence of the $SiMe_3$ groups as expected from the X-ray data.

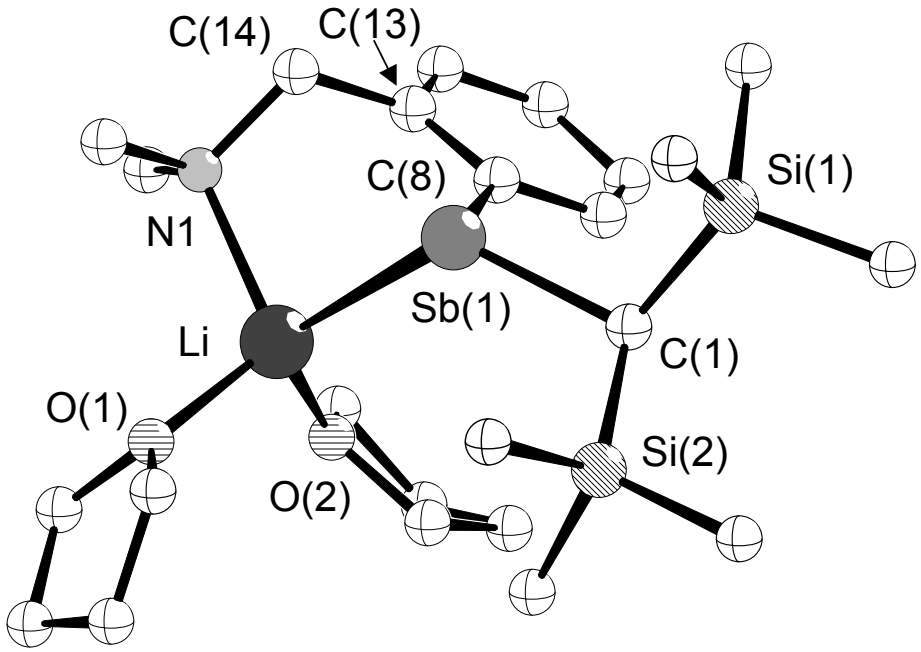

Figure 9. Structure and atom numbering scheme for *R*-**8.**

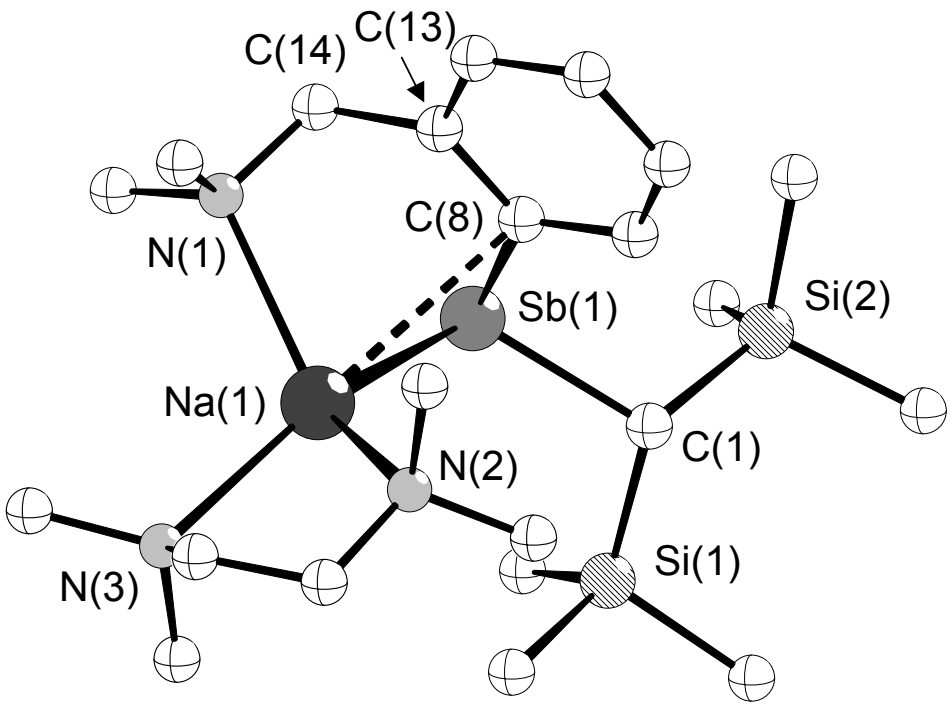

Figure 10. Structure and atom numbering scheme for *S*-**9**.

Single crystals for X-ray diffraction studies have been obtained by cooling a solution of **8** in thf to –28 ºC, and a solution of **9** in Et_2O to –28 ºC. X-ray diffraction studies revealed that **8** and **9** crystallize as racemates. The molecular structures of the *R* isomer of **8** and of the *S* isomer of **9** are shown in Figures 9 and 10. Selected bond distances and angles are given in Table 4.

Table 4. Selected interatomic distances (pm) and angles (º) in **8** and **9**.

[2-(Me_2NCH_2)C_6H_4][($Me_3Si)_2$CH]SbLi·2thf (**8**)			
Sb(1)-Li	285.60	C(1)-Sb(1)-C(8)	98.69
Sb(1)-C(1)	223.90	C(13)-C(8)-Sb(1)	119.00
Sb(1)-C(8)	218.00	C(1)-Sb(1)-Li	123.43
Li-N(1)	212.30	N(1)-C(14)-C(13)	112.50
Li-O(1)	193.30	C(8)-Sb(1)-Li	71.84
Li-O(2)	195.80	Li-N(1)-C(14)	111.60
		N(1)-Li-Sb(1)	91.00
[2-(Me_2NCH_2)C_6H_4][($Me_3Si)_2$CH]SbNa·tmeda (**9**)			
Sb(1)-Na(1)	310.10	C(1)-Sb(1)-C(8)	97.70
Sb(1)-C(1)	225.50	C(13)-C(14)-N(1)	112.70
Sb(1)-C(8)	218.60	C(8)-Sb(1)-Na(1)	67.69
N(2)-Na(1)	245.40	C(14)-N(1)-Na(1)	108.70
N(3)-Na(1)	247.20	Sb(1)-C(8)-C(13)	120.00
C(8)···Na(1)	304.10	N(1)-Na(1)-Sb(1)	83.18
N(1)-Na(1)	250.20	C(8)-C(13)-C(14)	120.50
		N(2)-Na(1)-N(3)	74.80

The bidentate Sb-N coordination of the amino antimonide ligand to the alkali metal forms six-membered chelate rings with a ligand bite angle of 91.0° in the case of **8** and 83.18° in the case of **9**. The six-membered chelate rings are puckered along the Sb-C(14) vectors generating a fold angle between the Sb(1)-C(8)-C(13)-C(14) and C(14)-N(1)-M-Sb(1) (M = Li, Na) planes of 94.9° in the case of **8** and 93.5° in the

case of **9**. The lithium atom in **8** lies in a tetrahedral environment coordinated by the antimony and nitrogen atoms of the amino antimonide ligand and the oxygen atoms of two tetrahydrofuran molecules. The Sb(1)-Li distance of 285.60 pm in **8** is comparable to the one found in $[Ph_2SbLi{\cdot}(thf)_3]$ (288.10 pm). The sodium atom in **9** is essentially four-coordinated with bonds to the Sb and N atoms of the antimonide ligand and to the nitrogen atoms of the tmeda ligand. The coordination geometry is distorted tetrahedral. The Na(1)-C(8) distance of 304.10 pm indicates a weak transanular interaction. A similar interaction was also found in the structure of $[2\text{-}(Me_2NCH_2)C_6H_4][(Me_3Si)_2CH]PNa{\cdot}$tmeda (Na**…**C*ipso* 300.40 pm).[46] The Sb(1)-Na(1) bond (310.10 pm) in **9** is shorter than the corresponding values in the triantimonide $[Na(pmdeta)^tBu_4Sb_3]$ (pmdeta = $(Me_2NCH_2CH_2)_2NMe$; Sb-Na 330.30 and 322.50 pm).[47] These differences reflect the lower coordination number of the sodium atom in **9**. The Na(1)-N(1) distance (250.20 pm) is only little longer than the two Na(1)-N(tmeda) distances (245.40 and 247.20 pm) in **9** and all three distances compare well with the Na-N distances in the triantimonide $[Na(pmdeta)^tBu_4Sb_3]$ (pmdeta = $(Me_2NCH_2CH_2)_2NMe$) (245.00 – 249.50 pm).[47]

3. Zintl compounds containing the Sb_7^{3-} anion

3.1. Introduction

The term "Zintl phases" entered the chemist's vocabulary more than 50 years ago to reflect the merits of Edward Zintl, who had discovered and studied a new class of compounds intermediate between typical salts and intermetallics.[48] Zintl investigated binary intermetallic compounds, of which one component is a rather electropositive element. He proposed an electron transfer from the electropositive to the electronegative atoms. In this way Zintl defined a class of compounds, which was at that time, a somewhat curious link between the well-known valence compounds and the obviously completely different intermetallic phases.[49]

In the last years, many polyatomic anions of the post transition elements, Bi_4^{2-},[50] Sb_7^{3-},[21] and As_{11}^{3-} [51] in group 15, for example, have been isolated as stable salts by the reaction of their alkali-metal alloys with 2,2,2-crypt-[4,7,13,16,21,24-hexaoxa-1,10-diazabicyclo-(8,8,8)hexacosane], an complexing agent for the metal cation. The chemistry of antimony is considerably modified compared with that of the lighter members of the group by the general decrease in bond strengths and the increase in metallic character. The homopolyatomic Sb_7^{3-} anion is usually prepared by fusing stoichiometric amounts of the alkali metal and antimony at 600 to 800 °C.[52] More recently, a methodology involving the thermolysis of the heterobimetallic phosphinidene complex $[\{Sb(PCy)_3\}_2Li_6 \cdot 6Me_2NH]$ (Cy = C_6H_{11}) at 30 to 40 °C has been proposed.[44] From this reaction the Zintl compound $[Sb_7Li_3 \cdot 6HNMe_2]$ could be isolated which with excess tmeda gives $[Sb_7Li_3(tmeda)_3] \cdot$toluene.[44] On the other hand heating $[\{Sb(PCy)_4\}Na \cdot tmeda]$ (Cy = C_6H_{11}) in solution to *ca*. 60 C° results in the formation of $[Sb_7Na_3 \cdot 3tmeda \cdot 3thf]$.[53,54] The compound $[(2,2,2\text{-crypt-K})_3Sb_7 \cdot 2en]$ has been prepared from the reaction of a KGeSb alloy with $C_{18}H_{36}N_2O_6$ (2,2,2-crypt) in ethylenediamine.[55] The first crystal structure of these type salts, has been reported by Corbett and co-workers in the early 1976's in the Zintl compound Na_3Sb_7[21] using 2,2,2-crypt which strongly complexes Na^+ cations and separates them from the polyatomic anions. The Sb_7^{3-} anion has been found to possess a P_4S_3 type structure:

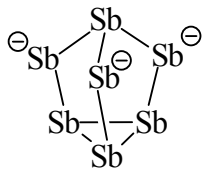

The fact that some of these compounds which possess "glass-like" thermal conductivity, have the ability to vary the electronic properties with doping level, and the relatively good electronic properties obtained in these semiconductor materials, make them interesting for thermoelectronic applications and also many other possible interesting properties that might lead to an entirely different range of applications from superconductivity to large band gap semiconductors.[22]

3.2. Synthesis and characterization of tris(tmeda-lithium)-, tris(pmdeta-sodium)- and tris(pmdeta-potassium)hepta-antimonide $[Sb_7Li_3{\cdot}(tmeda)_3]$, $[Sb_7Na_3{\cdot}(pmdeta)_3]$, $[Sb_7K_3{\cdot}(pmdeta)_3]$

When $RSbH_2$ (R = C_6H_5, 2-$[(CH_3)_2NCH_2]C_6H_4$, 2,4,6-$(CH_3)_3C_6H_2$ or $[(CH_3)_3Si]_2CH$) is treated with *n*-BuLi in thf at –70 ºC in the presence of tmeda (tmeda = tetramethylethylenediamine), red solutions of the Zintl compound $[Sb_7Li_3{\cdot}(tmeda)_3]$ (**11**) form.

$$RSbH_2 \xrightarrow[\text{thf / -70 °C}]{\text{BuLi / tmeda}} [Sb_7Li_3(tmeda)_3] \quad (\mathbf{11})$$

R = C_6H_5, 2-$[(CH_3)_2NCH_2]C_6H_4$,
2,4,6-$(CH_3)_3C_6H_2$ or $[(CH_3)_3Si)]_2CH$

The reaction of $PhSbH_2$ with Na or K in liquid ammonia in the presence of pmdeta (pmdeta = pentamethyldiethylenetriamine) provides access to the Zintl compounds $[Sb_7Na_3{\cdot}(pmdeta)_3]$ (**12**) and $[Sb_7K_3{\cdot}(pmdeta)_3]$ (**13**).

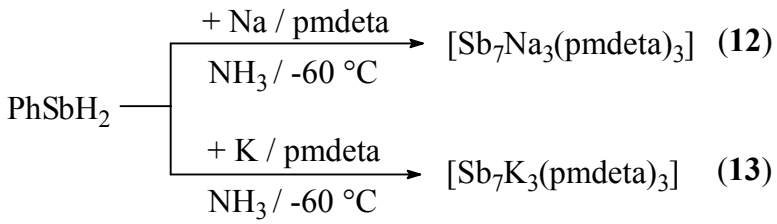

Complexes **11-13** are isolated as air- and moisture-sensitive red crystals in yields that vary between 53 and 65%. They are soluble in thf and can be stored under inert atmosphere and at –28º C for weeks without any sign of decomposition.

Although the presence of the Sb_7^{3-} anion is not unprecedented, the simple preparation of these complexes using easily accessible primary stibanes represents an important route to Zintl compounds.

Low-temperature X-ray diffraction studies of **11** (Figure 11), **12** (Figure 12) and **13** (Figure 13) show that they consist of discrete heterobimetallic cage molecules in which Sb_7^{3-} ions are coordinated at the equatorial Sb atoms by three Lewis base solvated metal cations. Selected bond distances and angles for **11**, **12**, and **13** are given in Tabele 5. A remarkable feature for all three structures is that the Sb-Sb bond distances (284.80 - 286.80 pm) in the triangular base are slightly longer than the Sb-Sb distances (273.60 - 275.80 pm) describing the edges of the cage.

Table 5. Selected interatomic distances (pm) and angles (º) for **11**, **12** and **13**.

$[Sb_7Li_3{\cdot}(tmeda)_3]$ (**11**)			
Sb-Li	287.90 - 289.80	Sb-Li-Sb	96.0 – 97.33
Sb(1)-Sb(2)	279.50	Sb(2)-Sb(1)-Sb(3)	100.80
Sb(1)-Sb(3)	279.50	Sb(3)-Sb(1)-Sb(4)	101.15
Sb(1)-Sb(4)	280.70	Sb(2)-Sb(1)-Sb(4)	101.15
Sb(2)-Sb(5)	275.20	Sb(6)-Sb(5)-Sb(7)	59.76
Sb(3)-Sb(6)	275.20	Sb(5)-Sb(6)-Sb(7)	59.76
Sb(4)-Sb(7)	275.80	Sb(5)-Sb(7)-Sb(6)	60.48
Sb(5)-Sb(6)	286.80	Sb(1)-Sb(2)-Sb(5)	99.39

Sb(6)-Sb(7)	284.80	Sb(2)-Sb(5)-Sb(7)	105.13
Sb(5)-Sb(7)	284.80	Sb(5)-Sb(7)-Sb(4)	106.01
		Sb(7)-Sb(4)-Sb(1)	98.43
$[Sb_7Na_3 \cdot (pmdeta)_3]$ (**12**)			
Sb-Na	320.80 – 325.80	Sb-Na-Sb	83.53 – 84.30
Sb(1)-Sb(2)	279.00	Sb(2)-Sb(1)-Sb(3)	101.81
Sb(1)-Sb(3)	278.70	Sb(3)-Sb(1)-Sb(4)	101.73
Sb(1)-Sb(4)	279.30	Sb(2)-Sb(1)-Sb(4)	101.66
Sb(2)-Sb(5)	275.40	Sb(6)-Sb(5)-Sb(7)	59.96
Sb(3)-Sb(6)	273.60	Sb(5)-Sb(6)-Sb(7)	60.26
Sb(4)-Sb(7)	273.70	Sb(5)-Sb(7)-Sb(6)	59.78
Sb(5)-Sb(6)	286.10	Sb(1)-Sb(2)-Sb(5)	98.26
Sb(6)-Sb(7)	286.60	Sb(2)-Sb(5)-Sb(7)	105.77
Sb(5)-Sb(7)	287.4	Sb(5)-Sb(7)-Sb(4)	104.93
		Sb(7)-Sb(4)-Sb(1)	98.51
$[Sb_7K_3 \cdot (pmdeta)_3]$ (**13**)			
Sb-K	320.70 – 326.30	Sb-K-Sb	83.95 – 85.06
Sb(1)-Sb(2)	279.40	Sb(2)-Sb(1)-Sb(3)	101.55
Sb(1)-Sb(3)	279.50	Sb(3)-Sb(1)-Sb(4)	101.89
Sb(1)-Sb(4)	279.20	Sb(2)-Sb(1)-Sb(4)	101.97
Sb(2)-Sb(5)	273.70	Sb(6)-Sb(5)-Sb(7)	60.37
Sb(3)-Sb(6)	275.60	Sb(5)-Sb(6)-Sb(7)	59.85
Sb(4)-Sb(7)	274.30	Sb(5)-Sb(7)-Sb(6)	59.78
Sb(5)-Sb(6)	286.50	Sb(1)-Sb(2)-Sb(5)	98.56
Sb(6)-Sb(7)	288.20	Sb(2)-Sb(5)-Sb(7)	104.95
Sb(5)-Sb(7)	286.70	Sb(5)-Sb(7)-Sb(4)	106.22
		Sb(7)-Sb(4)-Sb(1)	98.31

In **11** all three Li^+ cations, each solvated by a chelating tmeda ligand, bond exclusively with the equatorial Sb centres of the Sb_7^{3-} anion. The Sb-Li bond lengths in **11** (average 288.85 pm) are comparable with those found in known Sb-Li bonded complexes, *i.e.* $[Li(NH_3)_4]_3[(NH_3)_2Li_2Sb_5]$[56] (average 282.63 pm), $[(Me_3Si)_2SbLi{\cdot}glyme]$[11] (glyme = $(MeOCH_2)_2$; average Sb-Li bond 293.34 pm) or $[(C_6H_5)_2SbLi{\cdot}(thf)_3]$ (average 288.14 pm). The complex **11** is isostructural with the P and As analogues $[P_7Li_3{\cdot}(tmeda)_3]$[57] and $[As_7Li_3{\cdot}(tmeda)_3]$[58].

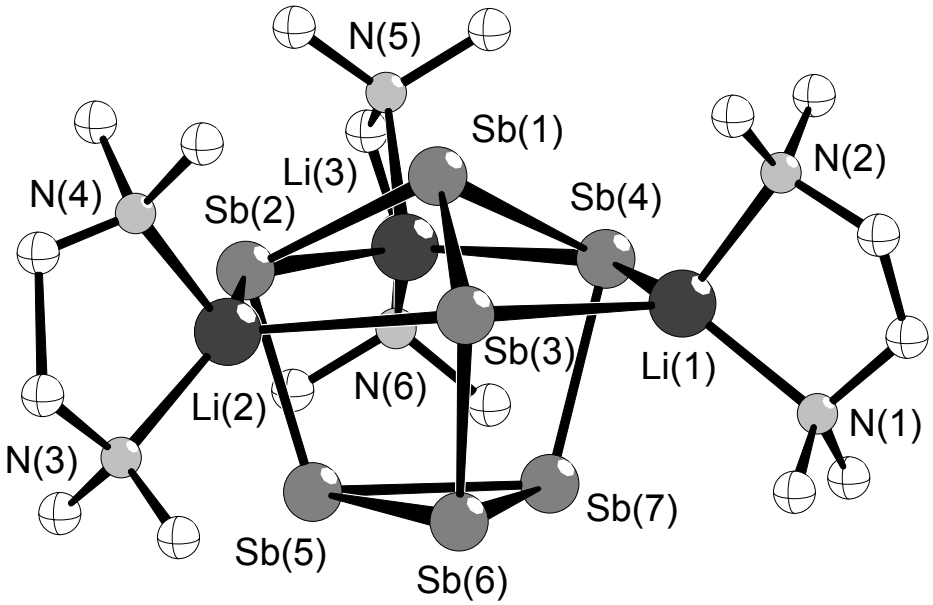

Figure 11. Structure and atom numbering scheme for **11**.

In complexes **12** and **13** the Sb_7^{3-} anions are bonded through their anionic centres to three alkali metal cations. The coordination number of the alkali metals is completed to five by three nitrogen atoms of a tridentate pmdeta ligand. The Sb-Na bond lengths in **12** (320.80 – 325.80 pm) are within the range observed in the closely related Zintl compound $[Sb_7Na_3{\cdot}(tmeda)_3{\cdot}(thf)_3]$[54] (319.69 – 356.30 pm).

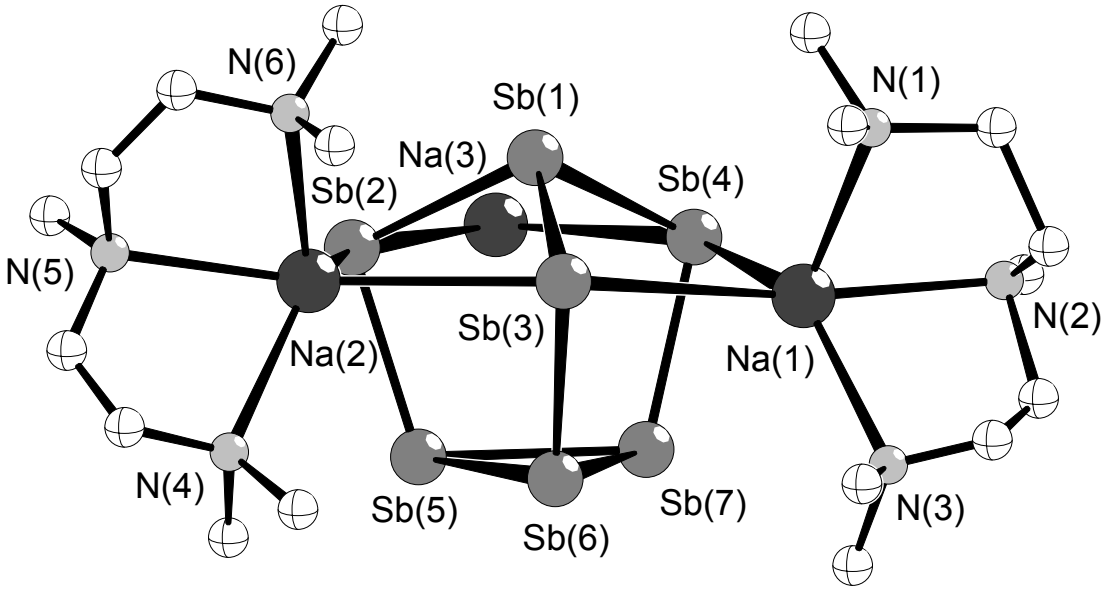

Figure 12. Structure and atom numbering scheme for **12**.

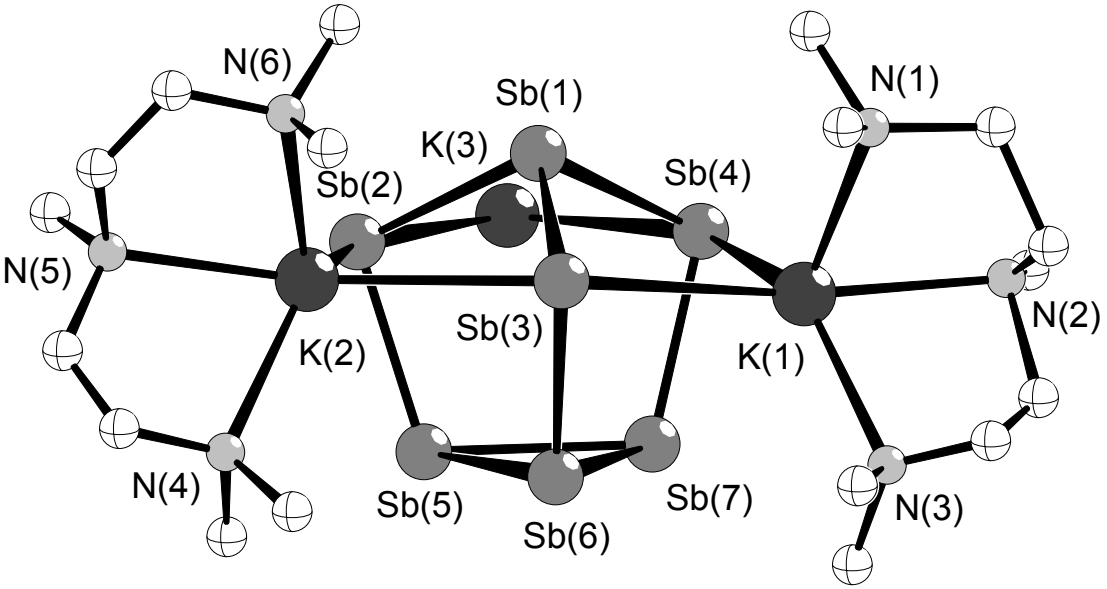

Figure 13. Structure and atom numbering scheme for **13**.

4. The cleavage of *cyclo*-(^{t}BuSb)$_4$ with alkali metals (Li, Na, and K)

4.1. Introduction

The number of reports on the reduction of cyclostibanes with alkali metals are few and often only mixtures containing various anions were obtained. Earlier work of Issleib and Balszuweit described the reduction of *cyclo*-(PhSb)$_6$ with appropriate amounts of sodium in liquid ammonia to give solutions of $Na_2[Ph_2Sb_2]$ or $Na_2[PhSb]$.[15] They suggest that these antimonides are suitable materials to prepare tertiary stibanes, distibanes and cyclic stibanes. In a separate work the dianionic diantimonide [^{t}Bu$_2$Sb$_2$]$^{2-}$ was suggested to form in solutions by the reduction of *cyclo*-(^{t}BuSb)$_4$ by electrochemical methods[59] (Scheme 1). However, when *cyclo*-(^{t}BuSb)$_4$ was reacted with K in thf at room temperature in the presence or absence of the stabilizer 18-crown-6 no anionic species could be isolated.[59] The only isolated products from these reactions were *cyclo*-(^{t}BuSb)$_4$ and ^{t}Bu$_3$Sb.

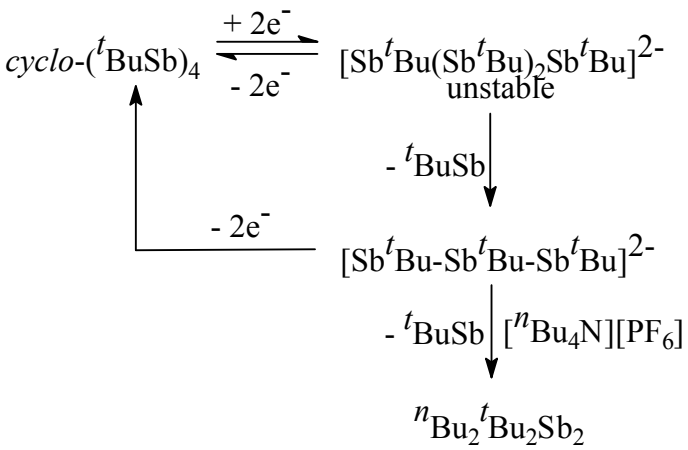

Scheme 1. Electroreduction of *cyclo*-(^{t}BuSb)$_4$

It is only recently that the first anionic species [(^{t}Bu$_4$Sb$_3$)][K(pmdeta)$_2$], could be isolated from the reaction of *cyclo*-(^{t}BuSb)$_4$ with potassium in boiling tetrahydrofuran, followed by the addition of pmdeta.[20] The triantimonide was characterized by X-ray diffraction analysis. The crystals contain amine coordinated potassium cations and [(^{t}Bu)$_2$Sb-Sb-Sb(^{t}Bu)$_2$]$^-$ anions.

Little work has been done also on the reduction of cycloarsanes with alkali metals and the mechanism of these reactions are not completely understood. It is known that the alkali metals cleave the cycloarsanes to give short-chain polyarsenides; the reaction has been used for the preparation of K(^{t}BuAs)$_4$K, K(^{t}BuAs)$_2$K from *cyclo*-(^{t}BuAs)$_4$ and potassium metal in thf or dioxane,[60] and of K(EtAs)$_5$K, K(EtAs)$_3$K and K(EtAs)$_2$K from *cyclo*-(EtAs)$_5$ in a similar manner.[61] The chain length of the formed arsenides can be regulated by the K : As ratio.

More detailed studies have been performed on the reactions of cyclophosphanes with alkali metals. Most of the work in this field has been done by the groups of *Issleib* and *Baudler*. Reactions of *cyclo*-(PhP)$_5$ with alkali metals (Li, Na or K) in tetrahydrofuran or dioxane lead to the formation of alkali metal phenylphosphides of type M$_2$(PhP)$_n$ (n = 4, 3, 2, 1).[62,63,64] These species were suggested to be cyclic. The compound K$_2$(PPh)$_3$ represents the only exception. NMR spectroscopic[65,66] and electrochemical investigations[67] revealed that K$_2$(PPh)$_3$ which has been described as the first derivate of a cyclotriphosphane[62] is in fact an open-chain species. Cleavage of *cyclo*-(^{t}BuP)$_4$ with potassium in boiling tetrahydrofuran gives not only the potassium phosphide of chain length 4[68,69], but also the phosphides K$_2$(P^{t}Bu)$_n$ (n = 3[70],2[70]). Because of its insolubility, K$_2$(P^{t}Bu)$_2$ can be easily isolated, representing an excellent synthon for the synthesis of cyclophosphanes[68,71] or P$_2$E[72] (E = group 13-16 element) heterocycles. In a recent reinvestigation of the ring cleavage of *cyclo*-(^{t}BuP)$_4$ with potassium in the presence of pmdeta the dimeric species [{(^{t}BuP)$_2$H}K·pmdeta]$_2$ was isolated and characterized by X-ray diffraction studies.[73] This compound is in fact a product of the hydrolysis of K$_2$(P^{t}Bu)$_2$.

4.2. Synthesis and characterization of [(^{t}Bu$_4$Sb$_3$)][Li(tmeda)$_2$], [(^{t}Bu$_4$Sb$_3$)Na(tmeda)], [(^{t}Bu$_4$Sb$_3$)Na(tmeda)$_2$], [(^{t}Bu$_4$Sb$_3$)Na(pmdeta)], [(^{t}Bu$_4$Sb$_3$)K(pmdeta)], [(^{t}Bu$_3$Sb$_2$)K(pmdeta)], [(^{t}Bu$_2$Sb)K(pmdeta)]

The reactions of *cyclo*-(^{t}BuSb)$_4$ with Li, Na, or K lead to cleavage of Sb-Sb bonds combined with migration of the tert. butyl groups, and after addition of

tetramethylethylenediamine or pentamethyldiethylenetriamine, complex salts containing the mono anions **A**, **B** or **C** form. The anions **A** are present in [(^{t}Bu$_4$Sb$_3$)][Li(tmeda)$_2$] (**14**), [(^{t}Bu$_4$Sb$_3$)Na(tmeda)] (**15**), [(^{t}Bu$_4$Sb$_3$)Na(tmeda)$_2$] (**16**), [(^{t}Bu$_4$Sb$_3$)Na(pmdeta)] (**17**), [(^{t}Bu$_4$Sb$_3$)K(pmdeta)] (**18**). The anion **B** was found to act as a bridging ligand in the potassium complex [(^{t}Bu$_3$Sb$_2$)K(pmdeta)] (**19**) and the anion **C**, which is the smallest anionic fragment that can be obtained from the cleavage of cyclo stibanes with alkali metals, was coordinated in the complex [(^{t}Bu$_2$Sb)K(pmdeta)] (**20**).

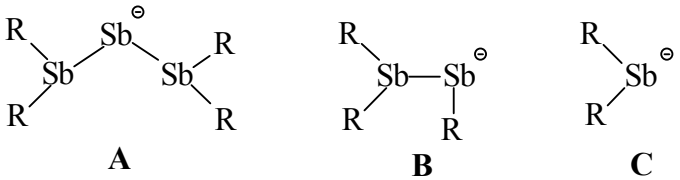

A **B** **C**

R = ^{t}Bu

These compounds are red or brown-red solids, which are extremely sensitive towards traces of moisture or air. The solubility of these complexes in petroleum ether is low; in tetrahydrofuran, benzene, toluene or other organic solvents they are readily soluble.

The progress of the reaction of *cyclo*-(^{t}BuSb)$_4$ with potassium in boiling thf was monitored by ^{1}H-NMR spectra of samples taken from the reaction mixture after 10 min, 1 h, 1.5 h, 2 h, and 2 h 45 min, which were worked up with addition of the triamine ligand, removal of the thf, and dissolution in C_6D_6. The spectra are shown in Figure 14. There is one singlet signal for the [^{t}Bu$_4$Sb$_3$]$^-$ moiety **A** (Figure 14b), as expected for the symmetric configuration [(^{t}Bu)$_2$Sb-Sb-Sb(^{t}Bu)$_2$]$^-$, which was confirmed by crystal structure determinations of **14**, **15**, **16**, **17** and **18**. The diantimonide [^{t}Bu$_3$Sb$_2$]$^-$ **B** gives rise to two singlets in the 2:1 ratio of intensities (Figure 14d). This pattern is characteristic for the [(^{t}Bu)$_2$Sb-Sb(^{t}Bu)]$^-$ configuration in a symmetric environment, as found in the crystal structure of **19**. The spectra of the monoantimonide [^{t}Bu$_2$Sb]$^-$ **C** shows the expected singlet for two equivalent ^{t}Bu

substituents, a structural pattern confirmed also by X-ray diffraction analysis on **20** (Figure 14e).

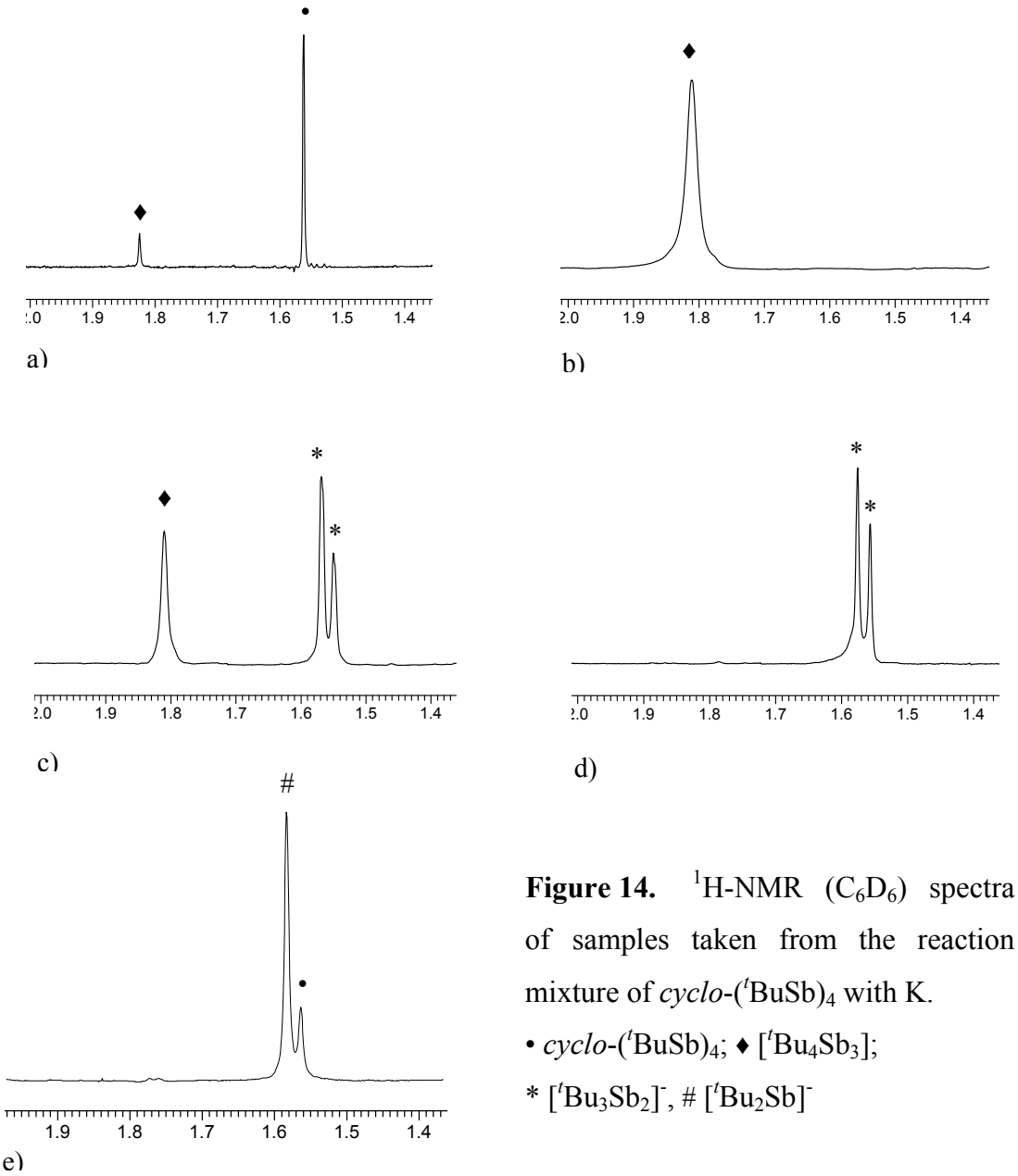

Figure 14. ^{1}H-NMR (C_6D_6) spectra of samples taken from the reaction mixture of *cyclo*-(^{t}BuSb)$_4$ with K.
• *cyclo*-(^{t}BuSb)$_4$; ♦ [^{t}Bu$_4$Sb$_3$];
* [^{t}Bu$_3$Sb$_2$]$^{-}$, # [^{t}Bu$_2$Sb]$^{-}$

Other intermediates of the reaction of *cyclo*-(^{t}BuSb)$_4$ with alkali metals were not observed spectroscopically. It is probable however that in the first step of the reduction the radical anion [^{t}Bu$_4$Sb$_4$]$^{-}$ should form. Migration of the *tert*-butyl groups and elimination of antimony can lead to [^{t}Bu$_4$Sb$_3$]$^{-}$. Precipitation of Sb was in fact

observed during the reaction. The second step, the transformation of $[^tBu_4Sb_3]^-$ to $[^tBu_3Sb_2]^-$ requires the elimination of a ^{t}BuSb unit, which, after tetramerization, should give the initial product *cyclo*-$(^t$BuSb$)_4$ and react with the alkali metals. It is remarkable that $[^tBu_3Sb_2]^-$ is not formed, when solutions of **18** in C_6D_6 are exposed to ambient temperature. Instead decomposition with formation of $^tBu_3Sb$ and *cyclo*-$(^t$BuSb$)_4$ is observed. Decomposition of the diantimonide $[^tBu_3Sb_2]^-$, after prolonged heating, leads to the monoantimonide $[^tBu_2Sb]^-$ and the starting material *cyclo*-$(^t$BuSb$)_4$, which were identified by NMR spectroscopy.

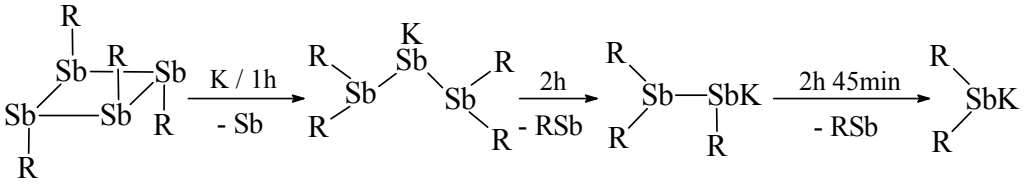

R = ^{t}Bu

Scheme 2. Reations of *cyclo*-$(^t$BuSb$)_4$ with potassium.

X-ray studies show that the triantimonide of type **A** in solid state can adopt either monomeric, polymeric or ion pair structure depending on the size of the cation (*i.e.* the coordination number of the cation) and the type and concentration of the co-ligands (Scheme 3). An excess of co-ligand will result in the separation of the antimonide from the alkali metal cation, which is suggestive for the poor bonding ability of the triantimonide of type **A**. The anion **A** is non-coordinating in **14**, whereas in the **15**, **16**, **17**, and **18** coordination to the alkali metal centers occurs.

Similar to the reaction of *cyclo*-$(^t$BuSb$)_4$ with potassium, treatment of *cyclo*-$(^t$BuSb$)_4$ in thf under reflux with excess lithium for 3 days or with excess sodium for 4 h results in the formation of red solutions containing $[^tBu_4Sb_3]^-$. The isolation of stable solids is achieved by addition of the amine ligand to the reaction mixture in molar ratios, [tmeda] : *cyclo*-$(^t$BuSb$)_4$ = 3 for **14** and **16**, [tmeda] : *cyclo*-$(^t$BuSb$)_4$ = 1.5 for **15**, [pmdeta] : *cyclo*-$(^t$BuSb$)_4$ = 1.5 for **17** and **18**, followed by cooling, filtration and removal of the solvent.

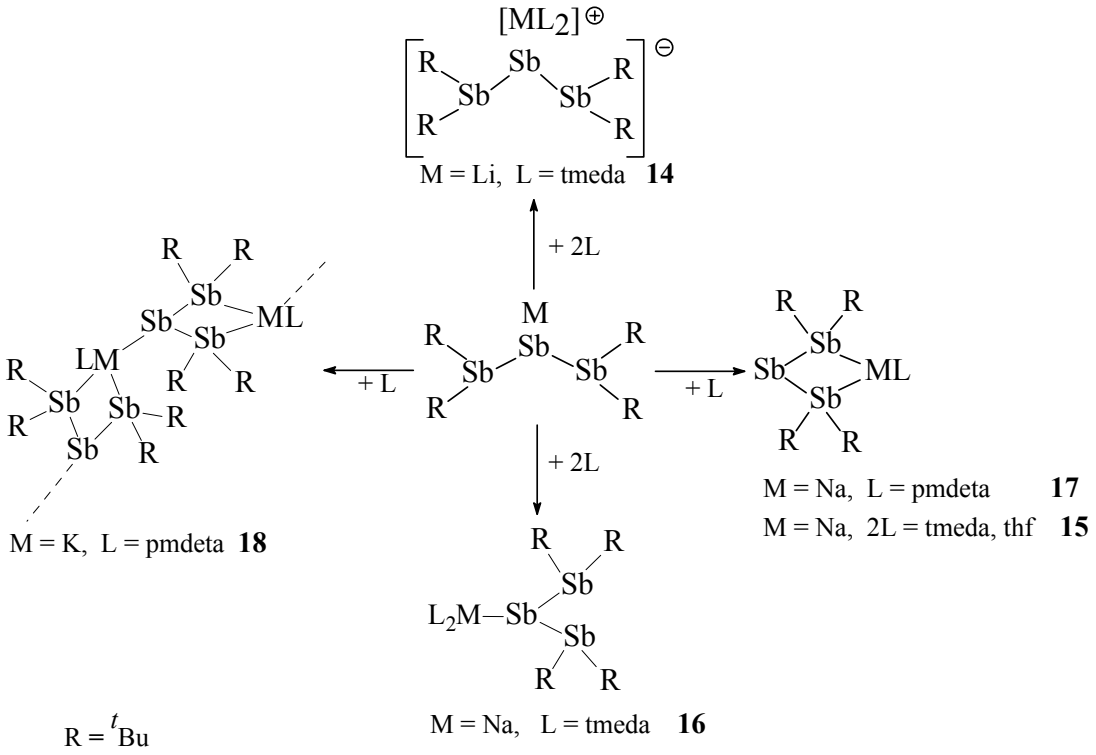

Scheme 3. Monoanions of type **A**.

In the ^{1}H-NMR spectra of C_6D_6 solutions containing **14**, **15**, **16**, **17**, or **18** the two ^{t}Bu groups bound to a terminal antimony atom were found equivalent and hence singlet signals were observed. The structures of this complexes were also confirmed by observation of the expected signals in the ^{13}C-NMR spectra.

The crystal structure determination showed that the lithium cation in **14** is coordinated by two of the bidentate amine ligands tmeda and there are no close contacts between the cation and the $[^{t}Bu_4Sb_3]^-$ ion. Closely related to **14** are the crystal structures of $[(^{t}Bu_4Sb_3)][K(pmdeta)_2]$[20] and $[(Ph_4Sb_3)][Li(12\text{-crown-4})]$[4]. The molecular structure of **14** is shown in Figure 15. The anions consist of bent Sb_3 chains with two *tert*-butyl groups bonded to each of the terminal antimony atoms. The central antimony atom is two coordinated and free of organic substituents. The mean Sb-Sb bond length in **14** is 276.9 pm. Similar values have been found for $[(^{t}Bu_4Sb_3)][K(pmdeta)_2]$ (276.50 pm[20]) and $[(Ph_4Sb_3)][Li(12\text{-crown-4})]$ (276.10

pm[4]). These distances are significantly shorter than the Sb-Sb single bond lengths in Ph_2Sb-$SbPh_2$ (283.70 pm[74]) and *cyclo*-($^tBu_4Sb_4$) (281.70 pm[75]) but longer than the Sb-Sb double bond in RSb=SbR, R = 2,4,6-$[(Me_3Si)_2CH]_3C_6H_2$ (264.20 pm[76]). The relatively short Sb-Sb bond in **14** has been related to possible (p_π-d_π) bonding[20]. The Sb-Sb-Sb bond angle in **14** is 89.36°. This is comparable with the Sb-Sb-Sb bond angle found in [($^tBu_4Sb_3$)][K(pmdeta)$_2$] (86.32°) or [(Ph_4Sb_3)][Li(12-crown-4)] (88.8°). The C-Sb-C angle in **14** (102.37°) is comparable with the value found in [($^tBu_4Sb_3$)][K(pmdeta)$_2$] (104.2°) and larger than that reported for [(Ph_4Sb_3)][Li(12-crown-4)] (92.7°). These values reflect the different sterical demand of the organic substituents bonded to antimony.

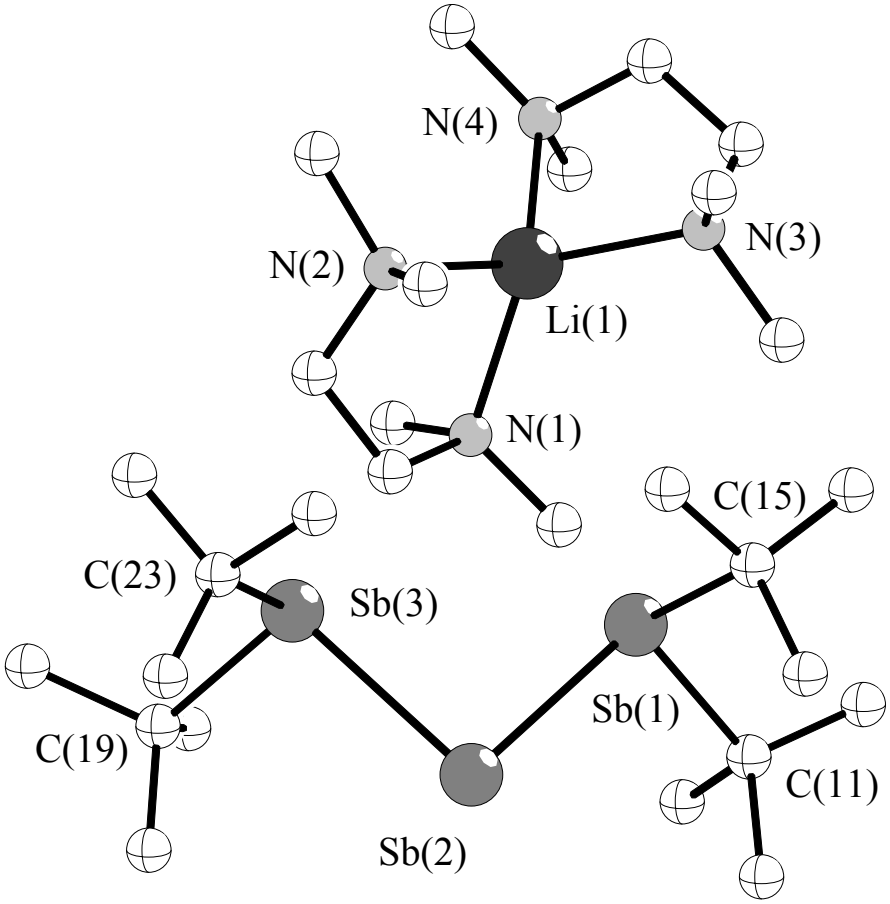

Figure 15. Structure and atom numbering scheme for **14**.

The distances between the terminal antimony atoms in **14** (389.4 pm) indicate weak bonding interactions because they are shorter than the sum of the van der Waals radii of two antimony atoms (440 pm). For the description of the conformation of $[(^t\text{Bu})_2\text{Sb-Sb-Sb}(^t\text{Bu})_2]^-$ in **14** the dihedral angles Φ (Sb-Sb-Sb-lp), where lp denotes the (assumed) direction of the lone pair of electrons at one of the terminal antimony atoms, are used.[77] For the *syn* conformation, Φ is close to 0° but close to 180° for the *anti* conformation. With $\Phi_1 = 3.46$ and $\Phi_2 = 17.25°$ as calculated from the C-Sb-Sb-Sb torsion angles given under Figure 15, the conformation of $[(^t\text{Bu})_2\text{Sb-Sb-Sb}(^t\text{Bu})_2]^-$ is close to *syn-syn.*

Single crystals of **15** and **17** were obtained by recrystallization from benzene and toluene respectively. The structures of **15** and **17** were determined by X-ray diffraction. The structures of **15** and **17** (Figure 16 and Figure 17) contain the $[(^t\text{Bu})_2\text{Sb-Sb-Sb}(^t\text{Bu})_2]^-$ ion, coordinated through the terminal antimony atoms as a bidentate chelating ligand to the sodium ion. The coordination number of sodium is completed to five by three nitrogen atoms of a tridentate pmdeta ligand in the case of **17** and two nitrogen atoms of a bidentate tmeda ligand and one oxygen atom of a thf molecule in the case of **15**.

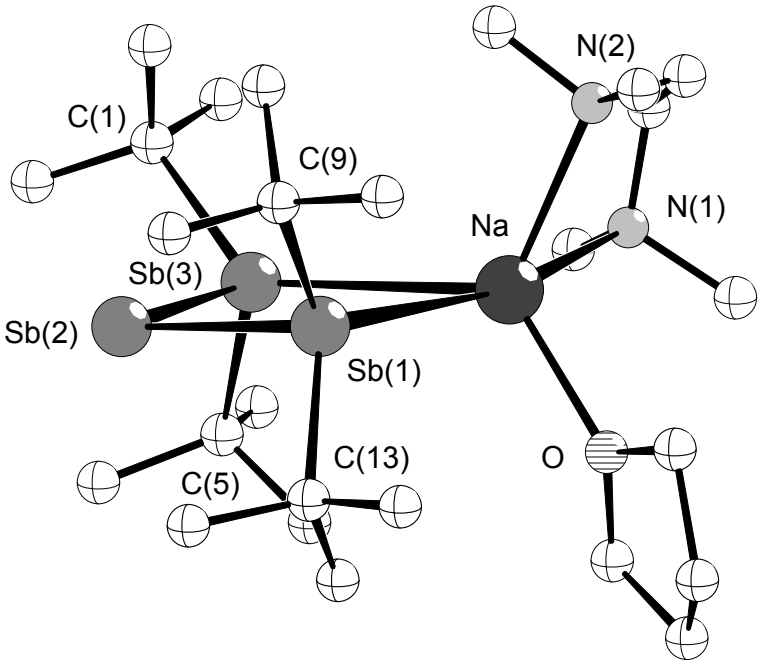

Figure 16. Structure and atom numbering scheme for **15.**

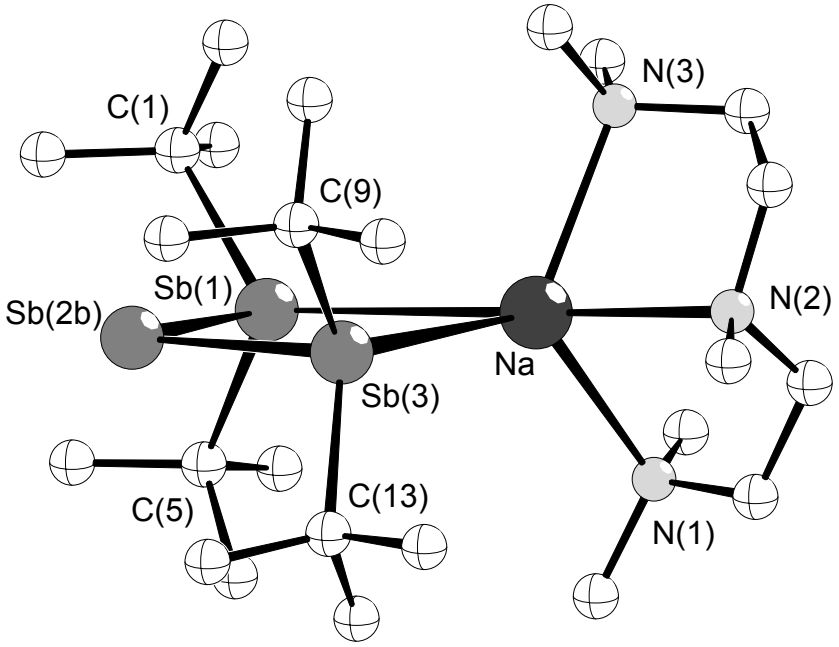

Figure 17. Structure and atom numbering scheme for **17**.

The coordination geometry around the sodium center in **15** and **17** is distorted trigonal bipyramidal with Sb(1), N(1) in axial and Sb(3), N(2), and O in equatorial positions in **15** and Sb(1) and N(2) in axial and Sb(3), N(1), and N(3) in equatorial positions in **17**. The central antimony atom of the $[(t\text{Bu})_2\text{Sb-Sb-Sb}(^t\text{Bu})_2]^-$ ion in **17** is disordered over two positions with an occupancy of 0.78 (Sb(2b)) and 0.22 (Sb(2a)), respectively. The Sb_3Na heterocycles are slightly folded; the Na-Sb-Sb/Sb-Sb-Sb dihedral angle is 175.5° in **15** and 176.1° and 171.4° in **17**. The Sb-Na bond lengths (330.40 and 322.50 pm in **17**; 324.00 and 343.00 pm in **15**) range between the sums of covalent (294.00 pm) and van der Waals radii[78] (450.00 pm) of Sb and Na, closer to the former. They compare well with the corresponding values found in $[\{(CyP)_4Sb\}Na\cdot Me_2NH\cdot tmeda]$[53] (322.90 pm) and $[Sb_7Na_3\cdot 3tmeda\cdot 3thf]$[54] (319.60 pm), which also contain coordinative bonds between antimonides and sodium cations. The coordination of the $[(^t\text{Bu})_2\text{Sb-Sb-Sb}(^t\text{Bu})_2]^-$ ion to Na^+ leads to small changes of the geometry of the ligand. This is shown by comparison with the structures of **14** and $[(^t\text{Bu}_4\text{Sb}_3)][\text{K(pmdeta)}_2]$[20], where the $[(^t\text{Bu})_2\text{Sb-Sb-Sb}(^t\text{Bu})_2]^-$ unit is not included in the coordination sphere of the cation. The Sb-Sb bond lengths

([(^{t}Bu$_4$Sb$_3$)][K(pmdeta)$_2$] 276.47 pm, **14** 276.9, **15** 275.85 and **17** 274.97 pm), the Sb-Sb-Sb bond angles ([(^{t}Bu$_4$Sb$_3$)][K(pmdeta)$_2$] 87.6°, **14** 89.36, **15** 88.37° and **17** 90.6) are similar, the SbC_2 and Sb_2C bond angles range between 101 and 105° in [(^{t}Bu$_4$Sb$_3$)][K(pmdeta)$_2$], 100 and 118° in **14**, 100 and 104° in **15**, and between 97 and 106° in **17**. In **15** and **17** the conformation is close to *syn-syn* (**15** Φ_1 = 2.12 and Φ_2 = 7.9 °; **17** Φ_1 = 11.44 and Φ_2 = 17.06°; where Φ = Sb-Sb-Sb-lp) with almost perfect orientation of the lone pairs of electrons to the Na centres. The conformations of the 'naked' anions in **14** (Φ_1 = 12 and Φ_2 = 21°) and [(^{t}Bu$_4$Sb$_3$)][K(pmdeta)$_2$] (Φ_1 = 7.23 and Φ_2 = 24.04°) are similar. As already mentioned, in **15** and **17** the [(^{t}Bu)$_2$Sb-Sb-Sb(^{t}Bu)$_2$]$^-$ ions act as chelating bidentate ligand. Other examples of this type of coordination are the complexes [Li(L)(R_4P_3)] (R = ^{t}Bu, ^{i}Pr; L = 2thf, tmeda).[79]

In **16** the triantimonide ligand is coordinated through the central antimony atom to the sodium center, which bears two molecules of the bidentate tmeda ligand as additional ligands (Figure 18).

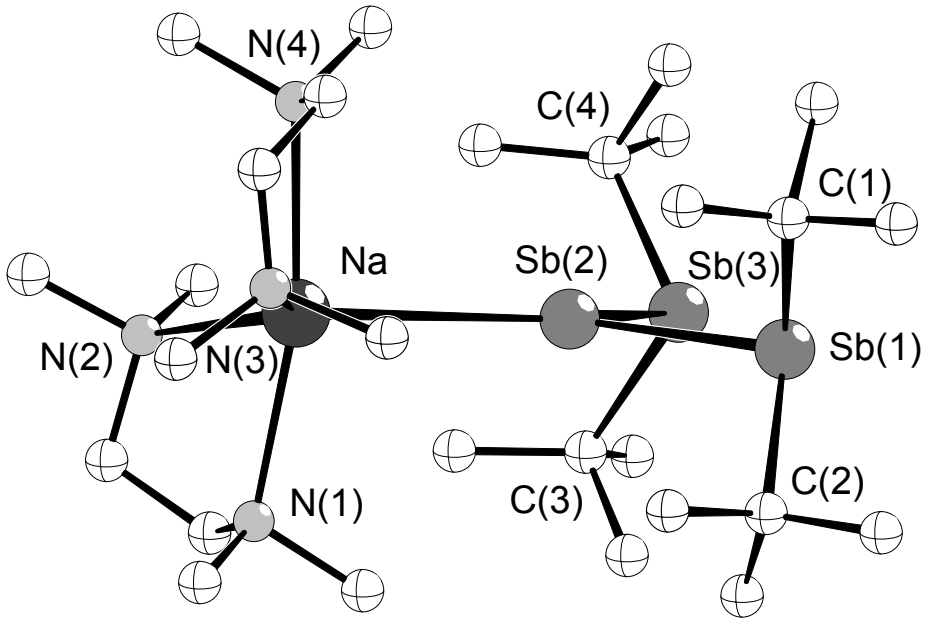

Figure 18. Structure and atom numbering scheme for **16**.

The sodium centre in **16** is distorted trigonal bipyramidal coordinated and, other than in **15** and **17**, two nitrogen atoms (N(1), N(4)) from the amine ligand are in axial and

the remaining two nitrogen atoms (N(2), N(3)) and Sb(2) in equatorial positions. The Sb-Na bond length (337.9 pm) and the Sb-Sb-Sb bond angle (86.49°) in **16** are comparable with the Sb-Na bond lengths and the Sb-Sb-Sb bond angles in **15** and **17**, where coordination through the terminal antimony atoms occurs. Also similar are the conformations of $[(^t\text{Bu})_2\text{Sb-Sb-Sb}(^t\text{Bu})_2]^-$ with $\Phi_1 = 3.52$ and $\Phi_2 = 4.01°$ in the case of **16**. An interesting feature of the structure of **16** is the close to trigonal planar coordination of the antimonido atom Sb(2) (sum of Sb_3 and Sb_2Na 359.85°). The Sb(2) atom lies 6.13 pm above the Sb(1)-Sb(3)-Na plane. The coordination of Sb(2) can be viewed as a result of an sp^2 hybridization at the Sb(2). The three hybrid orbitals are used in the bond to Sb(1), Sb(3), and Na. The remaining unhybridized p orbital contains the lone pairs of electrons and is perpendicular to the plane formed by Sb(1)-Sb(3)-Na. An alternative interpretation would be to consider no hybridization at Sb(2). In this case two of the p orbitals, each of which containing two electrons, are involved in the bond to Sb(1), Sb(3), and Na. Known compounds with an antimony atom in trigonal planar environment are the stibinidene complexes $(BrSb)[Mn(CO)_2(C_5H_4CH_3)]_2$[80], $(ClSb)[Mo(CO)_3(C_5H_5)]_2$[81], $(BrSb)[Cr(CO)_2(C_6H_6)]_2$[82]. For these compounds an *sp²* hybridization at the antimony atom was proposed.

Other compounds containing a three coordinated planar antimony atom, but with the antimony atom in a T-shaped environment, are the hypervalent 10-Sb-3[83] compounds reported by *Arduengo*.[84,85] In these compounds the lone pair of electrons is considered to possess *s*-character and the bond from antimony to the two oxygen atoms is three-centered four-electron and implies one of the *p*-orbitals of the antimony atom.

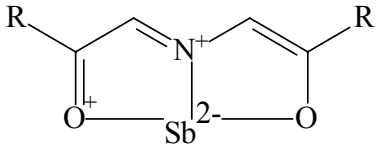

R = 1-adamantyl, *t*-Bu

In crystals of **18** the coordination of the triantimonide as a bridging tridentate ligand is realized. Not only the terminal but also the central antimony atoms are coordinated to neighbouring potassium cations and helical chains, $[K(L)\{(^t\text{Bu}_2\text{Sb})_2\text{Sb}\}]_n$ result. The C_6H_6 molecules lie between the chains. A section of this unique structure is depicted in Figure 19. The Sb_3K heterocycle is slightly folded with an Sb_3-Sb_2K dihedral angle of 160.8°. The central antimony atom is in a trigonal pyramidal

environment (sum of bond angles at Sb(2) = 338.59°). The bond lengths, bond angles and conformation of the ligand in **18** (Sb-Sb 275.94 pm, Sb(1)-Sb(2)-Sb(3) 87.59°, Φ_1 = 1.84; Φ_2 = 22.22°) are similar to the corresponding values for **15** or **17**.

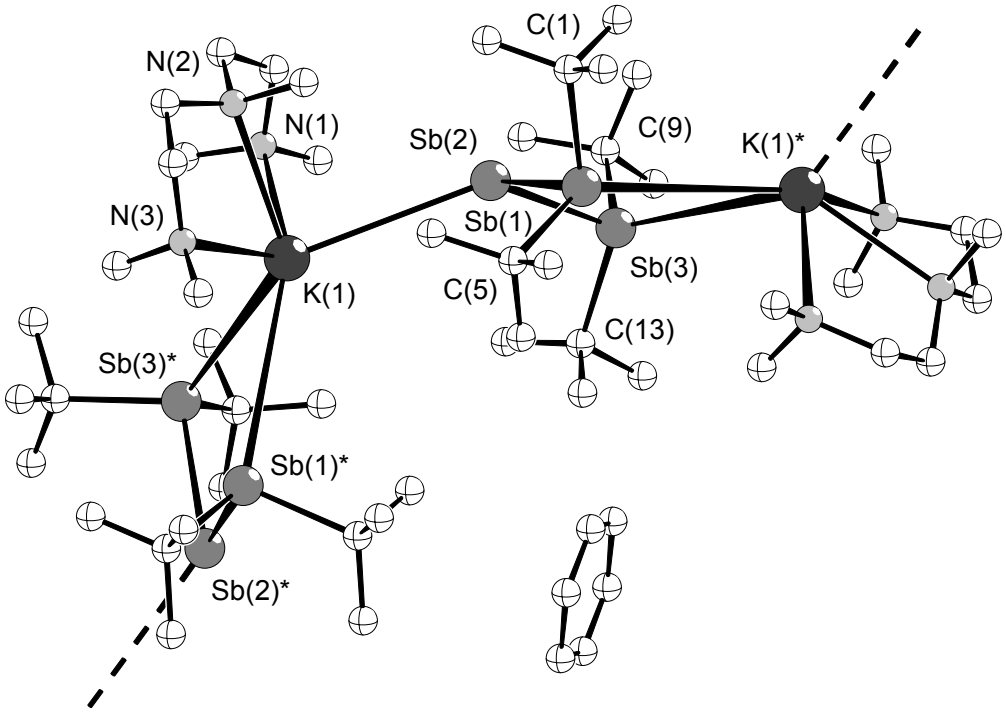

Figure 19. Structure and atom numbering scheme for **18**.

The coordination number about each potassium is completed to six by three nitrogen atoms of a pmdeta ligand. The Sb-K bond lengths in **18** (Sb(1)-K(1)* 415.70, Sb(3)-K(1)* 399.70, Sb(2)-K(1) 383.30 pm) vary in a large range. The shortest bond results from the monodentate coordination of the central antimony atom; the longer bonds represent the asymmetric bidentate coordination through the terminal atoms. All Sb-K bonds lie between the sum of the covalent (368.00 pm) and van der Waals radii (500.00 pm) for Sb and K. Shorter K-Sb bonds (348.60-361.80 pm) were found in $[K(thf)_{1/4}(\textit{cyclo}\text{-}Et_4C_4Sb)]$[86].

Table 6. Selected interatomic distances (pm) and angles (º) in **14**, **15**, **16**, **17**, **18**.

[(^{t}Bu$_4$Sb$_3$)][Li(tmeda)$_2$] (**14**)			
Sb(1)-Sb(2)	277.20	Sb(1)-Sb(2)-Sb(3)	89.54
Sb(2)-Sb(3)	276.80	C(11)-Sb(1)-Sb(2)	100.2
Sb(1)-C(11)	219.20	C(15)-Sb(1)-Sb(2)	103.1
Sb(1)-C(15)	226.10	C(11)-Sb(1)-C(15)	102.9
Sb(3)-C(19)	218.00	C(23)-Sb(3)-Sb(2)	102.8
Sb(3)-C(23)	218.00	C(19)-Sb(3)-Sb(2)	100.7
Li(1)-N(1)	212.00	C(19)-Sb(3)-C(23)	102.9
Li(1)-N(2)	211.00	N(1)-Li(1)-N(2)	87.0
Li(1)-N(3)	211.00	N(1)-Li(1)-N(4)	122.0
Li(1)-N(4)	209.00	N(1)-Li(1)-N(3)	122.3
		N(2)-Li(1)-N(3)	120.0
		N(3)-Li(1)-N(4)	89.0
[(^{t}Bu$_4$Sb$_3$)Na(tmeda)] (**15**)			
Sb(1)-Sb(2)	276.40	Na-Sb(1)-Sb(2)	98.11
Sb(2)-Sb(3)	275.30	Na-Sb(1)-C(9)	127.77
Sb(1)-Na	343.00	Na-Sb(1)-C(13)	118.53
Sb(3)-Na	324.00	Sb(1)-Sb(2)-Sb(3)	88.37
Sb(1)-C(9)	224.40	Na-Sb(3)-Sb(2)	102.96
Sb(1)-C(13)	226.10	Na-Sb(3)-C(1)	131.45
Sb(3)-C(1)	223.60	Na-Sb(3)-C(5)	109.07
Sb(3)-C(5)	222.60	N(1)-Na-Sb(1)	168.98
Na-N(1)	253.20	N(1)-Na-Sb(3)	103.35
Na-N(2)	246.0	N(1)-Na-N(2)	73.26
Na-O	228.3	N(1)-Na-O	98.80
[(^{t}Bu$_4$Sb$_3$)Na(tmeda)$_2$] (**16**)			
Sb(1)-Sb(2)	277.60	C(1)-Sb(1)-C(2)	102.45
Sb(2)-Sb(3)	276.20	C(1)-Sb(1)-Sb(2)	102.96

Sb(1)-C(1)	227.700	C(2)-Sb(1)-Sb(2)	102.76
Sb(1)-C(2)	223.20	Sb(1)-Sb(2)-Sb(3)	86.49
Sb(3)-C(4)	216.90	C(4)-Sb(3)-C(3)	103.52
Sb(3)-C(3)	225.00	C(4)-Sb(3)-Sb(2)	101.70
Sb(2)-Na	337.90	C(3)-Sb(3)-Sb(2)	100.78
Na-N(1)	250.50	Sb(1)-Sb(2)-Na	137.74
Na-N(2)	253.70	Sb(3)-Sb(2)-Na	135.62
Na-N(3)	254.00	Sb(2)-Na-N(1)	97.61
Na-N(4)	250.40	Sb(2)-Na-N(2)	117.18
		Sb(2)-Na-N(3)	114.97
		Sb(2)-Na-N(4)	93.96

[(^{t}Bu$_4$Sb$_3$)Na(pmdeta)] (**17**)

Sb(1)-Sb(2a)	272.00	Sb(2a)-Sb(1)-C	96.9 - 107.7
Sb(1)-Sb(2b)	277.60	Sb(2b)-Sb(1)-C	100.5 - 103.84
Sb(2a)-Sb(3)	274.10	Sb(2a)-Sb(3)-C	97.3 - 106.6
Sb(2b)-Sb(3)	276.20	Sb(2b)-Sb(3)-C	99.3 - 104.2
Sb(1)-Na	330.40	C(1)-Sb(1)-C(5)	102.7
Sb(3)-Na	322.50	C(9)-Sb(3)-C(13)	104.2
Sb(1)-C(1)	222.80	Sb(1)-Sb(2a)-Sb(3)	91.4
Sb(1)-C(5)	223.60	Sb(1)-Sb(2b)-Sb(3)	89.80
Sb(3)-C(9)	221.60	Na-Sb(1)-C	120.92 - 126.8
Sb(3)-C(13)	219.20	Na-Sb(3)-C	117.0(2)-128.45(18)
Na-N(1)	248.20	Sb(1)-Na-Sb(3)	73.54(4)
Na-N(2)	245.50	N-Na-N	74.97(17) – 75.79(17)
Na-N(3)	246.40	C(1)-Sb(1)-Sb(2b)-Sb(3)	132.7
		C(5)-Sb(1)-Sb(2b)-Sb(3)	121.26
Na-Sb(1)-Sb(2a)	96.44	C(9)-Sb(3)-Sb(2b)-Sb(1)	134.9
Na-Sb(1)-Sb(2b)	97.18	C(13)-Sb(3)-Sb(2b)Sb(1)	117.84

[(^{t}Bu$_4$Sb$_3$)K(pmdeta)] (**18**)			
Sb(1)-Sb(2)	276.30	K(1)-Sb(2)-Sb(3)	130.24
Sb(2)-Sb(3)	276.60	K(1)-Sb(2)-Sb(1)	120.97
Sb(1)-K(1)*	415.50	Sb(1)-Sb(2)-Sb(3)	87.60
Sb(3)-K(1)*	399.50	Sb(2)-Sb(1)-C(1)	101.6
Sb(2)-K(1)	383.30	Sb(2)-Sb(1)-C(5)	102.2
Sb(1)-C(1)	220.00	C(1)-Sb(1)-C(5)	105.0
Sb(1)-C(5)	224.70	Sb(2)-Sb(3)-C(9)	99.7
Sb(3)-C(9)	222.900	Sb(2)-Sb(3)-C(13)	103.0
Sb(3)-C(13)	225.50	C(9)-Sb(3)-C(13)	104.7
K(1)-N(1)	289.10	Sb(3)*-K(1)-Sb(2)	130.24
K(1)-N(2)	299.40	Sb(1)*-K(1)-Sb(2)	121.03
K(1)-N(3)	295.20	Sb(2)-Sb(1)-K(1)*	104.09
		Sb(2)-Sb(3)-K(1)*	108.12
C(1)-Sb(1)-K(1)*	104.03	N-K(1)-N	60.3 – 61.7
C(5)-Sb(1)-K(1)*	135.60	C(1)-Sb(1)-Sb(2)-Sb(3)	125.03
C(9)-Sb(3)-K(1)*	113.80	C(5)-Sb(1)-Sb(2)-Sb(3)	126.87
C(13)-Sb(3)-K(1)*	124.30	C(9)-Sb(3)-Sb(2)-Sb(1)	137.16
		C(13)-Sb(3)-Sb(2)-Sb(1)	114.94

The crystal structure of **19**, a diantimonide of type **B**, consists of a centrosymetric dimer in which two [(^{t}Bu)$_2$Sb-Sb(^{t}Bu)]$^-$ anions are coordinated through the antimonido atoms as bridging ligands to two potassium ions (Figure 20). The central K_2Sb_2 unit has a rhombic shape, (K(1)-Sb(2)-K(1)* 101.37, Sb(2)-K(1)-Sb(2)* 78.63°), with almost equal Sb-K bond lenghts, (K(1)-Sb(2) 356.55, K(1)-Sb(2)* 359.26 pm). The potassium ions are five-coordinate by two antimony ligands and one triamine. An unexpected aspect of the structure of **19** is the trigonal pyramidal coordination of the antimonido atoms Sb*(2) and Sb(2)* (sum of Sb_2K angles at Sb(2), respectively Sb(2)* 358.89°), which is very unusual for four-coordinate antimony atoms and contrasts with the distorted tetrahedral geometry of the arsenido atoms in [Li(thf)(^{t}Bu$_3$As$_2$)]$_2$.[87] This difference may result from steric effects.

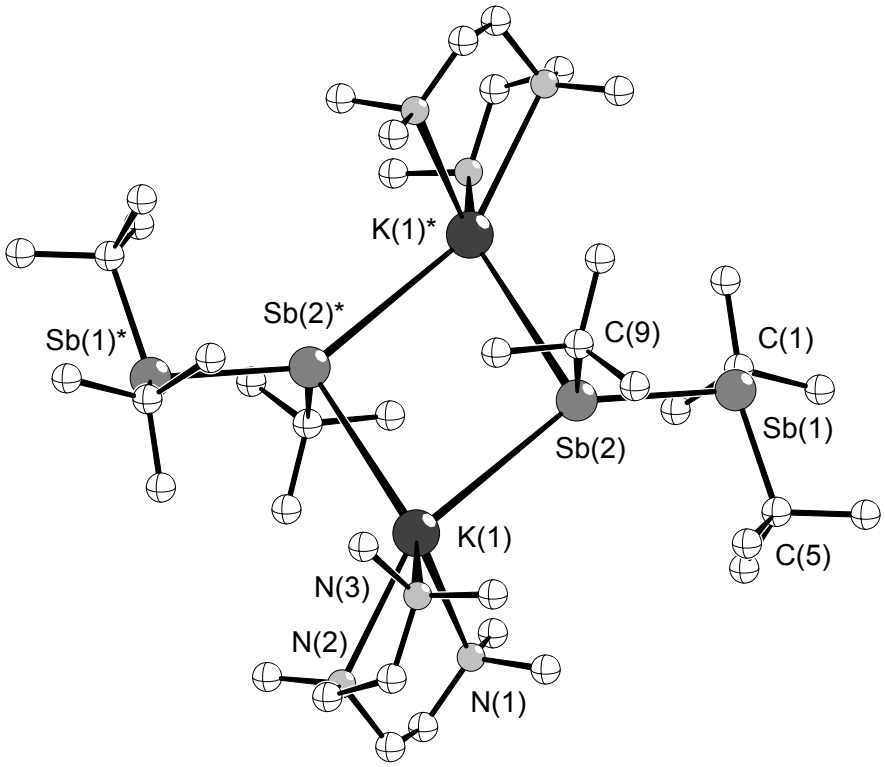

Figure 20. Structure and atom numbering scheme for **19**.

The most straightforward interpretation for the coordination geometry in **19** is to consider a sp^2 hybridization for the Sb(2), respectively Sb(2)* atoms. Two of the hybrid orbitals contain the lone pairs of electrons for the coordinative bond to the potassium ion, one is used for the Sb-Sb bond. The remaining unhybridized p orbital of Sb(2) is involved in the bond to the C(9) carbon atom of the ^{t}Bu group (C(9)-Sb(2)-Sb(1) 94.88, C(9)-Sb(2)-K(1)* 93.740, C(9)-Sb(2)-K(1) 90.02°). An alternative interpretation would be to assume no hybridization at Sb(2) and to consider a p orbital orthogonal to the Sb-Sb bond for the interaction with the K atoms.

The crystal structure analysis revealed that **20** is a polymeric compound containing zig-zag chains of alternating antimony and potassium atoms. There are no close contacts between the polymeric chains.

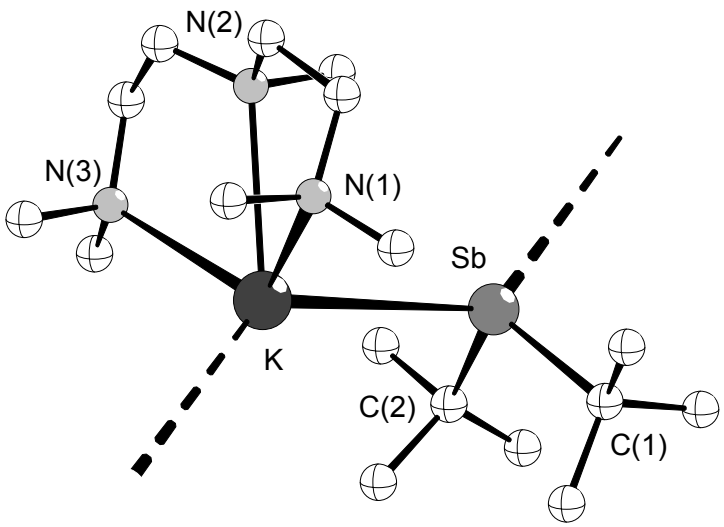

Figure 21. Structure and atom numbering scheme for **20**.

Only two other examples of diorganoantimonides with known crystal structures, $[Ph_2Sb][Li(12\text{-crown-}4)_2]\cdot{}^1/_3thf$[4] and $[\{(Me_3Si)_2SbLi\cdot DME\}_\infty]$[11] (DME = 1,2-dimethoxyethane), have been described in the literature. The crystals of $[\{(Me_3Si)_2SbLi\cdot DME\}_\infty]$ consist of polymeric chains built up by bis(trimethylsilyl)stibino groups and DME-coordinated lithium atoms in an alternating sequence. A different type of structure was found in the crystal of $[Ph_2Sb][Li(12\text{-crown-}4)_2]\cdot{}^1/_3thf$, where no close contacts between the lithium cation and the $[Ph_2Sb]^-$ ion exist. The structure of **20** is depicted in Figure 21. Selected bond lenghts and angles are given in Table 7. The coordination around the Sb atom can be best described as distorted tetrahedral with K-Sb-K 131.85, K-Sb-C 110.3 - 100.61, and C(1)-Sb-C(2) 103.51°. The Sb-K bond distance is 368.9 pm and lies in the range of Sb-K bond lenghts found in **18** and **19**.

In an approach to synthesize *catena*-stibanes with terminal $^tBu_2Sb$ groups the reaction of $[(^tBu_2Sb)_2Sb][K(pmdeta)]$ (pmdeta = pentamethyldiethylenetriamine) with MeI in thf between –80° and –30° was investigated. As a product of this reaction $^tBu_2Sb\text{-}SbMe\text{-}Sb^tBu_2$ could be identified by NMR methods, and mass spectrometry, from a mixture containing other unidentified products. $^tBu_2Sb\text{-}SbMe\text{-}Sb^tBu_2$ was also prepared by reduction of $^tBu_2SbCl$ and $MeSbCl_2$ (2:1 molar ratio) with magnesium in

tetrahydrofuran.[88] However, in this reaction the tristibane forms together with $^{t}Bu_2Sb(SbMe)_2Sb^{t}Bu_2$ as an inseparable mixture.

Table 7. Selected interatomic distances (pm) and angles (º) in **19**, **20**.

[($^{t}Bu_3Sb_2$)K(pmdeta)] (**19**)			
Sb(1)-Sb(2)	276.13	K(1)-Sb(2)-K(1)*	101.37
K(1)-Sb(2)	356.55	Sb(1)-Sb(2)-K(1)	113.85
K(1)-Sb(2)*	359.26	Sb(1)-Sb(2)-K(1)*	143.669
Sb(1)-C(1)	221.90	Sb(1)-Sb(2)-C(9)	94.88
Sb(1)-C(5)	223.40	C(9)-Sb(2)-K(1)*	93.70
K(1)-N(1)	282.80	C(9)-Sb(2)-K(1)	90.02
K(1)-N(2)	287.50	Sb(2)-Sb(1)-C(1)	100.11
K(1)-N(3)	285.90	Sb(2)-Sb(1)-C(5)	104.17
		C(1)-Sb(1)-C(5)	102.77
		Sb(2)-K(1)-Sb(2)*	78.63
[($^{t}Bu_2Sb$)K(pmdeta)] (**20**)			
K-Sb	368.90	K-Sb-C(1)	110.3
Sb-C(1)	225.20	K-Sb-C(2)	100.61
Sb-C(2)	223.70	K-Sb-K*	131.85
K-N(1)	287.50	C(1)-Sb-K*	105.67
K-N(2)	292.50	C(1)-Sb-C(2)	103.51
K-N(3)	295.50	C(2)Sb-K*	100.95

5. 2-(3',5'-Dimethylphenyl)-5,7-dimethylstibindolyl potassium·pmdeta

5.1. Introduction

Alkali-metal complexes of cyclic hydrocarbons with delocalised π systems have been studied frequently because they are important as reagents for organometallic syntheses and their special bonding situation is remarkable. Among heterocylic analogues with heavier pnicogen (Pn) atoms the complexes with anionic phospholyl and the phosphindolyl ligands (type I, P_n = P; M = Li,[89] Na,[90] K,[89-91] Rb,[92] Cs,[92] and type II, Pn = P; M = Li,[93] K,[94]) have received attention. With arsenic or antimony only two derivatives of type I containing the arsolyl, respectively stibolyl anion (Pn = As, M = Li;[95] Pn = Sb, M = K[86]) were described. Complexes with stibindolyl anions (type II, Pn = Sb) are not known, but neutral aryl or alkyl stibindoles have been described.[96-98]

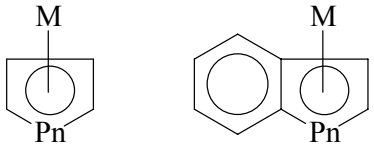

I II

type I: Pn = P; M = Li, Na, K, Rb, Cs

Pn = As; M = Li

Pn = Sb; M = K

type II: Pn = P; M = Li, K

5.2. Synthesis and characterization of 2-(3',5'-dimethylphenyl)-5,7-dimethylstibindolyl potassium·pmdeta

The synthesis of 2-(3',5'-dimethylphenyl)-5,7-dimethylstibindolyl potassium·pmdeta (**21**) is achieved in an one pot reaction of trimesitylantimony with potassium and pmdeta in tetrahydrofuran. After recrystallisation from tetrahydrofuran/toluene (1/3) **21** is obtained in 62 % yield. **21** is a deep red solid which is soluble in tetrahydrofuran

but not in hexane, petroleum ether, benzene or other organic solvents. In air it is self igniting and also very sensitive to traces of water, but stable in an inert atmosphere up to 176 °C.

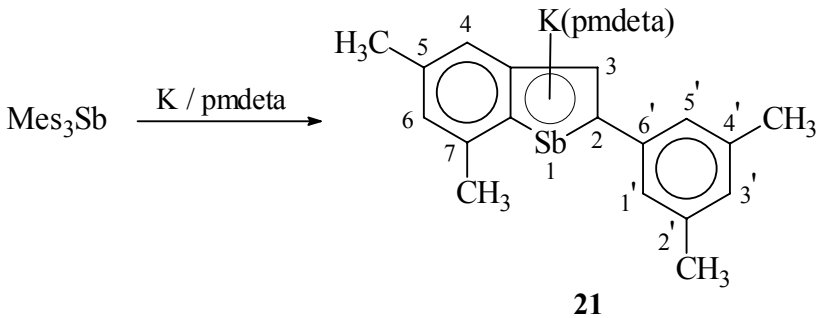

21

The mechanism of the remarkably specific formation of **21** is not known. By analogy with the reaction of trimesitylantimony with lithium giving mesityl lithium and lithium dimesitylantimonide[3] we propose the formation of MesK and Mes_2SbK in the first step. The following steps probably include the migration of a Sb-C bond, removal and shifting of hydrogen atoms and C-C coupling.

It is noteworthy that the carbon framework in the stibindolyl anion corresponds to two mesityl moieties.

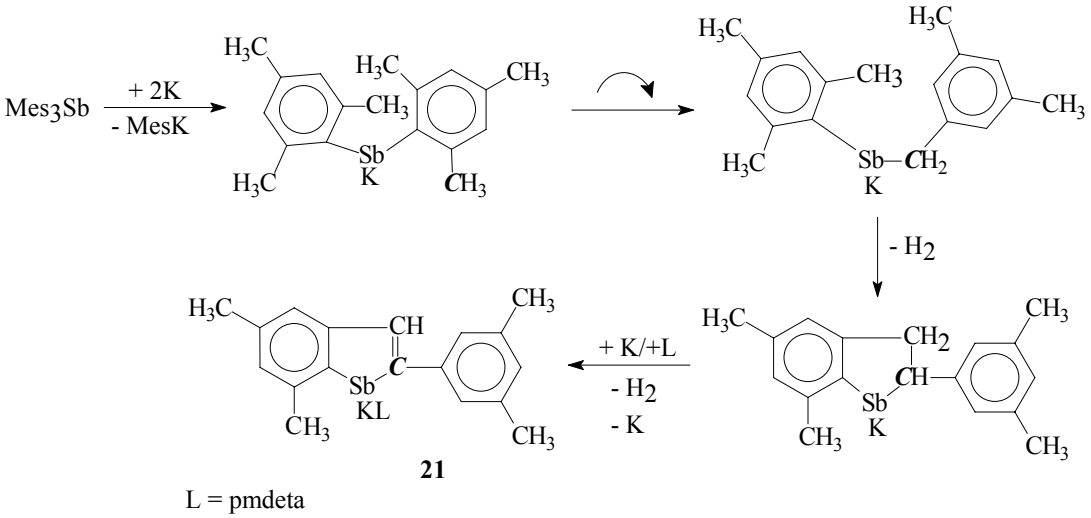

Scheme 4. Proposed mechanism for the formation of **21**.

The characterisation of **21** was achieved by X-ray diffractometry on single crystals obtained from thf/benzene and by NMR spectroscopy. The structure consists of stacks built of dimethyl(dimethylphenyl) stibindolyl anions and (pmdeta)K^+ cations in bridging positions between each other. The repeating unit (Figure 22) contains two pairs of anions and cations which are crystallographically independent but have very similar geometries.

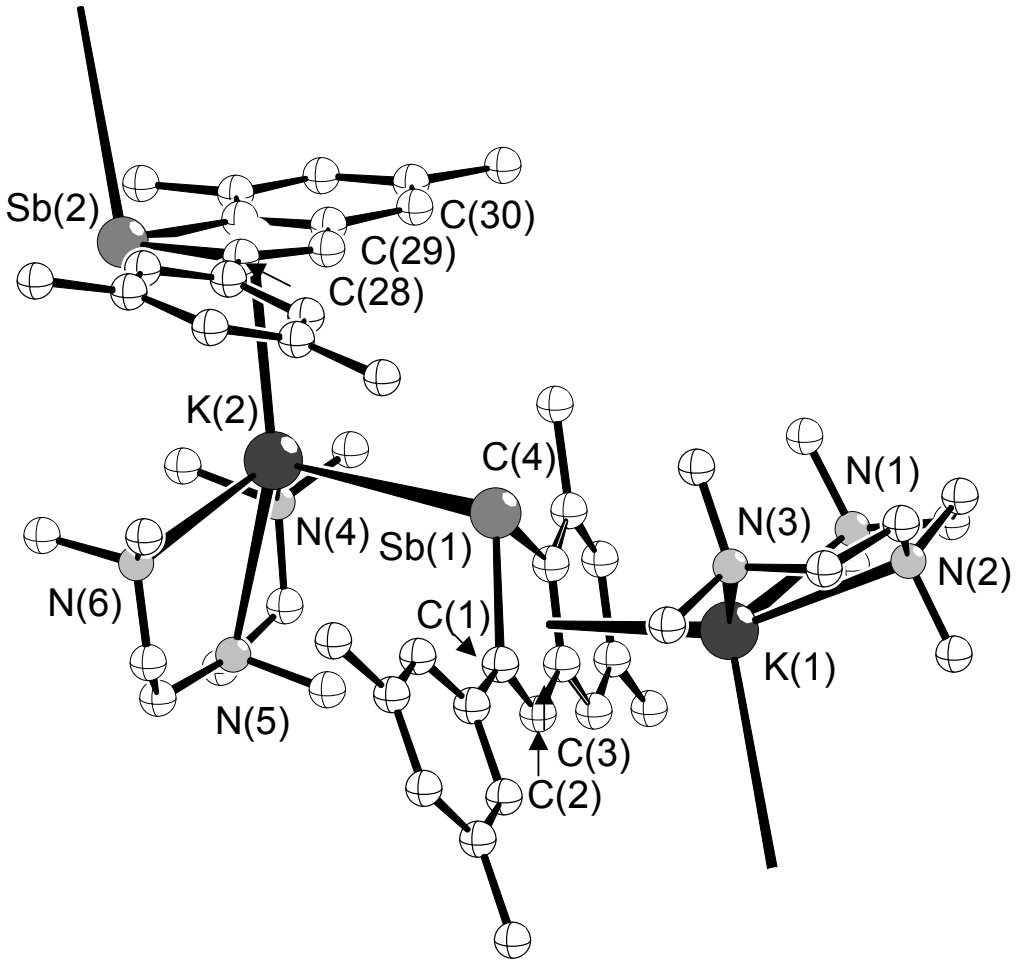

Figure 22. Structure and atom numbering scheme for **21**.

An important structural feature of the stibindolyl anions is the perfect planarity of the condensed C_4Sb and C_6 rings, which corresponds to considerable delocalisation in the 10 π electron system where also one of the lone pairs of antimony is involved. Only

between the rings there is subtle bending along the common C-C bond (dihedral angle 3°). Rotation of the dimethyl phenyl ring, which is not involved in the 10 π system, leads to a dihedral angle between the C_6- and the C_4Sb-planes of 16.8°. The Sb-C distances (212.10 – 212.80 pm) in **21** are almost equal. They lie between the values for single and double bonds (cf.: Sb-C : Mes_3Sb (218.10 – 218.50 pm),[99] Sb=C: RC(O)Sb=C(OH)R (R = $^tBu_3C_6H_2$) (207.8 pm)[100] and compare well with the Sb-C bond lengths (208.50 – 211.50 pm) in tetraethylstibolyl-potassium·0.25 thf.[86] Also the SbC_2 angles in **21** (80.6, 80.5°) are similar to the analogous values found in the stibolide (81.1(3)°).[86] The C-C bond lengths in the stibindolyl ligand of **21** are not equal, they vary in the SbC_4 ring between 139.00 and 144.30 pm. The cations feature the tridentate coordination of the pmedta ligands to the potassium centers where the K centers lie 127.00 and 130.00 pm above the N_3 planes. In the repeating unit (Figure 22) two different types of interactions between the cations and the anions can be distinguished. The position of K(1) above the C_4Sb ring of the stibindolyl anion containing Sb(1) or of K(2) relative to the anion containing Sb(2) corresponds to η^5-coordination with K-Sb distances of 368.7 and 368.8 pm and K-C distances ranging between 316.80 and 368.80 pm. The distances between the K(1) or K(2) atoms and the centers (Z) of the $C_4Sb(1)$ or $C_4Sb(2)$ rings are both 311.0 pm. The η^5 coordination is slightly acentric with shorter distances between K and the peripheral carbon atoms C(2), C(3) or C(28), C(29). The angles between the Z-K vector and the C_4Sb plane are 79.3 and 79.6 °. Another type of interaction exists between K(2) and the stibindolyl ion containing Sb(1). Here the geometric parameters (Sb(1)-K(2) 375.5 pm; K-C distances > 400 pm) correspond rather to an η^1 coordination through the p-orbital of the antimony atom of the stibindolyl ion than to η^5 interactions. Most likely repulsive steric interactions between the pmedta ligands and between neighboring stibindolyl anions, which are almost perpendicular relative to each other, are responsible for the pronounced bending and the alternation of the type of coordination in the stacks. A sterically less congested situation exists in the structure of the type I compound tetraethylstibolid·(0.25thf)[86] where alternating cations and almost parallel anions with exclusive η^5-coordination form a polydecker type

structure which is much closer to linearity. In fact the modest bending in the stibolid structure is mainly related to Sb-K contacts between neighboring stacks. In the structure of **21** there are no short contacts between the stacks.

Table 8. Selected interatomic distance (pm) and angles (°) in **21**.

2-(3',5'-dimethylphenyl)-5,7-dimethylstibindolyl potassium·pmdeta (**21**)			
Sb(1)-K(2)	375.50	K(2)-C(30)	341.70
K(1)-Sb(1)	368.70	K(2)-C(31)	362.20
K(1)-C(1)	320.00	K(2)-Z(2)	311.30
K(1)-C(2)	316.80	Sb(2)-C(28)	212.80
K(1)-C(3)	341.40	Sb(2)-C(31)	212.00
K(1)-C(4)	361.90	C(28)-C(29)	136.70
K(1)-Z(1)	311.00	C(29)-C(30)	143.80
Sb(1)-C(1)	212.10	C(30)-C(31)	140.30
Sb(1)-C(4)	212.80	K-N	283.30 – 288.90
C(1)-C(2)	139.40		
C(2)-C(3)	144.30	C(1)-Sb(1)-C(4)	80.60
C(3)-C(4)	139.00	C(28)-Sb(2)-C(31)	80.53
Sb(2)-K(1)	374.30	Z(1)-Sb(1)-K(2)	98.99
K(2)-Sb(2)	368.70	K(2)-Z(2)-Sb(2)	93.72
K(2)-C(28)	320.90	Z(2)-K(2)-Sb(1)	105.79
K(2)-C(29)	316.80	Z(1)-K(1)-Sb(2)*	105.44

Solutions of **21** contain only one type of stibindolyl groups. ^{1}H- and ^{13}C-NMR spectra in thf-d_8 show one set of all the expected signals for the CH groups of the stibindolyl moiety. Signals for the methyl groups are partially overlapping with the methyl signals of the pmdeta ligand. Characteristic for the stibindolyl anion is the low-field shift of the signals due to the protons from the 10 π system (7.30 – 7.99 ppm), compared with the chemical shift of the aromatic protons from the starting material, Mes_3Sb (6.72 ppm).

6. Experimental Section

6.1. General Comments

All the reactions and manipulations were performed under dry, oxygen free argon atmosphere, using a vacuum line and standard Schlenk techniques. The glass equipment was heated under vacuum ($1x10^{-3}$ mbar) and filled with argon. The solvents were refluxed under an argon atmosphere with the appropriate drying agent[101-103] and freshly distilled prior to their use. As drying agent potassium (tetrahydrofuran), sodium chunks (toluene), sodium wire/benzophenone (diethyl ether) were used. Tetrahydrofuran and diethyl ether were initially stored over potassium hydroxide.

NMR spectra were run on a Bruker DPX 200 spectrometer. Chemical shifts are reported in δ units (ppm) referenced to TMS. The signals are indicated using the usual abbreviations: s (singlet), d (doublet), dd (doublet of doublets), t (triplet), m (multiplet), br (broad). As internal standard C_6D_5H with δ = 7.15 ppm in the ^1H - and C_6D_6 with δ = 128.00 ppm in the ^{13}C-spectra or $C_6D_5CD_2H$ with δ = 2.09 ppm in the ^1H - and $C_6D_5CD_3$ with δ = 20.4 ppm in the ^{13}C-spectra were used. The programs 1D - and 2D - WinNMR were used for the handling of the NMR Spectra.[104] The C, H correlation was performed by use of HSQC spectra, and to define the assignment of the signals to the same or to different organic groups. Mass spectra were recorded on Finnigan MAT CH7 (A) and Finnigan MAT 822 spectrometers. The pattern of antimony containing ions was compared with theoretical values. For this the program MASPEC was used.[105]

For the IR spectra a Perkin Elmer FT-IR SPECTRUM 1000 instrument was used. The samples were measured as solutions in diethyl ether and the absorption spectra of the respective pure solvent was subtracted from the spectrum of the sample. The intensity of the bands is indicated in the usual way: br (broad), vs (very strong), s (strong), sh (shoulder), m (mean).

The starting materials $[2,4,6\text{-}(CH_3)_3C_6H_2]_2SbH$,[3] $[2\text{-}(Me_2NCH_2)C_6H_4][(Me_3Si)_2CH]SbH$,[47] $[2\text{-}(Me_2NCH_2)C_6H_4]SbCl_2$,[106]

$(C_6H_5)_2SbCl$,[107] $C_6H_5SbCl_2$,[107] $[2,4,6\text{-}(CH_3)_3C_6H_2]SbCl_2$,[108] *cyclo*-$(^tBuSb)_4$,[109] $(Me_3Si)_2CHSbH_2$,[34] $^tBu_2SbCl$,[39] $^tBuSbCl_2$,[109] were prepared according to the reported procedures.

The data for X-ray structure analysis were collected on a Siemens P4 four-circle or a Stoe IPDS diffractometer using graphite-monochromated Mo Kα radiation (λ = 71.073 pm). For this propose the crystals were attached with Kel-F oil to a glass fibre and cooled in a nitrogen stream to 173 K. The structures were solved, after Lp correction, by direct methods. All non-hydrogen atoms were refined with anisotropic thermal parameters. The hydrogen atoms were refined with a riding model and a mutual isotropic thermal parameter. For structure solving and refinement the software package SHELX-93 or SHELX-97[110,111] was used. The drawings were created with the Diamond program by Crystal Impact GbR.[112] Crystallographic data for the structural analysis of some of the crystal structures (mgh 8, mgh 10i, mgh 11, mgh 9, mgh 7i and mgh14i,) have been deposited with the respective Cambridge Crystallographic Data Centre CCDC number (appendix). Copies of the information may be obtained free of charge from The Director, CCDC, 12 Union Road, Cambridge CB2 1EZ, UK (fax: +44-1223-336-033; Email: deposit@ccdc.cam.ac.uk or www:http//www.ccdc.cam.ac.uk).

6.2. Primary and secondary stibanes

Phenylstibane $(C_6H_5)SbH_2$ (1)

A solution of $(C_6H_5)SbCl_2$ (2.00 g, 7.40 mmol) in Et_2O (30 mL) was added dropwise

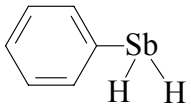

to a cold (–80 °C) suspension of $LiAlH_4$ (0.61 g, 16.05 mmol) in Et_2O (20 mL). The mixture was warmed to –20 °C and filtered through a cooled (–20 °C) frit covered with kieselguhr. Removal of the solvent under reduced pressure at –20 °C gave 1.38 g (93 %; lit. yield 42,[32] 70,[35] 96[36] %) of $(C_6H_5)SbH_2$ as a white solid unstable at room temperature (m.p. –35 °C; dec. –5 - 0 °C).

^{1}H-NMR (200 MHz, C_6D_6): 3.70 (s, 2H, SbH_2), 7.04 – 6.89 (m, 3H, C_6H_3 – *m* +*p*), 7.49 – 7.42 (m, 2H, C_6H_2 - *o*).

^{13}C-NMR (50 MHz, C_6D_6): 128.24 (s, C_6H_5), 129.01 (s, C_6H_5), 138.30 (s, C_6H_5), 139.47 (s, C_6H_5).

IR (Et_2O): $\nu_{(Sb\text{-}H)}$ 1791 cm^{-1} br.

2,4,6-Trimethylphenylstibane $[2,4,6\text{-}(CH_3)_3C_6H_2]SbH_2$ (2)

A solution of $[2,4,6\text{-}(CH_3)_3C_6H_2]SbCl_2$ (2.00 g, 6.43 mmol) in Et_2O (30 mL) was

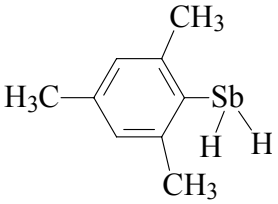

added dropwise to a cold (–80 °C) suspension of $LiAlH_4$ (0.52 g, 13.89 mmol) in Et_2O (20 mL). The mixture was warmed to –10 °C and filtered through a cooled (–10 °C) frit covered with kieselguhr. Removal of the solvent under reduced pressure at –10 °C gave 1.42 g (92 %) of $[2,4,6\text{-}(CH_3)_3C_6H_2]SbH_2$ as a white solid unstable at room temperature (m.p. -18 °C; dec. 15-18 °C). Suitable crystals for X–ray diffraction studies were grown by cooling a Et_2O solution of $MesSbH_2$ at –28 °C.

^{1}H-NMR (200 MHz, C_6D_6): 2.10 (s, 3H, C*H*$_3$ - *p*), 2.23 (s, 6H, C*H*$_3$ - *o*), 3.11 (s, 2H, Sb*H*$_2$), 6.75 (s, 2H, C$_6$*H*$_2$ - *m*).

^{13}C-NMR (50 MHz, C_6D_6): 20.88 (s, *C*H$_3$ - *p*), 27.90 (s, *C*H$_3$ - *o*), 128.07 (s, *C*$_6$H$_2$), 128.29 (s, *C*$_6$H$_2$), 137.84 (s, *C*$_6$H$_2$), 144.11 (s, *C*$_6$H$_2$).

IR (Et_2O): $\nu_{(Sb\text{-}H)}$ 1863 cm^{-1} br.

MS (EI, 70 eV) m/z (%): 242 (43) [M$^+$], 119 (100) [Mes$^+$], 105 (86) [Mes$^+$ - CH$_3$], 91 (40) [Mes$^+$ - 2CH$_3$] Mes = 2,4,6-(CH$_3$)$_3$C$_6$H$_2$.

HRMS (EI, 70 eV): 242.00528 (calcd 242.00555 amu, $C_9H_{13}Sb^{121}$).

2-(Dimethylaminomethyl)phenylstibane [2-(Me$_2$NCH$_2$)C$_6$H$_4$]SbH$_2$ (3)

A solution of 1.00 g (3.05 mmol) of [2-(Me$_2$NCH$_2$)C$_6$H$_4$]SbCl$_2$ in Et_2O (30 mL) was added dropwise to a cold (-80 °C) suspension of $LiAlH_4$ (0.25 g, 6.57 mmol) in Et_2O (20 mL). The mixture was warmed to -30 °C and filtered through a cooled (–30 °C) D4 frit covered with kieselguhr. Removal of the solvent under reduced pressure gave 0.68 g (87 %) of [2-(Me$_2$NCH$_2$)C$_6$H$_4$]SbH$_2$ as a white powder, unstable at room temperature (m.p. –23 °C; dec. 11-14 °C).

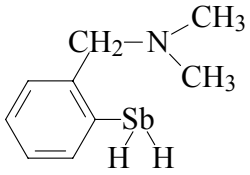

^{1}H-NMR (200 MHz, C_6D_6): 1.98 (s, 6H, N(C*H*$_3$)$_2$), 3.18 (s, 2H, C*H*$_2$N), 4.43 (s, 2H, Sb*H*$_2$), 6.86 (d, 1H, C$_6$*H*$_4$, $^3J_{HH}$ = 7.2 Hz), 7.19 – 7.32 (m, 2H, C$_6$*H*$_4$), 8.03 (d, 1H, C$_6$*H*$_4$, $^3J_{HH}$ = 6.7 Hz).

^{13}C-NMR (50 MHz, C_6D_6): 45.14 (s, N(*C*H$_3$)$_2$), 65.46 (s, *C*H$_2$N), 124.27 (s, *C*$_6$H$_4$), 126.79 (s, *C*$_6$H$_4$), 128.30 (s, *C*$_6$H$_4$), 138.56 (s, *C*$_6$H$_4$),145.25 (s, *C*$_6$H$_4$).

IR (Et_2O): $\nu_{(Sb\text{-}H)}$ 1806 cm^{-1} br.

MS (EI, 70 eV) m/z (%): 255 (65) [RSb$^+$], 179 (28) [Me$_2$NCH$_2$Sb]$^+$, 134 (40) [R$^+$], 58 (100) [Me$_2$NCH$_2^+$] R = Me$_2$NCH$_2$C$_6$H$_4$.

Diphenylstibane $(C_6H_5)_2SbH$ (4)

A solution of $(C_6H_5)_2SbCl$ (2.00 g, 6.42 mmol) in Et_2O (30 mL) was added dropwise

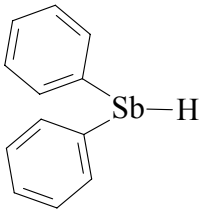

to a cold (–80 °C) suspension of $LiAlH_4$ (0.26 g, 6.84 mmol) in Et_2O (20 mL). The mixture was warmed to 0 °C and filtered through a cooled (0 °C) frit covered with kieselguhr. Removal of the solvent under reduced pressure at 0 °C gave 1.62 g (92 %; lit.[5] yield 50 %) of $(C_6H_5)_2SbH$ as a white solid unstable at room temperature (m.p. –5; dec. 20 °C).

^{1}H-NMR (200 MHz, C_6D_6): 5.70 (s, H, Sb*H*), 7.01 - 7.06 (m, 3H, C_6H_5 – *m* + *p*), 7.44 – 7.53 (m, 2H, C_6H_5 - *o*).

^{13}C-NMR (50 MHz, C_6D_6): 129.24 (s, C_6H_5), 134.01 (s, C_6H_5), 136.68 (s, C_6H_5), 138.15 (s, C_6H_5).

IR (Et_2O): $\nu_{(Sb\text{-}H)}$ 1819 cm^{-1} br.

Tetra-*tert*-butyl distibane $(^tBu_2Sb)_2$ (5)

A solution of 3.60 g (13.26 mmol) of $^tBu_2SbCl$ in Et_2O (70 mL) was added dropwise

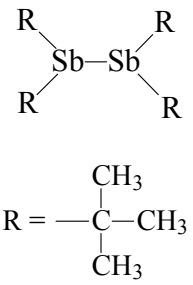

to a cold (-80 °C) suspension of $LiAlH_4$ (0.55 g, 14.47 mmol) in Et_2O (30 mL). The mixture was warmed to –50 °C, stirred for 2 h at this temperature and 1 h at –30 °C. The solution was then filtered through a cooled (-30 °C) frit covered with kieselguhr. Removal of the solvent under reduced pressure (20 mbar) gave 2.60 g (83 %) of $(^tBu_2Sb)_2$ as a yellow solid, decomposing above 7 °C. Attempts were made to grow single crystals from thf or Et_2O solution but only amorphous solids were obtained.

^{1}H-NMR (200 MHz, C_6D_6): 1.36 (s, 36H, C*H*$_3$).

^{13}C-NMR (50 MHz, C_6D_6): 22.27 (s, *C*Me$_3$), 23.85 (s, *C*H$_3$).

MS (CI_{neg}, NH_3) m/z (%): 658 (25) [$^tBu_3Sb_4^-$], 415 (30) [$^tBu_3Sb_2^-$], 359 (100) [$^tBu_2Sb_2^-$].

6.3. Mononuclear alkali organoantimonides

Lithium diphenylantimonide $[(C_6H_5)_2SbLi\cdot(thf)_3]$ (6)

A solution of $(C_6H_5)_2SbH$ (3.00 g, 10.83 mmol) in thf (50 mL) was treated dropwise with *n*-BuLi (6.76 mL, 1.6 M in hexane) at –70 °C. The red solution was warmed to –10 °C with stirring. Reducing the volume of the solution in *vacuo* to 20 mL and cooling overnight at –28 °C gave 4.20 g (78 %) red crystals of $[(C_6H_5)_2SbLi\cdot(thf)_3]$ (dec. 29 °C).

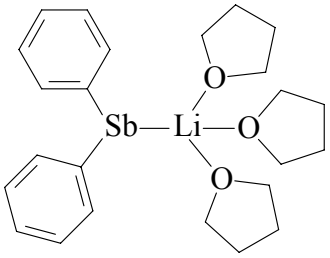

^{1}H-NMR (200 MHz, C_6D_6): 1.39 (12H, thf), 3.56 (12H, thf), 7.03 – 7.09 (m, 6H, C_6H_5 – *m* + *p*), 7.41 – 7.46 (m, 4H, C_6H_5 - *o*).

Lithium 2,4,6-trimethylphenylantimonide $[(2,4,6\text{-}(CH_3)_3C_6H_2)_2SbLi\cdot(thf)_3]$ (7)

A solution of $[2,4,6\text{-}(CH_3)_3C_6H_2]_2SbH$ (3.00 g, 8.31 mmol) in thf (50 mL) was treated dropwise with *n*-BuLi (5.19 mL, 1.6 M in hexane) at –70 °C. The red solution was warmed to –10 °C with stirring. Reducing the volume of the solution in *vacuo* to 20 mL and cooling overnight at –28 °C gave 2.97g (61 %) orange crystals of $[(2,4,6\text{-}(CH_3)_3C_6H_2)_2SbLi\cdot(thf)_3]$ (dec. 36 °C).

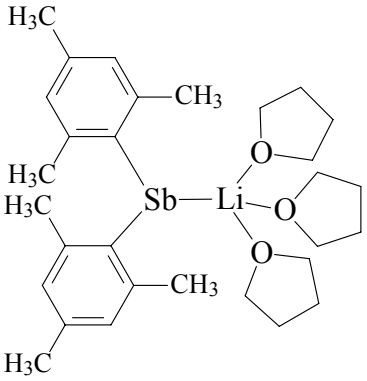

^{1}H-NMR (200 MHz, C_6D_6): 1.32 (12H, thf), 2.30 (s, 6H, CH_3 – *p*), 2.73 (s, 12H, CH_3 – *o*), 3.45 (12H, thf), 6.97 (s, 4H, C_6H_2 – *m*).

Potassium di *tert*-butylantimonide·pmdeta [(^{t}Bu$_2$Sb)K(pmdeta)] (20)

To a solution of *cyclo*-(^{t}BuSb)$_4$ (1.00 g, 1.4 mmol) in 40 mL thf, 0.30 g (7.7 mmol) small pieces of K were added and stirred with reflux for 2½ h. To the refluxing solution 0.88 mL (4.2 mmol) pmdeta were added, the red-brown solution was cooled with stirring to r. t. and filtered through a frit covered with kieselguhr. Removal of the solvent under reduced pressure gave 0.17 g (15 %) of [(^{t}Bu$_2$Sb)K(pmdeta)] as a red-brown solid (dec.113 - 117 °C). Suitable crystals for X-ray analysis were grown by cooling thf solutions of [(^{t}Bu$_2$Sb)K(pmdeta)] at -28 °C.

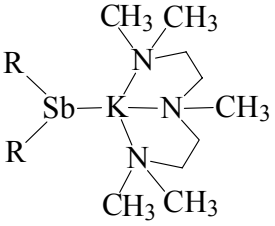

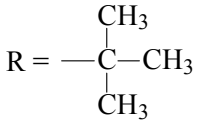

^{1}H-NMR (200 MHz, C_6D_6): 1.58 (s, 18H, C(CH_3)$_3$), 2.08 (s, 12H, N(CH_3)$_2$), 2.12 (s, 3H, NCH_3), 2.23 - 2.41 (m, 8H, CH_2).

^{13}C-NMR (50 MHz, C_6D_6): 29.59 (s, *C*(CH$_3$)$_3$), 31.93 (s, C(*C*H$_3$)$_3$), 42.96 (s, N*C*H$_3$), 45.98 (s, N(*C*H$_3$)$_2$), 56.85 (s, *C*H$_2$), 58.22 (s, *C*H$_2$).

Lithium[2-(dimethylaminomethyl)phenyl]-[bis(trimethylsilyl)methyl] antimonide [2-(Me$_2$NCH$_2$)C$_6$H$_4$][(Me$_3$Si)$_2$CH]SbLi·2thf (8)

A solution of [2-(Me$_2$NCH$_2$)C$_6$H$_4$][(Me$_3$Si)$_2$CH]SbH (1.80 g, 4.42 mmol) in thf (40 mL) was treated dropwise with 2.7 mL *n*-BuLi (15 % in hexane) at -80 °C. The reaction mixture was warmed to –30 °C with stirring and the color became red. Filtration through a cooled (-30 °C) frit covered with kieselguhr, reducing the volume in *vacuo* for 50 % and cooling for 12 h at -28 °C gave 1.50 g (62 %) red crystals of [2-(Me$_2$NCH$_2$)C$_6$H$_4$]-[(Me$_3$Si)$_2$CH]SbLi·2thf (dec. 48 - 52 °C).

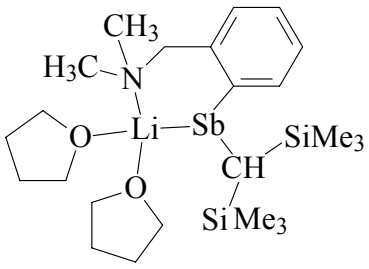

^{1}H-NMR (200 MHz, C_6D_6): -0.38 (s, 1H, C*H*), 0.04 (s, 18H, SiCH_3), 1.19 (m, 8H, thf), 2.07 (s, 6H, NCH_3), AB spin system with A: 3.22, B: 3.35 (2H, CH_2,

$^2J_{HH}$ = 11.6 Hz), 3.56 (m, 8H, thf), 7.33 – 6.74 (m, 3H, C_6H_4), 7.84 – 7.63 (m, 1H, C_6H_4).

Sodium[2-(dimethylaminomethyl)phenyl]-[bis(trimethylsilyl)methyl] antimonide [2-(Me_2NCH_2)C_6H_4][($Me_3Si)_2$CH]SbNa·tmeda (9)

A solution of 1.00 g (1.76 mmol) [2-(Me_2NCH_2)C_6H_4][($Me_3Si)_2$CH]SbLi·2thf in 30 mL Et_2O was added at –50 °C to a slurry of 0.18 g (1.87 mmol) NaO^{t}Bu in 10 mL Et_2O. The reaction mixture was warmed with stirring to 10 °C and then filtered at -30 °C through a frit covered with kieselguhr. Addition of 0.25 mL (1.72 mmol) tmeda and stirring at –30 °C for 1 h followed by reduction of the volume to 10 mL gave 0.43 g (44 %) [2-(Me_2NCH_2)C_6H_4][($Me_3Si)_2$CH]SbNa·tmeda as orange crystals (dec. 65-70 °C).

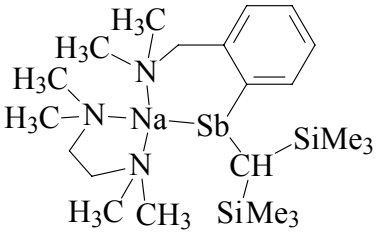

^{1}H-NMR (200 MHz, C_6D_6, 20 °C): 0.08 (s, 1H, C*H*), 0.60 (s, 18H, SiCH_3, $^2J_{SiH}$ = 6.2 Hz), 1.76 (s, 12H, tmeda), 1.80 (s, 4H, tmeda), 1.93 (s, 6H, NCH_3), 3.42 (s, br, 2H, CH_2), 6.67 – 6.97 (m, 3H, C_6H_4), 8.00 (dd, 1H, C_6H_4, $^3J_{HH}$ = 7.6 Hz, $^4J_{HH}$ = 1.2 Hz).

^{1}H-NMR (200 MHz, $C_6D_5CD_3$, 20 °C): 0.21 (s, 1H, C*H*), 0.52 (s, 18H, SiCH_3, $^2J_{SiH}$ = 6.2 Hz), 1.77 (s, 12H, tmeda), 1.82 (s, 4H, tmeda), 1.99 (s, 6H, NCH_3), 3.37 (s, br, 2H, CH_2), 6.63 – 7.16 (m, 3H, C_6H_4), 7.91 (d, 1H, C_6H_4, $^3J_{HH}$ = 7.4 Hz).

^{1}H-NMR (200 MHz, $C_6D_5CD_3$, -85 °C): 0.38 (s, 1H, C*H*), 0.70 (s, br, 9H, SiCH_3), 0.77 (s, br, 9H, SiCH_3), 1.69 – 1.93 (m, 22H, tmeda + NCH_3), 3.52 (s, br, 2H, CH_2), 6.75 – 8.02 (m, 4H, C_6H_4).

Potassium[2-(dimethylaminomethyl)phenyl]-[bis(trimethylsilyl)methyl] antimonide [2-(Me_2NCH_2)C_6H_4][($Me_3Si)_2$CH]SbK·pmdeta (10)

[2-(Me_2NCH_2)C_6H_4][($Me_3Si)_2$CH]SbH (2.00 g, 4.80 mmol) in thf (40 mL) was added to 0.20 g K (5.12 mmol) in 30 mL liquid ammonia, resulting in the formation of a red solution. After addition of pmdeta (1.10 mL, 5.27 mmol) the reaction mixture was allowed to warm to room temperature and the ammonia was evaporated. Removal of the solvent at reduced pressure gave [2-(Me_2NCH_2)C_6H_4][($Me_3Si)_2$CH]SbK·pmdeta as a red powder, which was washed with *n*-hexane. (yield: 2.10 g, 70 %).

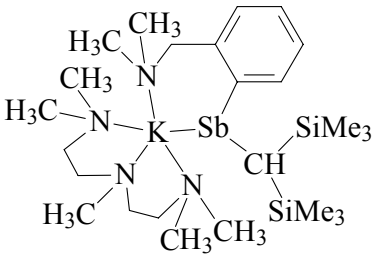

^{1}H-NMR (200 MHz, C_6D_6): -0.38 (s, 1H, C*H*), 0.04 (s, 18H, SiCH_3), 2.07 (s, 6H, NCH_3), 2.10 (s, 12H, NCH_3), 2.14 (s, 3H, NCH_3), 2.27 – 2.45 (m, 8H, CH_2), 3.24 (s, br, 2H, CH_2), 7.36 – 7.05 (m, 3H, C_6H_4), 8.12 – 7.91 (m, 1H, C_6H_4).

6.4. Dinuclear alkali organoantimonides

Potassium tri *tert*-butyldiantimonide·pmdeta [(^{t}Bu$_3$Sb$_2$)K(pmdeta)] (19)

To a solution of *cyclo*-(^{t}BuSb)$_4$ (1.00 g, 1.40 mmol) in 40 mL thf 0.30 g (7.70 mmol) small pieces of K were added and stirred with reflux for 2 h. After addition of 0.88 mL (4.2 mmol) pmdeta and further stirrring for 1 h at room temperature the reaction mixture was filtered and the solution concentrated to 15 mL. Cooling at 7 °C for 1 day gives 0.46 g (53 %) of [(^{t}Bu$_3$Sb$_2$)K(pmdeta)] as orange crystals (dec. 80 - 90 °C).

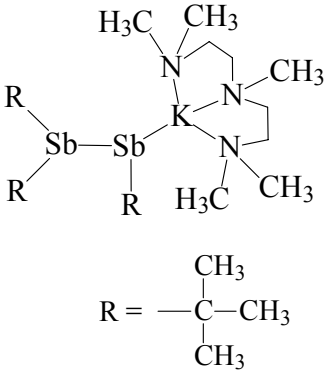

^{1}H-NMR (200 MHz, C_6D_6): 1.55 (s, 18H, C(CH_3)$_3$), 1.57 (s, 9H, C(CH_3)$_3$), 2.11 (s, 12H, N(CH_3)$_2$), 2.17 (s, 3H, NCH_3), 2.34 - 2.46 (m, 8H, CH_2).

^{13}C-NMR (50 MHz, C_6D_6): 30.52 (s, *C*(CH$_3$)$_3$), 31.03(s, *C*(CH$_3$)$_3$), 34.99 (s, C(*C*H$_3$)$_3$), 35.61 (s, C(*C*H$_3$)$_3$), 43.26 (s, N*C*H$_3$), 46.12 (s, N(*C*H$_3$)$_2$), 57.05 (s, *C*H$_2$), 58.45 (s, *C*H$_2$).

MS (CI_{neg}, NH_3): 415 (100) [^{t}Bu$_3$Sb$_2$]$^-$.

6.5. Trinuclear alkali organoantimonides

Lithium tetra *tert*-butyltriantimonide·tmeda [(^{t}Bu$_4$Sb$_3$)][Li(tmeda)$_2$] (14)

To a solution of *cyclo*-(^{t}BuSb)$_4$ (1.00 g, 1.40 mmol) in 40 mL thf 0.97 g (138.6 mmol) Li wires (Φ = 0.6 mm) were added and stirred with reflux for 3 days. After addition of 0.61 mL (4.13 mmol) tmeda and further stirring for 1 h at room temperature, the reaction mixture was filtered through a frit covered with kieselguhr. Cooling at – 28 °C gives 0.20 g (17 %) of [(^{t}Bu$_4$Sb$_3$)Li(tmeda)$_2$] as red crystals (67 – 71 °C dec.).

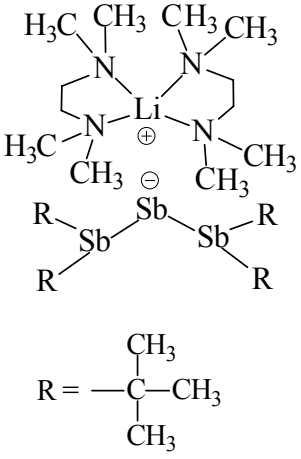

^{1}H-NMR (200 MHz, C_6D_6): 1.83 (s, 36H, C(CH_3)$_3$), 2.08 (s, 24H, N(CH_3)$_2$), 2.20 (s, 8H, CH_2).

^{13}C-NMR (50 MHz, C_6D_6): 32.56 (s, *C*(CH$_3$)$_3$), 35.42 (s, C(*C*H$_3$)$_3$), 48.31 (s, N(*C*H$_3$)$_2$), 59.27 (s, *C*H$_2$).

Sodium tetra *tert*-butyltriantimonide·tmeda [(^{t}Bu$_4$Sb$_3$)Na(tmeda)] (15)

1.00 g (1.4 mmol) *cyclo*-(^{t}BuSb)$_4$ was reacted for 4 h with small pieces of Na (0.4 g, 17.4 mmol) in 40 mL thf. Afterwards 0.30 mL (2.06 mmol) tmeda were added and stirred for 1 h until r.t.. After filtration and removal of the solvent under reduced

pressure 0.82 g of red solid (78 - 84 °C dec.) was obtained. After recrystallization from toluene at -28 °C 0.60 g (54 %) of [(^{t}Bu$_4$Sb$_3$)Na(tmeda)] formed as red crystals.

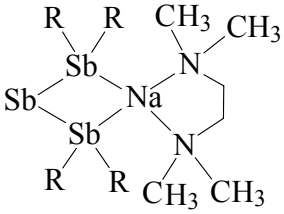

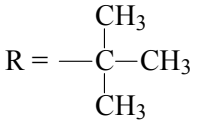

^{1}H-NMR (200 MHz, C_6D_6): 1.77 (s, 36H, C(CH_3)$_3$), 1.95 (s, 4H, CH_2), 2.02 (s, 12H, NCH_3).

^{13}C-NMR (50 MHz, C_6D_6): 25.75 (s, thf), 30.42 (s, *C*(CH$_3$)$_3$), 34.89 (s, C(*C*H$_3$)$_3$), 46.05 (s, N(*C*H$_3$)$_2$), 57.77 (s, *C*H$_2$), 67.80 (s, thf).

Sodium tetra *tert*-butyltriantimonide·2tmeda [(^{t}Bu$_4$Sb$_3$)Na(tmeda)$_2$] (16)

1.00 g (1.40 mmol) *cyclo*-(^{t}BuSb)$_4$ was reacted for 4 h with 0.40 g (17.40 mmol) small pieces of Na in 40 mL thf. Afterwards 0.62 mL (4.13 mmol) tmeda were added and stirred for 1 h until r.t.. After filtration and removal of the solvent under reduced pressure 0.76 g of the red solid was obtained. After recrystallization from toluene at -28 °C 0.55 g (47 %) of [(^{t}Bu$_4$Sb$_3$)Na(tmeda)$_2$] formed as red crystals. (81 - 85 °C dec.)

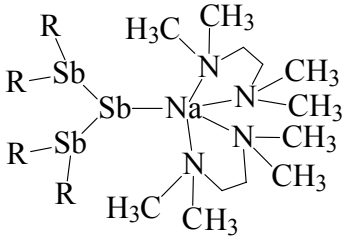

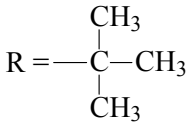

^{1}H-NMR (200 MHz, C_6D_6): 1.57 (s, 36H, C(CH_3)$_3$), 2.03 (s, 24H, NCH_3), 2.06 (s, 8H, CH_2).

^{13}C-NMR (50 MHz, C_6D_6): 34.21 (s, *C*(CH$_3$)$_3$), 38.07 (s, C(*C*H$_3$)$_3$), 49.15 (s, N(*C*H$_3$)$_2$), 61.32 (s, *C*H$_2$).

Sodium tetra *tert*-butyltriantimonide·pmdeta [(^{t}Bu$_4$Sb$_3$)Na(pmdeta)] (17)

1.00 g (1.40 mmol) *cyclo*-(^{t}BuSb)$_4$ were reacted for 4 h with 0.4 g (17.40 mmol) small pieces of Na in 40 mL thf. Afterwards 0.43 mL (2.08 mmol) pmdeta were added and stirred for 1 h until room temperature. After filtration and removal of the solvent under reduced pressure 0.80 g of a red solid was obtained. After

recrystallization from benzene at 7 °C 0.64 g (58 %) of [(^{t}Bu$_4$Sb$_3$)Na(pmdeta)] formed as red crystals. (82 – 88 °C dec.)

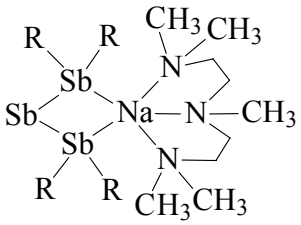

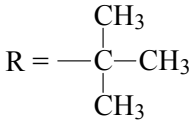

^{1}H-NMR (200 MHz, C_6D_6): 1.77 (s, 36H, C(C*H*$_3$)$_3$), 2.07 (s, 12H, N(C*H*$_3$)$_2$), 2.10 (s, 3H, NC*H*$_3$), 2.15 - 2.21 (m, 8H, C*H*$_2$).

^{13}C-NMR (50 MHz, C_6D_6): 30.42 (s, *C*(CH$_3$)$_3$), 34.88 (s, C(*C*H$_3$)$_3$), 43.14 (s, N*C*H$_3$), 46.02 (s, N(*C*H$_3$)$_2$), 56.94 (s, *C*H$_2$), 58.35 (s, *C*H$_2$).

Potassium tetra *tert*-butyltriantimonide·pmdeta [(^{t}Bu$_4$Sb$_3$)K(pmdeta)] (18)

To a solution of *cyclo*-(^{t}BuSb)$_4$ (1.00 g, 1.40 mmol) in 40 mL thf small pieces of K (0.30 g, 7.7 mmol) were added and stirred with reflux for 1 h. To the refluxing solution 0.43 mL (2.1 mmol) pmdeta were added and the red-brown solution further stirred until room temperature, than filtered through a frit covered with kieselguhr. Removal of the solvent under reduced pressure gave 0.76 g (68 %) of [(^{t}Bu$_4$Sb$_3$)K(pmdeta)] as a red-brown solid (90 - 110 °C dec.). Crystals of [(^{t}Bu$_4$Sb$_3$)K(pmdeta)]·0.5C$_6$H$_6$ suitable for X-ray analysis were grown by cooling solutions of [(^{t}Bu$_4$Sb$_3$)K(pmdeta)] in benzene at 7 °C for 1 day.

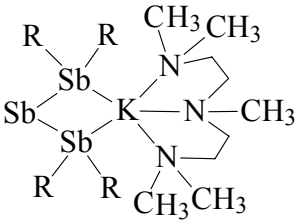

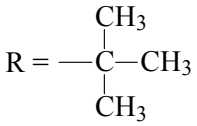

^{1}H-NMR (200 MHz, C_6D_6): 1.81 (s, 36H, C(C*H*$_3$)$_3$), 2.10 (s, 12H, N(C*H*$_3$)$_2$), 2.14 (s, 3H, NC*H*$_3$), 2.26 - 2.34 (m, 8H, C*H*$_2$).

^{13}C-NMR (50 MHz, C_6D_6): 24.80 (s, *C*(CH$_3$)$_3$), 34.89 (s, C(*C*H$_3$)$_3$), 43.61 (s, N*C*H$_3$), 45.73 (s, N(*C*H$_3$)$_2$), 56.40 (s, *C*H$_2$), 57.83 (s, *C*H$_2$).

6.6. Stibindolyl anion

2-(3',5'-Dimethylphenyl)-5,7-dimethylstibindolyl potassium-pmdeta (21)

Addition of potassium pieces (0.32 g, 8.20 mmol) to a solution of Mes_3Sb (1.00 g, 2.08 mmol) in 20 mL thf and stirring at room temperature for 1 h results in a colour change to dark red. The remaining potassium pieces are removed by filtration and pmdeta (0.80 mL, 4.17 mmol) is added to the reaction mixture. After 1 h of stirring and removal of the solvent at reduced pressure a red powder remains which is washed twice with *n*-hexane; recrystallisation from tetrahydrofuran:toluene (3:1) gives 0.73 g (1.28 mmol, 62 %) of 2-(3',5'-dimethylphenyl)-5,7-dimethylstibindolyl potassium-pmdeta as a red powder. M. p. 176 °C (dec.).

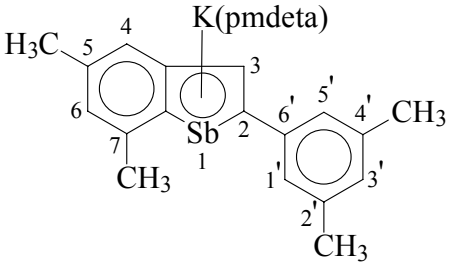

^{1}H-NMR (200 MHz, C_4D_8O): 2.14 (12H, s, NCH_3), 2.18 (3H, s, NCH_3), 2.22 (6H, s, CH_3 – C3' and C5'), 2.26 –2.45 (14H, m, CH_3 - C4, CH_3 - C6 and NCH_2), 6.64 (1H, s, C_6H_3 - C4'), 6.74 (2H, s, C_6H_3 – C2' and C6'), 7.30 (1H, s, C*H* - C4 or C6), 7.32 (1H, C*H* - C6 or C4), 7.99 (1H, s, C*H* - C3).

^{13}C-NMR (50 MHz, C_4D_8O): 13.88 (s, *C*H_3), 22.97 (s, *C*H_3), 31.98 (s, *C*H_3), 42.71 (s, N(*C*H_3)$_2$), 45.65 (s, N*C*H_3), 56.85 (s, N*C*H_2), 58.28 (s, N*C*H_2), 117.69 (s, C*H*), 123.95 (s, *C*H), 124.34 (s, *C*H), 124.78 (s, *C*H), 125.96 (s, *C*H), 127.00 (s, *C*H), 128.54 (s, *C*H), 136.68 (s, *C*H), 137.49 (s, *C*H), 141.74 (s, *C*H), 148.26 (s, *C*H), 149.07 (s, *C*H).

6.7. Zintl compounds containing the Sb_7^{3-} anion

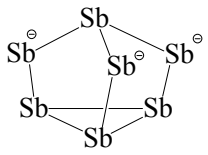

Tris(pmdeta-lithium) hepta-antimonide [Sb_7Li_3·(tmeda)$_3$] (11)

a) A solution of $(C_6H_5)SbH_2$ (2.00 g, 9.95 mmol) in thf (30 mL) was cooled to –70 °C and *n*-BuLi (12.44 mL, 1.6 M in hexanes) was added *via* syringe. The solution was allowed to warm to 0 °C with stirring. At this temperature tmeda (2.96 mL) in 10 mL toluene was added dropwise and the mixture stirred for 1 h. Cooling to –28 °C afforded 1.21 g (65 %) red crystals of [Sb_7Li_3(tmeda)$_3$]. Dec. 149-152 °C. The identity of the compound was proven by XRD (XRD = X-ray diffractometry).

b) The reaction of [2,4,6-$(CH_3)_3C_6H_2$]SbH_2 (2.00 g, 8.23 mmol) with *n*-BuLi (10.29 mL, 1.6 M in hexanes) and tmeda (2.45 mL) in thf (30 mL) and the workup procedures were performed in a manner analogous to the reaction of $PhSbH_2$ with *n*-BuLi. 0.87 g (58 %) of [Sb_7Li_3(tmeda)$_3$] were obtained as red crystals.

c) The reaction of [2-$(Me_2NCH_2)C_6H_4$]SbH_2 (1.00 g, 3.87 mmol) with *n*-BuLi (4.74 mL, 1.6 M in hexanes) and tmeda (1.14 mL) in thf (20 mL) and the workup procedures were performed in a manner analogous to the reaction of $PhSbH_2$ with *n*-BuLi. 0.41 g (57 %) of [Sb_7Li_3(tmeda)$_3$] were obtained as red crystals.

d) The reaction of $(Me_3Si)_2CHSbH_2$ (1.50 g, 5.3 mmol) with *n*-BuLi (6.55 mL, 1.6 M in hexanes) and tmeda (1.57 mL) in thf (20 mL) and the workup procedures were performed in a manner analogous to the reaction of $PhSbH_2$ with *n*-BuLi. 0.52 g (53 %) of [Sb_7Li_3(tmeda)$_3$] were obtained as red crystals.

Tris(pmdeta-sodium) hepta-antimonide [Sb_7Na_3·$(pmdeta)_3$] (12)

$(C_6H_5)SbH_2$ (2.00 g, 9.95 mmol) in 30 mL thf was added to 0.22 g Na (9.56 mmol) in 20 mL liquid ammonia resulting in the formation of a red solution. After addition of pmdeta (2.07 mL, 9.94 mmol) in 10 mL toluene, the reaction mixture was allowed to warm to room temperature and the ammonia evaporated. Storage of the solution at – 28 °C gave 1.14 g (56 %) of $[Sb_7Na_3(pmdeta)_3]$ as red crystals. The identity of the compound was proven by XRD.

Tris(pmdeta-potassium) hepta-antimonide [Sb_7K_3·$(pmdeta)_3$] (13)

$(C_6H_5)SbH_2$ (2.00 g, 9.95 mmol) in 30 mL thf was added to 0.38 g K (9.74 mmol) in 20 mL liquid ammonia resulting in the formation of a red solution. After addition of pmdeta (2.07 mL, 9.94 mmol) in 10 mL toluene, the reaction mixture was allowed to warm to room temperature and the ammonia evaporated. Storage of the solution at – 28 °C gave 1.30 g (58 %) of $[Sb_7K_3(pmdeta)_3]$ as red crystals. The identity of the compound was proven by XRD.

7. Summary

The primary arylstibanes $(C_6H_5)SbH_2$, $[2,4,6\text{-}(CH_3)_3C_6H_2]SbH_2$ and $[2\text{-}(Me_2NCH_2)C_6H_4]SbH_2$ were prepared in high yields by the reaction of the corresponding arylantimony dichlorides, $RSbCl_2$ with $LiAlH_4$. A low temperature X-ray crystal structure analysis revealed that crystals of $[2,4,6\text{-}(CH_3)_3C_6H_2]SbH_2$ consist of discrete molecules. This is the second primary stibane to be crystallographically characterized. The only primary stibane with known crystal structure, {2,6-[2,4,6-triisopropylphenyl]$_2C_6H_3$}SbH_2, was reported by *Power*. Other than dimesitylstibane, $[2,4,6\text{-}(CH_3)_3C_6H_2]_2SbH$, which was isolated in the group of *Cowley* as an air stable solid, monomesityltibane, $[2,4,6\text{-}(CH_3)_3C_6H_2]SbH_2$ exists only as an extremely air sensitive liquid at room temperature.

Reactions of the secondary arylstibanes $(C_6H_5)_2SbH$ and $[2,4,6\text{-}(CH_3)_3C_6H_2]_2SbH$ with one equivalent ^{n}BuLi in thf gave the solvated lithium antimonides $[(C_6H_5)_2SbLi\cdot(thf)_3]$ and $[(2,4,6\text{-}(CH_3)_3C_6H_2)_2SbLi\cdot(thf)_3]$, respectively. Both compounds were characterized by X-ray diffraction studies. Their crystals consist of discrete molecules with the antimony atoms in trigonal-pyramidal environments.

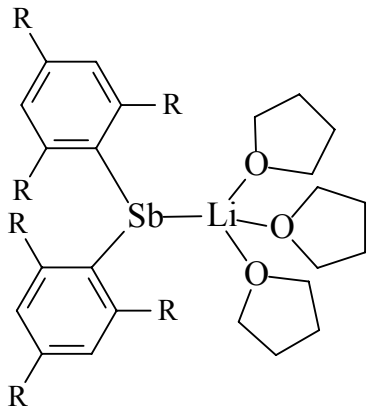

The chiral lithium alkylarylantimonide $[2\text{-}(Me_2NCH_2)C_6H_4][(Me_3Si)_2CH]\text{-}SbLi\cdot 2thf$ forms by metalation of $[2\text{-}(Me_2NCH_2)C_6H_4][(Me_3Si)_2CH]SbH$ with *n*-BuLi.

Treatment of [2-$(Me_2NCH_2)C_6H_4$][$(Me_3Si)_2CH$]SbH with K in liquid ammonia followed by addition of pentamethyldiethylenetriamine gives [2-$(Me_2NCH_2)C_6H_4$][$(Me_3Si)_2CH$]SbK·pmdeta. Transmetalation of [2-$(Me_2NCH_2)C_6H_4$][$(Me_3Si)_2CH$]SbLi·2thf with sodium *tert*-butoxide in the presence of tetramethylethylenetriamine leads to [2-$(Me_2NCH_2)C_6H_4$][$(Me_3Si)_2CH$]SbNa·tmeda. The crystal structures of [2-$(Me_2NCH_2)C_6H_4$][$(Me_3Si)_2CH$]-SbLi·2thf and [2-$(Me_2NCH_2)C_6H_4$][$(Me_3Si)_2CH$]SbNa·tmeda have been determined. These are the first asymmetrically substituted mononuclear alkali diorganoantimonides to be structurally characterized. Both compounds crystallize as racemates and their molecular structures revealed the formation of six-membered C_3SbMN (M = Li, Na) rings in which the amino antimonide ligand functions as a chelating bidentate donor through the antimony and nitrogen atoms.

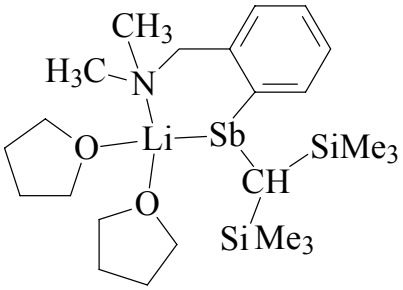

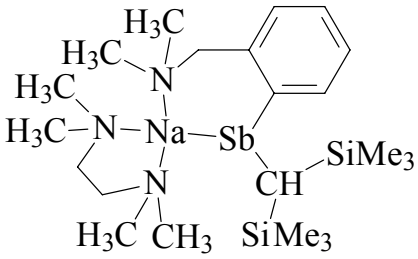

This contrasts the structure of [2-$(Me_2NCH_2)C_6H_4$][$(Me_3Si)_2CH$]SbCl, where coordination of the pendant Me_2N group to the antimony center was found.

Reaction of primary stibanes $RSbH_2$ (R = C_6H_5, 2-$((CH_3)_2NCH_2)C_6H_4$, 2,4,6-$(CH_3)_3C_6H_2$ or $[(CH_3)_3Si]_2CH$) with 2 equivalents of *n*-BuLi or treatment of $PhSbH_2$ with Na or K in liquid ammonia does not lead to the dianionic species $RSb^{2-}M^{+}_2$ (M = Li, Na, K) but instead the Zintl compounds $[Sb_7Li_3\cdot(tmeda)_3]$, $[Sb_7Na_3\cdot(pmdeta)_3]$ and $[Sb_7K_3\cdot(pmdeta)_3]$ have been isolated in yields ranging from 50 to 65 %.

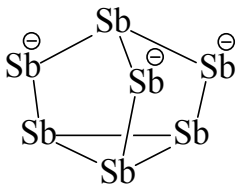

This was found to be a more effective approach for the synthesis of Zintl compounds containing the Sb_7^{3-} anion than the procedure reported earlier, *i.e.* by fusing stoichiometric amounts of the alkali metal and antimony at 600 to 800 °C.[7] The identity of these compounds were proven by X-ray diffractometry.

The reactions of *cyclo*-(^{t}BuSb)$_4$ with Li, Na, or K lead to cleavage of Sb-Sb bonds combined with migration of the tert. butyl groups, and after addition of tetramethylethylenetriamine or pentamethyldiethylenetriamine, complex salts containing the mono anions **A**, **B** or **C** form.

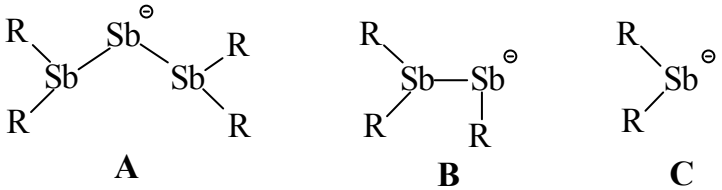

A **B** **C**

R = ^{t}Bu

The crystal structures of [(^{t}Bu$_4$Sb$_3$)][Li(tmeda)$_2$], [(^{t}Bu$_4$Sb$_3$)Na(tmeda)(thf)], [(^{t}Bu$_4$Sb$_3$)Na(tmeda)$_2$], [(^{t}Bu$_4$Sb$_3$)Na(pmdeta)], [(^{t}Bu$_4$Sb$_3$)K(pmdeta)] [(^{t}Bu$_3$Sb$_2$)K(pmdeta)] and [(^{t}Bu$_2$Sb)K(pmdeta)] have been determined.

The synthesis of 2-(3',5'-dimethylphenyl)-5,7-dimethylstibindolyl potassium·pmdeta is achieved in one pot reaction of trimesitylantimony with potassium and pentamethyldiethylenetriamine in tetrahydrofuran. This illustrates the difference in reactivity of trimesitylantimony towards different alkali metals since its reaction with lithium is known to give the dimesityl antimonide [2,4,6-(CH$_3$)$_3$C$_6$H$_2$]$_2$SbLi.

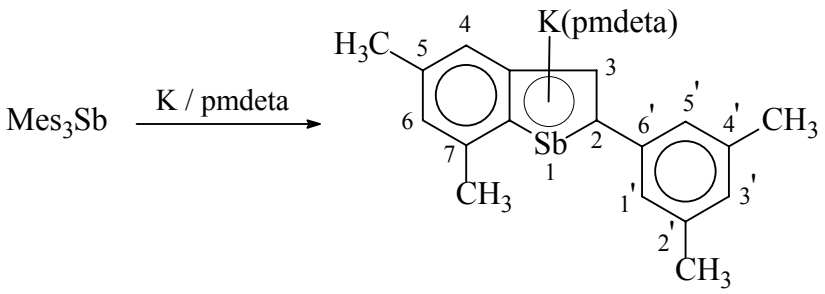

The characterisation of 2-(3',5'-dimethylphenyl)-5,7-dimethylstibindolyl potassium·pmdeta was achieved by X-ray diffractometry on single crystals. The structure consists of stacks built of dimethyl(dimethylphenyl) stibindolyl anions and $(pmdeta)K^+$ cations in bridging positions between each other. The simple synthesis of potasium stibindolyl should encourage further work towards the synthesis of transition metal complexes supported by the stibindolyl ligand.

8. References

[1] H. J. Breunig, D. Müller, *J. Organomet. Chem.* **1983**, *253*, C21.

[2] W. Levason, K. G. Smith, C. A. McAuliffe, F. P. McCullough, R. D. Sedgwick, S. G. Murray, *J. Chem. Soc., Dalton Trans.* **1979**, 1718.

[3] A. H. Cowley, R. A. Jones, C. M. Nunn, D. L. Westmoreland, *Angew. Chem.* **1989**, *101*, 1089. *Angew. Chem. Int. Engl.* **1989**, *28*, 1018.

[4] R. A. Bartlett, H. V. Rasika Dias, H. Hope, B. D. Murray, M. M. Olmstead, P. P. Power, *J. Am. Chem. Soc* **1986**, *108*, 6921.

[5] K. Issleib, B. Hamann, *Z. Anorg. Allg. Chem.* **1966**, *343*, 196.

[6] H. A. Meinema, H. F. Martens, J. G. Noltes, N. Bartazzi, R. Berbieri, *J. Organomet. Chem.* **1977**, *136*, 173.

[7] W. Becker, H. Nöth, *Chem. Ber.* **1972**, *105*, 1962.

[8] N. Kuhn, M. Winter, *Chem.-Ztg.* **1983**, *107*, 342.

[9] A. H. Cowley, R. A. Jones, C. M. Nunn, D. L. Westmoreland, *Chem. Mater.* **1990**, *2*, 221.

[10] L. I. Vyshinskaya, S. P. Korneva, G. P. Kulikova, T. A. Visnyakova, *Metalloorg. Khim.* **1989**, *2*, 1163.

[11] G. Becker, A. Münch, C. Witthauer, *Z. Anorg. All. Chem.* **1982**, *492*, 15.

[12] H. J. Breunig, J. Probst, *J. Organomet. Chem.* **1998**, *571*, 297.

[13] L. D. Freedman, G. O. Doak, in *The Chemistry of the Metal Carbon Bond*; F. R. Hartley ed.; Wiley and Sons: New York **1989**; Vol. 5, 397.

[14] Y. Z. Huang, Y. Sheng, C. Chen, *Tetrahedron Lett.* **1985**, *26*, 5171.

[15] K. Issleib, A. Balszuweit, *Z. Anorg. Allg. Chem.* **1976**, *419*, 87.

[16] A. N. Nesmayanov, A. E. Borisov, N. V. Novikova, *Izv. Akad. Nauk, Ser. Khim.* **1967**, 815.

[17] S. Sato, Y. Matsumura, R. Okawara, *J. Organomet. Chem.* **1972**, *43*, 333.

[18] K.-Y. Akiba, Y. Yamamoto, in *The Chemistry of Organic Arsenic, Antimony and Bismuth Compounds*; S. Patai ed.; Wiley and Sons: New York **1994**, 761.

[19] E. Shewchuk, S. B. Wild, *J. Organomet. Chem.* **1981**, *210*, 181.

[20] H. Althaus, H. J. Breunig, J. Probst, R. Rösler, E. Lork, *J. Organomet. Chem.* **1999**, *585*, 285.

[21] D. G. Adolphson, J. D. Corbett and D. J. Merryman, *J. Am. Chem. Soc.* **1976**, *98*, 7234.

[22] G. Nolas, J. Sharp, H. Goldsmid, *Thermoelectrics basic principles and new materials developments* **2001**, Springer.

[23] M. Wiberg, *Gmelin Handbook of Inorganic Chemistry*, Springer Verlag: Berlin, **1981**; Sb Organoantimony Compounds, part. 2.

[24] G. Balazs, H. J. Breunig, E. Lork, *Organometallics* **2002**, *21*, 2584 and references therein.

[25] D. G. Hendershot, J. C. Pazik, A. D. Berry, *Chem. Mater.* **1992**, *4*, 833.

[26] D. G. Hendershot, A. D. Berry, *J. Organomet. Chem.* **1993**, *449*, 119.

[27] G. Balazs, H. J. Breunig, E. Lork, S. Mason, *Organometallics* **2003**, *22*, 576.

[28] N. Wiberg, *Hollemann-Wiberg, Lehrbuch der Anorganischen Chemie;* de Gruyter: Berlin **1985**.

[29] F. E. Saalfeld, H. J. Svec, *Inorg. Chem.* **1963**, *2*, 51.

[30] F. A. Cotton, G. Wilkinson, *Advanced Inorganic Chemistry*, Wiley-Interscience: New York **1988**, p 390.

[31] C. J. Carmalt, N. C. Norman, *Chemistry of Arsenic, Antimony, and Bismuth*; Blackie Academic and Professional: London **1998**; p 20.

[32] E. Wiberg, K. Mödritzer, *Z. Naturforsch.* **1957**, *12B*, 128.

[33] B. Twamley, C.-S. Hwang, N. J. Hardmann, P. P. Power, *J. Organomet. Chem.* **2000**, *609*, 152.

[34] G. Balazs, H. J. Breunig, E. Lork, *Organometallics* **2001**, *20*, 2666.

[35] M. Ates, H. J. Breunig, S. Gülec, *Phosphorus Sulfur Silicon Relat. Elem.* **1989**, *44*, 129

[36] K. Issleib, A. Balszuweit, *Z. Anorg. Allg. Chem.* **1975**, *418*, 158.

[37] E. Wiberg, K. Mödritzer, *Z. Naturforsch.* **1956**, *11b*, 753.

[38] R. A. Rossi, J. F. Bunnett, *J. Am. Chem. Soc.* **1974**, *96*, 112.

[39] K. Issleib, B. Hamann, L. Schmidt, *Z. Anorg. Allg. Chem.* **1965**, *339*, 298.

[40] H. J. Breunig, T. Severengiz, *Z. Naturforsch.* **1982**, *37B*, 395.

[41] R. A. Bartlett, M. M. Olmstead, P. P. Power, *Inorg. Chem.* **1986**, *25*, 1243.

[42] R. A. Bartlett, M. M. Olmstead, P. P. Power, G. A. Siegel, *Inorg. Chem.* **1987**, *26*, 1941.

[43] M. F. Lappert, P. P. Power, A. R. Sanger, R. C. Srivastava, *Metal and Metalloid Amides*; Ellis.Horwood: Chichester, **1980**.

[44] M. A. Beswick, N. Choi, C. N. Harmer, A. D. Hopkins, M. McPartlin, D. S. Wright, *Science* **1998**, *281*, 1500.

[45] H. Hope, M. M. Olmstead, P. P. Power, Xiaojie Xu, *J. Am. Chem. Soc* **1984**, *106*, 819.

[46] W. Clegg, S. Doherty, K. Izod, H. Kagerer, P. O'Shaughnessy, J. M. Sheffield, *J. Chem. Soc., Dalton Trans.* **1999**, 1825.

[47] H. J. Breunig, M. E. Ghesner, E. Lork, *J. Organomet. Chem.* **2002**, *660*, 167.

[48] A. Shevelkov, M. Shatruk, *Russ. Chem. Bull. Int. Ed.* **2001**, *50*, 338.

[49] R. Nesper, *Prog. Solid St. Chem.* **1990**, *20*, 1.

[50] A. Cisar, J. D. Corbett, *Inorg. Chem.* **1977**, *16*, 2482.

[51] C. H. E. Belin, *J. Am. Chem. Soc.* **1980**, *102*, 6036.

[52] E. Zintl, W. Dullenkopf, *Z. Phys. Chem.* **1932**, *B16*, 183.

[53] M. A. Beswick, N. Choi, A. D. Hopkins, M. E. G. Mosquera, M. McPartlin, P. R. Raithby, A. Rothenberger, D. Stalke, A. E. H. Wheatley and D. S. Wright, *Chem. Commun*. **1998**, 2485.

[54] A. Bashall, M. A. Beswick, N. Choi, A. D. Hopkins, S. J. Kidd, Y. G. Lawson, M. E. G. Mosquera, M. McPartlin, P. R. Raithby, A. A. E. H. Wheatley, J. A. Wood and D. S. Wright, *J. Chem. Soc., Dalton Trans*. **2000**, 479.

[55] S. C. Critchlow and J. D. Corbett, *Inorg. Chem*. **1984**, 23, 770.

[56] N. Korber, F. Richter, *Angew. Chem.* **1997**, *109*, 1575; *Angew. Chem. Int. Ed. Engl.* **1997**, *36*, 1512.

[57] W. Hönle, H. G. Schnering, A. Schmidpeter, G. Burget, *Angew. Chem.* **1984**, *96*, 796; *Angew. Chem., Int. Ed. Engl.* **1984**, *23*, 817.

[58] D. Stalke, T. Kottke, *J. Appl. Crystallogr.* **1993**, *26*, 615.

[59] Y. Mourad, A. Atmani, Y.Mugnier, H. J. Breunig, K. H. Ebert, *J. Organomet. Chem.* **1994**, *476*, 47.

[60] A. Tzschach, V. Kiesel, *J. Prakt. Chem.* **1971**, *313*, 259.

[61] H. Köpf, U. Georges, *Z. Naturforsch.* **1981**, *36b*, 1205.

[62] K. Issleib, E. Fluck, *Angew. Chem.* **1966**, *78*, 597; *Angew. Chem. Int. Ed. Engl.* **1966**, *5*, 587.

[63] K. Issleib, K. Krech, *Chem. Ber.* **1966**, *100*, 1310.

[64] M. Baudler, A. Zarkadas, *Chem. Ber.* **1973**, *106*, 3970.

[65] M. Baudler, D. Koch, E. Tolls, K. M. Diedrich, B. Kloth, *Z. Anorg. Allg. Chem.* **1976**, *420*, 146.

[66] P. R. Hoffman, K. G. Caulton, *J. Am. Chem. Soc.* **1975**, *97*, 6370.

[67] T. J. DuPont, J. L. Mills, *Inorg. Chem.* **1973**, *12*, 2487.

[68] K. Issleib, C. Rockstroh, I. Duchek, E. Fluck, *Z. Anorg. Allg. Chem.* **1968**, *360*, 77.

[69] K. Issleib, M. Hoffmann, *Chem. Ber.* **1966**, *100*, 1320.

[70] M. Baudler, Ch. Grunter, G. Fastener, B. Cloth, F. Saykowski, U. Özer, *Z. Anorg. Allg. Chem.* **1978**, *446*, 169.

[71] M. Baudler, C. Gruner, *Z. Naturforsch.* **1976**, *31b*, 1311.

[72] M. Baudler, K. Glinka, in: I. Haiduc, D. B. Sowerby (Eds.), The Chemistry of Inorganic Homo- and Heterocycles, vol. 2, Academic Press, London, **1987**, p. 447.

[73] M. A. Beswick, A. D. Hopkins, L. C. Kerr, M. E. G. Mosquera, J. S. Palmer, P. R. Raithby, A. Rothenberger, D. Stalke, A. Steiner, A. E. H. Wheatley, D. S. Wright, *Chem. Commun.* **1998**, 1527.

[74] K. Deuten, D. Rehder, *Crystal Struct. Commun.* **1980**, *9*, 167.

[75] O. Mundt, G. Becker, H.-J. Wessely, H. J. Breunig, H. Kischkel, *Z. Anorg. Allg. Chem.* **1982**, *486*, 70.

[76] N. Tokitoh, Y. Arai, T. Sasamori, R. Okazaki, S. Nagase, H. Uekusa, Y. Ohashi, *J. Am. Chem. Soc.* **1998**, *120*, 433.

[77] H. J. Breunig, R. Rösler, *Coord. Chem. Rev.* **1997**, *163*, 33.

[78] J. E. Huheey, E. A. Keiter, R. L. Keiter, *Anorganische Chemie*, Walter de Gruyter, Berlin **1995**, p. 335.

[79] I. Kovacs, H. Krautscheid, E. Matern, E. Sattler, G. Fritz, W. Hönle, H. Borrmann, H. G. von Schering, *Z. Anorg. Allg. Chem.* **1996**, *622*, 1564.

[80] U. Weber, L. Zsolnai, G. Huttner, *J. Organomet. Chem.* **1984**, *260*, 281.

[81] A. M. Barr, M. D. Kerlogue, N. C. Norman, P. M. Webster, L. J. Farrugia, *Polyhedron* **1989**, *8*, 2495.

[82] F. Bringewski, G. Huttner, W. Imhof, L. Zsolnai, *J. Organomet. Chem.* **1992**, *439*, 33.

[83] C. W. Perkins, J. C. Martin, A. J. Arduengo III, W. Lau, A. Alegria, J. K. Kochi, *J. Am. Chem. Soc.* **1980**, *102*, 7753.

[84] C. A. Stewart, R. L. Harlow, A. J. Arduengo III, *J. Am. Chem. Soc.* **1985**, *107*, 5543.

[85] A. J. Arduengo III, C. A. Stewart, F. Davidson, D. A. Dixon, J. Y. Becker, S. A. Culley, M. B. Mizen, *J. Am. Chem. Soc.* **1987**, *109*, 627.

[86] M. Westerhausen, Ch. Gückel, M. Warchhold, H. Nöth, *Organometallics* **2000**, *19*, 2393.

[87] A. M. Arif, R. A. Jones, K. B. Kidd, *J. Chem. Soc. Chem. Commun.* **1986**, 1440.

[88] I. Ghesner, *PhD Thesis*, Universität Bremen, **2002**.

[89] T. Douglas, K. H. Theopold, *Angew. Chem.* **1989**, *101*, 1394. *Angew. Chem., Int. Ed. Engl.* **1989**, *28*, 1367.

[90] F. Paul, D. Carmichael, L. Ricard, F. Mathey, *Angew. Chem.* **1996**, *108*, 1204. *Angew. Chem., Int. Ed.* **1996**, *35*, 1125.

[91] H.-J. Gosink, F. Nief, L. Ricard, F. Mathey, *Inorg. Chem.* **1995**, *34*, 1306.

[92] F. Nief, L. Ricard, *J. Organomet. Chem.* **2002**, *642*, 208.

[93] E. Niecke, M. Nieger, P. Wenderoth, *Angew. Chem.* **1994**, *106*, 362. *Angew. Chem., Int. Ed. Engl.* **1994**, *33*, 353.

[94] F. Nief, L. Ricard, *J. Organomet. Chem.* **1994**, *464*, 149.

[95] S. C. Sendlinger, B. S. Haggerty, A. L. Rheingold, K. H. Theopold, *Chem. Ber.* **1991**, *124*, 2453.

[96] J. Kurita, M. Ishii, S. Yasuike, T. Tsuchiya, *J. Chem. Soc., Chem. Commun.* **1993**, 1309.

[97] J. Kurita, F. Usuda, S. Yasuike, T. Tsuchiya, Y. Tsuda, F. Kiuchi, S. Hosoi, *J. Chem. Soc., Chem. Commun.* **2000**, 191.

[98] S. L. Buchwald, R. A. Fisher, B. M. Foxman, *Angew. Chem.* **1990**, *102*, 820. *Angew. Chem., Int. Ed. Engl.* **1990**, *102*, 771.

[99] M. Ates, H. J. Breunig, K. H. Ebert, R. Kaller, M. Dräger, U. Behrens, *Z. Naturforschung* **1992**, *47b*, 503.

[100] C. Jones, J. W. Steed, R. C. Thomas, *J. Chem. Soc.*, *Dalton Trans*. **1999**, 1541.

[101] D. R. Burfield, K.-H. Lee, R. H. Smithers, *J. Org. Chem*. **1977**, *42*, 3060.

[102] D. R. Burfield, R. H. Smithers, *J. Org. Chem*. **1978**, *43*, 3966.

[103] D. R. Burfield, R. H. Smithers, *J. Org. Chem*. **1983**, *48*, 2420.

[104] Bruker-Franzen Analytik GmbH, *Win-NMR Version 6.0*, **1997**.

[105] Mass Spectrometry Service Ltd., *MASPEC Data System for Windows*, **1996**.

[106] D. A. Atwood, A. H. Cowley, J. Ruiz, *Inorg. Chim. Acta* **1992**, *198/200*, 271.

[107] N. Nunn, D. B. Sowerby, D. M. Wesolek, *J. Organomet. Chem*. **1983**, *251*, C45.

[108] M. Ates, H.J. Breunig, A. Soltani-Neshan, M. Tegeler, *Z. Naturforsch.* **1986**, *41B*, 321

[109] R. Rösler, PhD Thesis, Universität Bremen, Germany, **1998**

[110] G. M. Sheldrick, SHELX-93, Universität Göttingen **1993**.

[111] G. M. Sheldrick, SHELX-97, Universität Göttingen **1997**.

[112] *DIAMOND-Visual Crystal Structure Information System*, CRYSTAL IMPACT, P Box 1251, D-53002 Bonn.

9. Appendix

9.1. Abbreviations

amu	atomic mass unit
CI_{neg}	chemical ionization, negative charged ions
CI_{pos}	chemical ionisation, positive charged ions
calcd.	calculated
dec.	decomposition
EI	electron ionization
Et_2O	diethyl ether
Et	ethyl
HRMS	high-resolution mass spectrometry
IR	infrared spectroscopy
m	meta
Me	methyl
Mes	mesityl
ν	stretching vibration
MS	mass spectrometry
m.p.	melting point
NMR	nuclear magnetic resonance
o	ortho
p	para
Ph	phenyl
pmdeta	pentamethyldiethylenetriamine
^{t}Bu	tertiary butyl
thf	tetrahydrofuran
tmeda	tetramethylethylenediamine
XRD	X-ray diffraction

1	$(C_6H_5)SbH_2$
2	$[2,4,6\text{-}(CH_3)_3C_6H_2]SbH_2$
3	$[2\text{-}(Me_2NCH_2)C_6H_4]SbH_2$
4	$(C_6H_5)_2SbH$
5	$(^tBu_2Sb)_2$
6	$[(C_6H_5)_2SbLi\cdot(thf)_3]$
7	$[(2,4,6\text{-}(CH_3)_3C_6H_2)_2SbLi\cdot(thf)_3]$
8	$[2\text{-}(Me_2NCH_2)C_6H_4][(Me_3Si)_2CH]SbLi\cdot 2thf$
9	$[2\text{-}(Me_2NCH_2)C_6H_4][(Me_3Si)_2CH]SbNa\cdot tmeda$
10	$[2\text{-}(Me_2NCH_2)C_6H_4][(Me_3Si)_2CH]SbK\cdot pmdeta$
11	$[Sb_7Li_3\cdot(tmeda)_3]$
12	$[Sb_7Na_3\cdot(tmeda)_3]$
13	$[Sb_7K_3\cdot(tmeda)_3]$
14	$[(^tBu_4Sb_3)][Li(tmeda)_2]$
15	$[(^tBu_4Sb_3)Na(tmeda)(thf)]$
16	$[(^tBu_4Sb_3)Na(tmeda)_2]$
17	$[(^tBu_4Sb_3)Na(pmdeta)]$
18	$[(^tBu_4Sb_3)K(pmdeta)]$
19	$[(^tBu_3Sb_2)K(pmdeta)]$
20	$[(^tBu_2Sb)K(pmdeta)]$
21	2-(3’,5’-Dimethylphenyl)-5,7-dimethylstibindolyl potassium-pmdeta

9.2. Details of crystal structure determination

Table 9.2.1. Crystal data and structure refinement for **[2,4,6-$(CH_3)_3C_6H_2$]SbH_2 (2)**

Identification code	mgh15	
Empirical formula	$C_9H_{13}Sb$	
Formula weight	240.93	
Temperature	163(2) K	
Wavelenght	71.073 pm	
Crystal system	Monoclinic	
Space group	P2	
Unit cell dimensions	a = 812.34(9) pm	α = 90°
	b = 713.92(8) pm	β = 101.325(8)°
	c = 831.35(9) pm	γ = 90°
Volume	4.7275(9) nm^3	
Z	2	
Diffractometer	Siemens P4	
Density (calculated)	1.693 Mg/m^3	
Absorption coefficient	2.847 mm^{-1}	
F(000)	232	
Crystal size	0.6 x 0.5 x 0.3 mm^3	
Theta range for data collection	2.56 to 27.50°	
Index ranges	-10<=h<=10, -8<=k<=9, -10<=l<=10	
Reflections collected	2722	
Independent reflections	1171 [R(int) = 0.0303]	
Completeness to theta = 27.50°	99.7 %	
Absorption correction	DIFABS	
Refinement method	Full-matrix least-squares on F^2	
Data / restraints / parameters	1171 / 0 / 66	
Goodness-of-fit on F^2	4.610	

Final R indices [I>2sigma(I)]	R1 = 0.0938, wR2 = 0.3439
R indices (all data)	R1 = 0.0986, wR2 = 0.3551
Largest diff. Peak and hole	3.906 and -3.324 e.Å^{-3}

Table 9.2.2. Atomic coordinates (x 10^4) and equivalent isotropic displacement parameters (pm^2 x 10^{-1}) for **[2,4,6-$(CH_3)_3C_6H_2$]SbH_2 (2)**. U(eq) is defined as one third of the trace of the orthogonalised Uij tensor.

	x	y	z	U(eq)
Sb(1)	1459(1)	2500	8189(1)	59(1)
C(1)	-718(13)	2500	6237(14)	25(2)
C(2)	-420(13)	2500	4560(15)	29(2)
C(3)	1400(15)	2500	4280(20)	45(3)
C(4)	-1729(14)	2500	3298(16)	30(2)
C(5)	-3412(14)	2500	3540(16)	32(2)
C(6)	-4814(16)	2500	2070(20)	51(4)
C(7)	-3613(12)	2500	5136(16)	32(2)
C(8)	-2348(15)	2500	6454(13)	30(2)
C(9)	-2804(19)	2500	8158(16)	45(3)

Table 9.2.3. Crystal data and structure refinement for **[$(C_6H_5)_2$SbLi·$(thf)_3$] (6)**

Identification code	mgh1	
Empirical formula	$C_{12}H_{10}SbLi \cdot 3C_4H_8$	
Formula weight	499.20	
Temperature	173(2) K	
Wavelenght	71.073 pm	
Crystal system	Triclinic	
Space group	$P\bar{1}$	
Unit cell dimensions	a = 914.90(10) pm	α = 95.38°
	b = 939.50(10) pm	β =100.63°

	c = 1595.7(2) pm γ = 113.73°
Volume	1.2124(2) nm^3
Z	2
Diffractometer	Siemens P4
Density (calculated)	1.367 Mg/m^3
Absorption coefficient	1.158 mm^{-1}
F(000)	512
Crystal size	0.60 x 0.50 x 0.40 mm^3
Theta range for data collection	2.51 to 27.50°
Index ranges	-16<=h<=1, -24<=k<=1, -45<=l<=45
Reflections collected	6635
Independent reflections	5500 [R(int) = 0.0185]
Completeness to theta = 27.50°	98.8 %
Absorption correction	DIFABS
Refinement method	Full-matrix least-squares on F^2
Data / restraints / parameters	5500 / 0 / 266
Goodness-of-fit on F^2	1.051
Final R indices [I>2sigma(I)]	R1 = 0.0270, wR2 = 0.0692
R indices (all data)	R1 = 0.0297, wR2 = 0.0708
Largest diff. Peak and hole	0.519 and -0.744 $e.Å^{-3}$

Table 9.2.4. Atomic coordinates (x 10^4) and equivalent isotropic displacement parameters (pm^2 x 10^{-1}) for **$[(C_6H_5)_2SbLi\cdot(thf)_3]$ (6)**. U(eq) is defined as one third of the trace of the orthogonalised Uij tensor.

	x	y	z	U(eq)
Sb(1)	-1129(1)	7311(1)	6846(1)	32(1)
O(1)	2928(2)	7570(2)	6041(1)	42(1)
O(2)	3348(2)	7411(2)	7960(1)	45(1)
O(3)	3691(2)	10486(2)	7381(1)	46(1)
Li(1)	2343(5)	8226(4)	7051(3)	36(1)

C(13)	-1040(2)	9642(2)	6837(1)	31(1)
C(19)	-933(2)	7210(2)	8204(1)	28(1)
C(1)	5082(3)	7813(4)	8125(2)	52(1)
C(2)	5638(4)	7965(5)	9076(2)	65(1)
C(3)	4093(4)	6938(4)	9352(2)	62(1)
C(4)	2721(3)	6392(3)	8545(2)	43(1)
C(5)	3763(4)	11601(4)	6824(2)	62(1)
C(6)	3500(4)	12898(4)	7319(2)	70(1)
C(7)	3680(4)	12644(4)	8245(2)	64(1)
C(8)	4287(4)	11371(3)	8246(2)	51(1)
C(9)	4361(3)	8411(3)	5727(2)	50(1)
C(10)	4590(3)	7173(4)	5160(2)	53(1)
C(11)	3795(3)	5688(3)	5529(2)	48(1)
C(12)	2366(3)	5894(3)	5765(2)	45(1)
C(14)	-906(3)	10227(3)	6064(2)	41(1)
C(15)	-926(3)	11667(3)	5966(2)	51(1)
C(16)	-1083(3)	12591(3)	6646(2)	52(1)
C(17)	-1229(3)	12034(3)	7415(2)	44(1)
C(18)	-1215(3)	10585(3)	7508(2)	35(1)
C(20)	66(3)	8451(2)	8900(1)	34(1)
C(21)	199(3)	8221(3)	9753(2)	42(1)
C(22)	-628(4)	6739(3)	9937(2)	48(1)
C(23)	-1588(3)	5489(3)	9263(2)	48(1)
C(24)	-1771(3)	5725(3)	8412(2)	37(1)

Table 9.2.5. Crystal data and structure refinement for **[(2,4,6-$(CH_3)_3C_6H_2)_2SbLi\cdot(thf)_3$] (7)**

Identification code	mgh6
Empirical formula	$C_{18}H_{22}SbLi\cdot 3C_4H_8O$
Formula weight	1166.72
Temperature	173(2)
Wavelenght	71.073
Crystal system / Space group	Monoclinic / P2(1)
Unit cell dimensions	a = 1007.9(2) α = 90
	b = 1836.8(3) β = 103.27°
	c = 1672.9(2) γ = 90°
Volume	3.0144(9) nm^3
Z	2
Diffractometer	Siemens P4
Density (calculated)	1.285 Mg/m^3
Absorption coefficient	0.941 mm^{-1}
F(000)	1216
Crystal size	0.050 x 0.40 x 0.20 mm^3
Theta range for data collection	2.50 to 27.50°
Index ranges	-13<=h<=1, -1<=k<=23, -21<=1<=21
Reflections collected	8887
Independent reflections	7491 [R(int) = 0.0305]
Completeness to theta = 27.50°	99.2 %
Absorption correction	DIFABS
Refinement method	Full-matrix least-squares on F^2
Data / restraints / parameters	7491 / 1 / 637
Goodness-of-fit on F^2	1.032
Final R indices [I>2sigma(I)]	R1 = 0.0378, wR2 = 0.0923
R indices (all data)	R1 = 0.0449, wR2 = 0.0971
Largest diff. Peak and hole	1.117 and –0.914 e.$Å^{-3}$

Table 9.2.6. Atomic coordinates (x 10^4) and equivalent isotropic displacement parameters (pm^2 x 10^{-1}) for **[(2,4,6-$(CH_3)_3C_6H_2)_2$SbLi·$(thf)_3$] (7)**. U(eq) is defined as one third of the trace of the orthogonalised Uij tensor.

	x	y	z	U(eq)
Sb(1)	-4925(1)	136(1)	4906(1)	37(1)
Li(1)	-7430(13)	-725(8)	4341(8)	45(3)
C(11)	-4895(6)	1066(4)	4093(3)	36(1)
C(21)	-3686(5)	-683(4)	4474(3)	36(1)
O(1)	-8677(4)	-514(3)	3282(3)	52(1)
O(2)	-8573(4)	-638(3)	5117(3)	53(1)
O(3)	-7086(5)	-1767(3)	4431(4)	68(2)
C(12)	-3731(8)	1274(4)	3823(4)	40(2)
C(13)	-3761(6)	1908(4)	3341(3)	38(1)
C(14)	-4921(7)	2329(4)	3117(3)	39(2)
C(15)	-6065(6)	2138(4)	3420(4)	41(2)
C(16)	-6057(6)	1520(4)	3909(3)	35(1)
C(17)	-2387(6)	882(4)	4064(4)	47(2)
C(18)	-4944(7)	3008(5)	2604(4)	52(2)
C(19)	-7260(8)	1388(4)	4267(5)	45(2)
C(22)	-2847(6)	-1128(4)	5062(3)	39(1)
C(23)	-2208(6)	-1752(3)	4822(4)	45(1)
C(24)	-2372(7)	-1950(4)	4018(4)	49(2)
C(25)	-3186(7)	-1517(4)	3434(4)	48(2)
C(26)	-3852(7)	-893(4)	3640(4)	41(2)
C(27)	-2643(7)	-972(4)	5984(4)	49(2)
C(28)	-1765(7)	-2636(4)	3769(5)	62(2)
C(29)	-4806(7)	-477(4)	2964(4)	54(2)
C(31)	-8587(6)	36(4)	2681(3)	47(2)
C(32)	-10014(6)	356(5)	2447(4)	55(2)
C(33)	-10874(7)	-321(5)	2432(4)	64(2)

C(34)	-10041(7)	-800(6)	3091(5)	67(2)
C(41)	-8177(11)	-940(7)	5919(5)	96(4)
C(42)	-8769(10)	-470(6)	6477(5)	78(3)
C(43)	-9296(11)	204(6)	5983(4)	90(3)
C(44)	-9549(8)	-74(5)	5122(5)	66(2)
C(51)	-5894(7)	-2194(4)	4512(5)	53(2)
C(52)	-6319(10)	-2822(5)	3950(5)	79(2)
C(53)	-7839(9)	-2914(5)	3916(6)	84(3)
C(54)	-8105(9)	-2302(5)	4471(7)	96(3)
Sb(2)	-9820(1)	322(1)	-33(1)	40(1)
Li(2)	-12142(14)	1227(7)	-738(9)	45(3)
C(61)	-8459(6)	1149(4)	-330(3)	36(1)
C(71)	-9717(5)	-579(4)	-860(3)	34(1)
O(4)	-11839(6)	2247(3)	-840(4)	71(2)
O(5)	-13401(5)	1198(4)	12(3)	63(2)
O(6)	-13404(4)	987(3)	-1801(3)	54(1)
C(62)	-7677(6)	1561(4)	329(4)	38(1)
C(63)	-6927(6)	2160(4)	160(4)	52(2)
C(64)	-6895(8)	2374(4)	-614(5)	56(2)
C(65)	-7661(7)	1968(4)	-1255(4)	53(2)
C(66)	-8431(8)	1369(4)	-1131(4)	44(2)
C(67)	-7662(8)	1380(6)	1207(4)	63(2)
C(68)	-6134(10)	3038(5)	-790(6)	90(3)
C(69)	-9333(7)	1010(4)	-1888(4)	54(2)
C(72)	-10871(6)	-1023(4)	-1107(3)	35(1)
C(73)	-10871	-1625(4)	-1615(3)	39(1)
C(74)	-9736(6)	-1819(4)	-1890(4)	42(2)
C(75)	-8564(7)	-1409(4)	-1605(4)	44(2)
C(76)	-8529(7)	-813(4)	-1101(4)	38(2)
C(77)	-12163(8)	-890(5)	-786(5)	47(2)

C(78)	-9751(8)	-2457(5)	-2470(5)	54(2)
C(79)	-7170(6)	-426(5)	-782(5)	55(2)
C(81)	-10782(11)	2703(5)	-437(6)	83(3)
C(82)	-10603(12)	3260(6)	-1048(6)	96(3)
C(83)	-12029(15)	3360(7)	-1478(10)	169(7)
C(84)	-12530(20)	2697(10)	-1386(18)	390(30)
C(91)	-13060(10)	1555(6)	780(5)	80(3)
C(92)	-13669(9)	1128(7)	1368(4)	81(3)
C(93)	-14124(12)	429(6)	881(5)	96(4)
C(94)	-14405(8)	655(5)	19(5)	66(2)
C(101)	-14796(7)	1265(5)	-2019(5)	66(2)
C(102)	-15623(9)	721(5)	-2585(5)	70(2)
C(103)	-14670(7)	87(5)	-2593(4)	57(2)
C(104)	-13276(6)	441(5)	-2398(3)	48(2)

Table 9.2.7. Crystal data and structure refinement for **[2-(Me_2NCH_2)C_6H_4][($Me_3Si)_2$CH]SbLi·2thf (8)**

Identification code	mgh8	
Empirical formula	$C_{24}H_{47}LiNO_2SbSi_2$	
CCDC-Number	207723	
Formula weight	566.50	
Temperature	173(2) K	
Wavelenght	0.71073 Å	
Crystal system	Monoclinic	
Space group	P2(1)/n	
Unit cell dimensions	a = 11.552(2) Å	α = 90°
	b = 16.518(3) Å	β = 96.11°
	c = 15.971(5) Å	γ = 90°
Volume	3030.2(12) $Å^3$	

Z	4
Diffractometer	Siemens P4
Density (calculated)	1.242 Mg/m^3
Absorption coefficient	1.007 mm^{-1}
F(000)	1184
Crystal size	0.6 x 0.5 x 0.1 mm^3
Theta range for data collection	2.57 to 27.51°
Index ranges	-15<=h<=1, -1<=k<=21, -20<=l<=20
Reflections collected	8538
Independent reflections	6872 [R(int) = 0.0304]
Completeness to theta = 27.50°	98.7 %
Absorption correction	DIFABS
Refinement method	Full-matrix least-squares on F^2
Data / restraints / parameters	6872 / 0 / 292
Goodness-of-fit on F^2	1.065
Final R indices [I>2sigma(I)]	R1 = 0.0595, wR2 = 0.1672
R indices (all data)	R1 = 0.0749, wR2 = 0.1787
Largest diff. Peak and hole	1.066 and -1.648 $e.Å^{-3}$

Table 9.2.8. Atomic coordinates (x 10^4) and equivalent isotropic displacement parameters (pm^2 x 10^{-1}) for **[2-(Me_2NCH_2)C_6H_4][(Me_3Si)$_2$CH]SbLi·2thf (8)**. U(eq) is defined as one third of the trace of the orthogonalised Uij tensor.

	x	y	z	U(eq)
Sb(1)	4151(1)	5815(1)	2730(1)	37(1)
Li	2529(7)	4790(5)	3449(5)	28(2)
C(1)	5186(4)	5423(3)	1693(3)	24(1)
C(8)	2460(4)	5951(2)	1996(3)	24(1)
N(1)	1638(4)	5811(2)	3871(3)	31(1)
O(1)	3135(3)	4162(2)	4419(3)	46(1)
O(2)	1551(3)	4042(2)	2734(3)	45(1)

Si(1)	5817(1)	6339(1)	1232(1)	31(1)
Si(2)	6192(1)	4590(1)	2080(1)	31(1)
C(2)	6962(6)	6825(5)	1983(5)	61(2)
C(3)	4687(6)	7119(4)	913(4)	52(2)
C(4)	6486(6)	6113(4)	244(4)	57(2)
C(5)	7273(6)	4329(4)	1332(4)	54(2)
C(6)	5392(6)	3631(4)	2244(5)	61(2)
C(7)	7055(5)	4850(5)	3107(4)	55(2)
C(9)	2215(4)	5711(3)	1151(3)	31(1)
C(10)	1111(5)	5804(3)	712(3)	39(1)
C(11)	220(4)	6148(3)	1103(3)	38(1)
C(12)	438(4)	6388(3)	1930(3)	34(1)
C(13)	1531(4)	6280(2)	2385(3)	25(1)
C(14)	1705(4)	6516(3)	3298(3)	32(1)
C(15)	412(5)	5593(4)	3912(4)	48(1)
C(16)	2169(6)	6026(4)	4714(4)	53(2)
C(17)	2448(7)	3590(6)	4830(7)	84(3)
C(18)	3236(8)	2927(5)	5158(8)	96(3)
C(19)	4390(7)	3128(4)	4920(6)	71(2)
C(20)	4331(5)	4008(4)	4705(4)	47(1)
C(21)	2182(6)	3583(6)	2155(8)	117(5)
C(22)	1438(7)	3472(4)	1373(5)	69(2)
C(23)	279(6)	3432(4)	1673(4)	56(2)
C(24)	371(5)	4062(4)	2376(4)	43(1)

Table 9.2.9. Crystal data and structure refinement for **[2-(Me_2NCH_2)C_6H_4][(Me_3Si)$_2$CH]SbNa·tmeda (9)**

Identification code	mgh10i	
Empirical formula	$C_{26}H_{57}N_3NaOSbSi_2$	
CCDC-Number	207724	
Formula weight	628.67	
Temperature	173(2) K	
Wavelenght	71.073 pm	
Crystal system	Monoclinic	
Space group	P2(1)/n	
Unit cell dimensions	a = 979.7(2) pm	α = 90°
	b = 2499.1(5) pm	β = 94.98(3)°
	c = 1434.8(3) pm	γ = 90°
Volume	3.4997(12) nm^3	
Z	4	
Diffractometer	Stoe IPDS	
Density (calculated)	1.193 Mg/m^3	
Absorption coefficient	0.889 mm^{-1}	
F(000)	1328	
Crystal size	0.50 x 0.40 x 0.30 mm^3	
Theta range for data collection	2.56 to 26.18°	
Index ranges	-11<=h<=11, -30<=k<=30, -17<=l<=17	
Reflections collected	35477	
Independent reflections	6428 [R(int) = 0.0852]	
Completeness to theta = 27.50°	91.7 %	
Absorption correction	DIFABS	
Refinement method	Full-matrix least-squares on F^2	
Data / restraints / parameters	6428 / 1 / 326	
Goodness-of-fit on F^2	1.031	
Final R indices [I>2sigma(I)]	R1 = 0.0571, wR2 = 0.1411	

R indices (all data)	R1 = 0.0918, wR2 = 0.1606
Largest diff. Peak and hole	0.701 and -0.440 e.Å^{-3}

Table 9.2.10. Atomic coordinates (x 10^4) and equivalent isotropic displacement parameters (pm^2 x 10^{-1}) for **[2-(Me_2NCH_2)C_6H_4][(Me_3Si)$_2$CH]SbNa·tmeda (9)**. U(eq) is defined as one third of the trace of the orthogonalised Uij tensor.

	x	y	z	U(eq)
Sb(1)	1715(1)	1828(1)	3024(1)	51(1)
Na(1)	3974(3)	2349(1)	1939(2)	58(1)
C(1)	1818(7)	927(2)	3022(4)	48(1)
C(8)	1060(7)	1938(2)	1541(4)	50(1)
N(1)	2392(6)	3137(2)	1877(4)	61(1)
N(2)	4943(6)	1915(3)	611(4)	62(1)
N(3)	6355(8)	2681(4)	1978(5)	80(2)
Si(1)	3287(2)	727(1)	3871(1)	54(1)
Si(2)	93(2)	643(1)	3172(1)	60(1)
C(2)	3421(11)	-32(3)	3981(7)	82(2)
C(3)	4964(9)	955(4)	3493(7)	76(2)
C(4)	3125(10)	989(4)	5087(6)	77(2)
C(5)	-1277(9)	894(4)	2280(7)	79(2)
C(6)	55(13)	-117(4)	3031(11)	110(4)
C(7)	-462(12)	807(6)	4372(7)	107(4)
C(9)	856(8)	1510(3)	905(5)	63(2)
C(10)	361(9)	1587(3)	-24(5)	68(2)
C(11)	26(9)	2102(4)	-343(5)	68(2)
C(12)	243(8)	2528(3)	249(5)	64(2)
C(13)	764(7)	2463(3)	1182(5)	56(2)
C(14)	966(8)	2941(3)	1802(5)	59(2)
C(15)	2610(11)	3517(3)	2678(6)	77(2)
C(16)	2691(10)	3421(3)	1015(6)	71(2)

C(17)	4150(10)	2120(4)	-218(6)	78(2)
C(18)	4758(13)	1336(4)	615(7)	90(3)
C(19)	6395(10)	2071(4)	631(7)	83(2)
C(20)	6709(10)	2605(5)	1016(7)	91(3)
C(21)	7132(11)	2347(4)	2664(7)	86(2)
C(22)	6633(13)	3249(5)	2219(9)	101(3)
O(1)	800(17)	4585(6)	3817(9)	173(6)
C(23)	2030(40)	4944(9)	4150(20)	250(20)
C(24)	3060(40)	4710(15)	4590(20)	250(20)
C(25)	-720(30)	4667(16)	3266(19)	320(30)
C(26)	-1740(50)	4372(18)	3410(40)	400(40)

Table 9.2.11. Crystal data and structure refinement for **[Sb_7Li_3·$(tmeda)_3$] (11)**

Identification code	mgh17	
Empirical formula	[Sb_7Li_3·$(tmeda)_3$]	
Formula weight	1411.92	
Temperature	173(2) K	
Wavelenght	71.073 pm	
Crystal system	Monoclinic	
Space group	P2(1)/m	
Unit cell dimensions	a = 1013.80(10) pm	α = 90°
	b = 2088.2(3) pm	β =92.040(10)°
	c = 1191.80(10) pm	γ = 90°
Volume	25.215(5) nm^3	
Z	2	
Diffractometer	Siemens P4	
Density (calculated)	1.860 Mg/m^3	
Absorption coefficient	3.718 mm^{-1}	
F(000)	1328	

Crystal size	0.4 x 0.3 x 0.1 mm^3
Theta range for data collection	2.59 to 27.50°
Index ranges	-13<=h<=1, -27<=k<=1, -15<=l<=15
Reflections collected	7403
Independent reflections	5936 [R(int) = 0.0244]
Completeness to theta = 27.50°	99.9 %
Absorption correction	DIFABS
Refinement method	Full-matrix least-squares on F^2
Data / restraints / parameters	5936 / 0 / 241
Goodness-of-fit on F^2	1.022
Final R indices [I>2sigma(I)]	R1 = 0.0446, wR2 = 0.1002
R indices (all data)	R1 = 0.0665, wR2 = 0.1100
Largest diff. Peak and hole	1.002 and -1.351 e.$Å^{-3}$

Table 9.2.12. Atomic coordinates (x 10^4) and equivalent isotropic displacement parameters (pm^2 x 10^{-1}) for **$[Sb_7Li_3 \cdot (tmeda)_3]$ (11)**. U(eq) is defined as one third of the trace of the orthogonalised Uij tensor.

	x	y	z	U(eq)
Sb(1)	-2236(1)	3187(1)	-1283(1)	55(1)
Sb(2)	-774(1)	2500	-2886(1)	54(1)
Sb(3)	1808(1)	2500	-2078(1)	40(1)
Sb(4)	-413(1)	3531(1)	374(1)	42(1)
Sb(5)	1329(1)	2500	227(1)	37(1)
Li(1)	1182(10)	3804(5)	-1523(9)	39(2)
Li(2)	-1756(15)	2500	1493(13)	45(3)
N(1)	744(6)	4480(3)	-2792(5)	52(1)
N(2)	2852(6)	4355(3)	-1060(5)	49(1)
N(3)	-1323(8)	2500	3217(6)	46(2)
N(4)	-3773(9)	2500	1847(7)	60(2)
C(1)	2906(12)	4561(7)	67(9)	134(6)

C(2)	4042(9)	4026(5)	-1349(14)	127(6)
C(3)	2666(13)	4904(6)	-1790(11)	118(5)
C(4)	1913(11)	4885(6)	-2755(11)	110(4)
C(5)	540(14)	4189(5)	6105(7)	110(5)
C(6)	-410(9)	4856(4)	-2558(9)	79(3)
C(7)	-450(20)	2000(9)	3573(10)	208(11)
C(8)	-2280(30)	2780(20)	3647(12)	600(50)
C(9)	-3774(11)	2500	3072(9)	61(3)
C(10)	-4440(12)	3057(8)	1444(10)	168(8)
C(11)	-3816(14)	3946(9)	5710(10)	151(7)
C(12)	-4740(20)	3993(10)	4925(11)	182(10)
C(13)	-5060(11)	4289(6)	4081(8)	88(3)
C(14)	-6180(15)	4245(9)	3344(17)	159(7)
C(15)	-7097(13)	3782(9)	3480(18)	160(9)
C(16)	-6480(40)	3386(9)	4810(30)	280(30)
C(17)	-5730(40)	3445(15)	5120(40)	400(50)

Table 9.2.17. Crystal data and structure refinement for **[Li(tmeda)$_2$(*t*-Bu$_4$Sb$_3$)] (14)**

Identification code	mgh12	
Empirical formula	$C_{28}H_{68}N_4LiSb_3 \cdot C_6H_6$	
Formula weight	911.16	
Temperature	173(2) K	
Wavelenght	71.073 pm	
Crystal system	Monoclinic	
Space group	P2/c	
Unit cell dimensions	a = 1780.2(2) pm	α = 90°
	b = 1708.4(2) pm	β = 93.60°
	c = 1462.2(2) pm	γ = 90°
Volume	4.4382(9) nm^3	

Z	7
Diffractometer	Siemens P4
Density (calculated)	1.364 Mg/m^3
Absorption coefficient	1.837 mm^{-1}
F(000)	1848
Crystal size	0.7 x 0.4 x 0.1 mm^3
Theta range for data collection	2.58 to 27.50°
Index ranges	-23<=h<=23, -22<=k<=7, -18<=l<=18
Reflections collected	12187
Independent reflections	11279 [R(int) = 0.0198]
Completeness to theta = 27.50°	99.1 %
Absorption correction	DIFABS
Refinement method	Full-matrix least-squares on F^2
Data / restraints / parameters	11279 / 2 / 803
Goodness-of-fit on F^2	1.003
Final R indices [I>2sigma(I)]	R1 = 0.0363, wR2 = 0.0733
R indices (all data)	R1 = 0.0634, wR2 = 0.0840
Largest diff. Peak and hole	0.677 and -0.964 $e.Å^{-3}$

Table 9.2.18. Atomic coordinates (x 10^4) and equivalent isotropic displacement parameters (pm^2 x 10^{-1}) for **[Li(tmeda)$_2$(*t*-Bu$_4$Sb$_3$)] (14)**. U(eq) is defined as one third of the trace of the orthogonalised Uij tensor.

	x	y	z	U(eq)
Sb(1)	8168(1)	3000(1)	416(1)	30(1)
Sb(2)	9695(1)	3038(1)	918(1)	38(1)
Sb(3)	9796(1)	1469(1)	469(1)	31(1)
Sb(4)	5341(1)	2999(1)	-3938(1)	30(1)
Sb(5)	3814(1)	3047(1)	-4427(1)	37(1)
Sb(6)	3719(1)	1472(1)	-4004(1)	30(1)
Sb(6)	3719(1)	1472(1)	-4004(1)	30(1)

Li(1)	6740(30)	784(1)	-1830(30)	42(5)
Li(2)	1690(20)	4481(7)	-6700(30)	29(4)
N(1)	7598(9)	1413(11)	-2457(14)	46(4)
N(2)	7611(9)	191(11)	-1064(15)	54(5)
N(3)	5878(10)	1350(11)	-1154(14)	60(6)
N(4)	7925(9)	134(10)	-2582(13)	46(4)
N(5)	10716(9)	4877(10)	-2043(11)	43(5)
N(6)	1225(10)	3856(12)	-5798(14)	45(5)
N(7)	12336(10)	3850(11)	-2229(13)	36(4)
N(8)	2783(9)	5124(9)	-6490(11)	42(5)
C(1)	7747(12)	1039(16)	-3328(10)	61(5)
C(2)	7528(8)	2237(13)	-2497(14)	68(6)
C(3)	8266(11)	1239(13)	-1850(14)	61(5)
C(4)	8277(14)	422(19)	-1608(18)	75(8)
C(5)	7680(12)	419(14)	-98(14)	73(7)
C(6)	7507(13)	-677(13)	-880(12)	80(7)
C(7)	5957(13)	2233(10)	-1146(15)	96(9)
C(8)	5882(14)	1139(17)	-161(16)	86(8)
C(8)	5882(14)	1193(17)	-161(16)	86(8)
C(9)	5222(9)	1098(17)	-1748(15)	94(10)
C(10)	5251(14)	302(17)	-2107(16)	58(5)
C(11)	8028(12)	4151(11)	-238(16)	42(5)
C(12)	8346(14)	4112(14)	-1179(17)	62(7)
C(13)	8555(10)	4795(8)	204(12)	46(3)
C(14)	7229(12)	4381(16)	-361(19)	67(7)
C(15)	7633(12)	3170(15)	1765(13)	36(5)
C(16)	6797(11)	3223(18)	1554(18)	771(9)
C(17)	7930(11)	3929(12)	2275(14)	47(4)
C(18)	7830(14)	2422(18)	2227(17)	75(9)
C(19)	10750(10)	1490(12)	-394(13)	47(6)

C(20)	1114(13)	640(16)	-513(19)	58(7)
C(21)	11374(11)	2062(15)	-70(16)	85(8)
C(22)	10417(13)	1652(12)	-1337(16)	50(5)
C(23)	10273(10)	947(9)	1736(12)	41(5)
C(24)	11030(10)	1222(14)	2143(15)	56(6)
C(25)	10255(10)	100(12)	1674(15)	50(5)
C(26)	9705(14)	1038(15)	2488(16)	79(8)
C(27)	10384(14)	4874(13)	-2995(19)	57(5)
C(28)	10804(14)	4091(10)	-1580(17)	70(7)
C(29)	10163(11)	5343(14)	-1586(16)	52(6)
C(30)	492(10)	4340(11)	-5707(15)	52(6)
C(31)	971(12)	3061(9)	-6108(19)	69(8)
C(32)	1612(8)	3736(15)	-4874(14)	48(5)
C(33)	11916(13)	3800(18)	1386(18)	80(8)
C(34)	12553(12)	3089(13)	2582(15)	64(7)
C(35)	12962(10)	4312(12)	2098(14)	54(6)
C(36)	3297(10)	4576(13)	-6962(17)	50(6)
C(37)	3021(14)	5298(12)	-5545(18)	51(5)
C(38)	2770(13)	5874(13)	-6896(13)	54(6)
C(39)	5456(11)	4175(12)	-3212(15)	42(5)
C(40)	5154(13)	4006(14)	-2312(16)	48(5)
C(41)	5168(13)	4836(13)	-3772(19)	115(11)
C(42)	6332(13)	4353(17)	-3062(17)	64(7)
C(43)	5829(12)	3152(15)	-5264(17)	47(6)
C(44)	6698(11)	3233(15)	-5162(10)	65(8)
C(45)	5529(14)	3761(14)	-5872(17)	100(10)
C(46)	5669(13)	2435(15)	-5840(16)	56(7)
C(47)	3263(10)	933(12)	-5354(11)	44(6)
C(48)	3814(12)	1203(12)	-6019(11)	44(4)
C(49)	2487(13)	1258(17)	-5612(16)	71(7)

C(50)	3184(15)	19(12)	-5157(19)	84(8)
C(51)	2711(11)	1484(12)	-3136(11)	38(5)
C(52)	2097(9)	2077(11)	-3420(11)	42(4)
C(53)	2443(14)	698(15)	-3077(18)	62(7)
C(54)	3035(12)	1847(12)	-2194(14)	44(4)
C(55)	8777(12)	2805(18)	-4960(20)	68(8)
C(56)	8993(16)	6951(16)	870(20)	75(8)
C(57)	9567(13)	2609(13)	-3577(15)	65(8)
C(58)	9876(12)	-2017(14)	1080(20)	53(6)
C(59)	9586(14)	-1747(14)	190(20)	72(8)
C(60)	-867(15)	2227(17)	-5307(18)	57(7)
C(61)	3948(15)	2712(13)	71(15)	69(8)
C(62)	3673(15)	1956(16)	400(20)	68(9)
C(63)	13860(12)	1750(13)	1247(13)	51(6)
C(64)	14432(14)	2119(17)	1801(17)	53(6)
C(65)	4640(14)	2882(14)	1455(19)	49(5)
C(66)	4426(12)	6871(12)	-4429(17)	48(5)
C(67)	5805(10)	528(12)	-3474(12)	41(4)
C(68)	5973(13)	-698(9)	-2575(18)	126(13)

Table 9.2.21. Crystal data and structure refinement for **[Na(tmeda)$_2$(*t*-Bu$_4$Sb$_3$)] (16)**

Identification code	Mgh24	
Empirical formula	$C_{28}H_{68}N_4NaSb_3$	
Formula weight	283.03	
Temperature	293(2) K	
Wavelenght	71.073 pm	
Crystal system	Monoclinic	
Space group	P2(1)/c	
Unit cell dimensions	a = 172.20(9) pm	α = 90°

	b = 124.69(5) pm	β =92.20(8)°
	c = 216.9(3) pm	γ = 90°
Volume	4.653(6) nm^3	
Z	12	
Diffractometer	Siemens P4	
Density (calculated)	1.212 Mg/m^3	
Absorption coefficient	1.755 mm^{-1}	
F(000)	1712	
Crystal size	0.70 x 0.40 x 0.30 mm^3	
Theta range for data collection	2.73 to 27.50°	
Index ranges	-10<=h<=22, -8<=k<=16, -28<=l<=28	
Reflections collected	12744	
Independent reflections	10512 [R(int) = 0.1538]	
Completeness to theta = 27.50°	98.3 %	
Absorption correction	DIFABS	
Refinement method	Full-matrix least-squares on F^2	
Data / restraints / parameters	10512 / 0 / 188	
Goodness-of-fit on F^2	1.793	
Final R indices [I>2sigma(I)]	R1 = 0.2351, wR2 = 0.5561	
R indices (all data)	R1 = 0.3444, wR2 = 0.5993	
Largest diff. Peak and hole	9.492 and -2.954 $e.Å^{-3}$	

Table 9.2.22. Atomic coordinates (x 10^4) and equivalent isotropic displacement parameters (pm^2 x 10^{-1}) for **[Na(tmeda)$_2$(*t*-Bu$_4$Sb$_3$)] (16)**. U(eq) is defined as one third of the trace of the orthogonalised Uij tensor.

	x	y	z	U(eq)
Sb(1)	1740(1)	1351(2)	2887(1)	36(1)
Sb(2)	2463(2)	2517(2)	1981(1)	59(1)
Sb(3)	3269(1)	3544(2)	2935(1)	38(1)

Na	2482(8)	2572(12)	426(7)	50(3)
N(1)	3600(20)	1280(30)	312(16)	62(9)
N(2)	3600(20)	3560(30)	-41(18)	71(10)
N(3)	1380(20)	1600(30)	-134(18)	72(10)
N(4)	1410(20)	3920(30)	295(18)	74(11)
C(1)	460(20)	1480(30)	2603(17)	48(8)
C(2)	2010(20)	-340(30)	2637(17)	50(9)
C(3)	4520(20)	3220(30)	2681(16)	42(8)
C(4)	3070(20)	5230(30)	2682(15)	41(8)
C(5)	270(30)	1400(40)	1970(20)	80(14)
C(6)	320(30)	2720(40)	2850(30)	90(16)
C(7)	30(20)	990(30)	3034(18)	58(10)
C(8)	1620(20)	-1010(30)	3105(19)	59(10)
C(9)	2830(30)	-360(40)	2720(20)	83(15)
C(10)	1740(30)	-650(50)	1960(20)	89(16)
C(11)	4990(40)	3720(50)	3140(30)	110(20)
C(12)	4590(30)	2100(40)	2790(20)	65(11)
C(13)	4700(20)	3420(30)	2014(19)	61(11)
C(14)	3220(20)	5520(30)	2046(17)	55(10)
C(15)	2210(30)	5320(40)	2830(20)	71(12)
C(16)	3390(40)	5880(60)	3180(30)	150(30)
C(17)	1350(30)	4760(40)	840(20)	81(14)
C(18)	1460(30)	4770(40)	-230(20)	85(15)
C(19)	780(40)	3270(50)	220(30)	110(20)
C(20)	820(30)	2390(50)	-240(30)	92(16)
C(21)	1580(30)	960(40)	-680(20)	65(11)
C(22)	1220(30)	860(40)	410(20)	84(15)
C(23)	3770(40)	660(50)	870(30)	110(20)
C(24)	3570(30)	480(50)	-140(30)	102(19)
C(25)	4280(40)	1930(60)	270(30)	110(20)

C(26)	4240(30)	2730(40)	-190(20)	78(14)
C(27)	3500(30)	4160(40)	-640(20)	69(12)
C(28)	3840(30)	4420(40)	390(20)	88(16)

Table 9.2.23. Crystal data and structure refinement for **[Na(pmdeta)(*t*-Bu_4Sb_3)] (17)**

Identification code	mgh11	
Empirical formula	$C_{25}H_{59}N_3NaSb_3 \cdot C_6H_6$	
CCDC-Number	184807	
Formula weight	868.10	
Temperature	173(2) K	
Wavelenght	71.073 pm	
Crystal system	Monoclinic	
Space group	C2/c	
Unit cell dimensions	a = 1248.80(10)pm	α = 90°
	b = 1876.5(3) pm	β = 91.660(10)°
	c = 3486.4(3) pm	γ = 90°
Volume	8.1665(16) nm^3	
Z	8	
Diffractometer	Siemens P4	
Density (calculated)	1.412 Mg/m^3	
Absorption coefficient	2.002 mm^{-1}	
F(000)	3488	
Crystal size	0.5 x 0.4 x 0.2 mm^3	
Theta range for data collection	2.60 to 27.50°	
Index ranges	-16<=h<=1, -24<=k<=1, -45<=l<=45	
Reflections collected	11472	
Independent reflections	9372 [R(int) = 0.0357]	
Completeness to theta = 27.50°	99.6 %	
Absorption correction	DIFABS	

Refinement method	Full-matrix least-squares on F^2
Data / restraints / parameters	9372 / 0 / 363
Goodness-of-fit on F^2	1.033
Final R indices [I>2sigma(I)]	R1 = 0.0528, wR2 = 0.1331
R indices (all data)	R1 = 0.0754, wR2 = 0.1586
Largest diff. Peak and hole	1.694 and -3.474 e.Å^{-3}

Table 9.2.24. Atomic coordinates (x 10^4) and equivalent isotropic displacement parameters (pm^2 x 10^{-1}) for **[Na(pmdeta)(*t*-Bu_4Sb_3)] (17)**. U(eq) is defined as one third of the trace of the orthogonalised Uij tensor.

	x	y	z	U(eq)
Sb(1)	4565(1)	3158(1)	1170(1)	34(1)
Sb(2)	5600(1)	1872(1)	1291(1)	54(1)
Sb(3)	7544(1)	2566(1)	1337(1)	32(1)
Na	6714(2)	4183(1)	1227(1)	37(1)
N(1)	6760(4)	4873(3)	616(2)	41(1)
N(2)	8343(4)	4906(3)	1293(2)	39(1)
N(3)	6481(4)	4901(3)	1818(2)	41(1)
C(1)	3257(6)	3099(4)	1592(3)	58(2)
C(2)	2757(6)	2366(4)	1618(2)	61(2)
C(3)	2406(10)	3653(6)	1485(4)	114(5)
C(4)	3798(11)	3279(7)	1976(3)	110(5)
C(5)	3690(5)	2980(4)	607(2)	44(1)
C(6)	3176(9)	3669(6)	483(3)	89(3)
C(7)	4561(8)	2814(6)	325(2)	76(3)
C(8)	2923(7)	2366(5)	611(3)	72(3)
C(9)	8268(6)	2062(4)	1857(2)	49(2)
C(10)	9459(8)	2198(6)	1888(3)	79(3)
C(11)	7709(11)	2410(7)	2188(2)	112(5)
C(12)	8055(6)	1261(4)	1876(3)	63(2)

C(13)	8428(6)	2089(5)	854(2)	53(2)
C(14)	9605(7)	2298(7)	880(3)	97(4)
C(15)	7913(10)	2414(8)	498(2)	122(6)
C(16)	8338(9)	1293(5)	834(3)	84(3)
C(17)	5951(7)	5414(5)	654(2)	64(2)
C(18)	6579(7)	4498(5)	252(2)	66(2)
C(19)	7842(5)	5187(4)	615(2)	47(2)
C(20)	8233(5)	5462(4)	996(2)	46(2)
C(21)	9338(5)	4506(4)	1251(2)	53(2)
C(22)	8362(5)	5226(4)	1683(2)	48(2)
C(23)	7279(6)	5472(4)	1810(2)	48(2)
C(24)	5412(6)	5221(5)	1853(3)	64(2)
C(25)	6656(6)	4424(4)	2140(2)	61(2)
C(26)	10416(6)	5530(4)	2374(2)	55(2)
C(27)	10831(6)	4894(5)	2250(2)	56(2)
C(28)	10417(6)	4260(4)	2373(2)	54(2)
C(29)	10375(7)	5594(5)	184(3)	72(3)
C(30)	10678(7)	4929(6)	312(3)	73(3)
C(31)	9703(7)	5661(5)	-131(3)	73(3)

Table 9.2.25. Crystal data and structure refinement for **[K(pmdeta)(*t*-Bu_4Sb_3)] (18)**

Identification code	mgh9
Empirical formula	$C_{25}H_{59}KN_3Sb_3 \cdot ½C_6H_6$
CCDC-Number	184806
Formula weight	884.16
Temperature	173(2) K
Wavelenght	71.073 pm
Crystal system	Monoclinic
Space group	P2(1)/c

Unit cell dimensions	a = 1234.4(4) pm	α = 90°
	b = 2065.2(5) pm	β = 111.47(5)°
	c = 1602(2) pm	γ = 90°
Volume	3.80(1) nm^3	
Z	4	
Diffractometer	Siemens P4	
Density (calculated)	1.477 Mg/m^3	
Absorption coefficient	2.245 mm^{-1}	
F(000)	1692	
Crystal size	0.8 x 0.8 x 0.2 mm^3	
Theta range for data collection	1.97 to 25.16°.	
Index ranges	-14<=h<=1, -24<=k<=24, -18<=l<=19	
Reflections collected	15457	
Independent reflections	6713 [R(int) = 0.1117]	
Completeness to theta = 27.50°	98.3 %	
Absorption correction	DIFABS	
Refinement method	Full-matrix least-squares on F^2	
Data / restraints / parameters	6713 / 0 / 336	
Goodness-of-fit on F^2	0.984	
Final R indices [I>2sigma(I)]	R1 = 0.0623, wR2 = 0.1272	
R indices (all data)	R1 = 0.1228, wR2 = 0.1514	
Largest diff. Peak and hole	1.191 and -1.279 $e.Å^{-3}$	

Table 9.2.26. Atomic coordinates (x 10^4) and equivalent isotropic displacement parameters (pm^2 x 10^{-1}) for **[K(pmdeta)(*t*-Bu_4Sb_3)] (18)**. U(eq) is defined as one third of the trace of the orthogonalised Uij tensor.

	x	y	z	U(eq)
Sb(1)	8082(1)	2329(1)	6919(1)	28(1)
Sb(2)	6211(1)	1958(1)	5418(1)	34(1)

Sb(3)	5013(1)	3006(1)	5731(1)	27(1)
K(1)	6641(2)	1425(1)	3269(2)	40(1)
N(1)	4572(9)	676(4)	2992(7)	43(3)
N(2)	6914(9)	70(4)	3943(7)	39(2)
N(3)	8625(9)	647(4)	3250(8)	47(3)
C(1)	8432(10)	1432(5)	7731(8)	37(3)
C(5)	9522(9)	2388(5)	6386(9)	35(3)
C(9)	3291(9)	2544(5)	5475(8)	32(3)
C(13)	4730(10)	3639(5)	4525(8)	35(3)
C(2)	7464(15)	1404(7)	8098(13)	82(6)
C(3)	9566(14)	1506(8)	8474(12)	94(7)
C(4)	8437(11)	817(5)	7213(9)	47(3)
C(6)	10651(12)	2503(11)	7105(13)	114(8)
C(7)	9639(13)	1793(6)	5895(13)	74(5)
C(8)	9277(14)	2970(6)	5853(13)	79(6)
C(10)	3446(11)	2177(5)	6328(9)	48(4)
C(11)	2335(10)	3071(6)	5312(11)	54(4)
C(12)	2929(11)	2057(6)	4689(10)	54(4)
C(14)	3976(12)	4230(5)	4549(10)	50(4)
C(15)	4246(15)	3290(6)	3693(10)	70(5)
C(16)	5945(12)	3894(6)	4688(11)	61(4)
C(17)	4227(13)	379(6)	2095(10)	61(4)
C(18)	3686(12)	1117(7)	3050(12)	71(5)
C(19)	4830(12)	184(6)	3699(10)	53(4)
C(20)	5824(11)	-266(5)	3758(9)	47(3)
C(21)	7439(12)	247(6)	4897(10)	55(4)
C(22)	7722(12)	-319(5)	3667(11)	56(4)
C(23)	8804(12)	38(6)	3740(11)	62(4)
C(24)	9733(12)	997(7)	3460(13)	78(6)
C(25)	8092(15)	523(7)	2300(11)	74(5)

C(26)	9380(20)	4705(8)	5432(14)	78(6)
C(27)	10530(20)	4562(7)	5661(12)	79(6)
C(28)	8856(14)	5158(8)	4751(15)	77(6)

Table 9.2.27. Crystal data and structure refinement for **[K(pmdeta)(*t*-Bu_3Sb_2)] (19)**

Identification code	mgh7i	
Empirical formula	$C_{21}H_{50}KN_3Sb_2$	
CCDC-Number	184805	
Formula weight	627.24	
Temperature	173(2) K	
Wavelenght	71.073 pm	
Crystal system	Monoclinic	
Space group	P2(1)/c	
Unit cell dimensions	a = 1047.7(2) pm	α = 90°
	b = 1666.6(3) pm	β = 106.24(3)°
	c = 1790.5(4) pm	γ = 90°
Volume	3.0016(10) nm^3	
Z	4	
Diffractometer	Stoe IPDS	
Density (calculated)	1.388 Mg/m^3	
Absorption coefficient	1.948 mm^{-1}	
F(000)	1272	
Crystal size	0.40 x 0.30 x 0.30 mm^3	
Theta range for data collection	2.02 to 26.07°.	
Index ranges	-12<=h<=12, -20<=k<=20, -21<=l<=21	
Reflections collected	40585	
Independent reflections	5811 [R(int) = 0.0782]	
Completeness to theta = 26.07°	97.8 %	
Absorption correction	DIFABS	

Refinement method	Full-matrix least-squares on F^2
Data / restraints / parameters	5811 / 0 / 260
Goodness-of-fit on F^2	0.877
Final R indices [I>2sigma(I)]	R1 = 0.0278, wR2 = 0.0455
R indices (all data)	R1 = 0.0564, wR2 = 0.0503
Largest diff. Peak and hole	0.653 and -0.359 e.Å^{-3}

Table 9.2.28. Atomic coordinates (x 10^4) and equivalent isotropic displacement parameters (pm^2 x 10^{-1}) for **[K(pmdeta)(*t*-Bu_3Sb_2)] (19)**. U(eq) is defined as one third of the trace of the orthogonalised Uij tensor.

	x	y	z	U(eq)
Sb(1)	7504(1)	4596(1)	2223(1)	34(1)
Sb(2)	9124(1)	4942(1)	3691(1)	34(1)
K(1)	8944(1)	3500(1)	5130(1)	39(1)
N(1)	10857(3)	2284(2)	5688(2)	42(1)
N(2)	8128(3)	1869(2)	4701(2)	48(1)
N(3)	6626(3)	2976(2)	5548(2)	52(1)
C(1)	5561(3)	4464(2)	2487(2)	43(1)
C(2)	5387(4)	5034(3)	3122(2)	55(1)
C(3)	4429(4)	4568(3)	1743(2)	55(1)
C(4)	5549(4)	3607(2)	2776(3)	59(1)
C(5)	7292(4)	5779(2)	1609(2)	41(1)
C(6)	6572(4)	5632(2)	750(2)	51(1)
C(7)	8713(4)	6059(2)	1674(2)	48(1)
C(8)	6583(4)	6416(2)	1949(2)	48(1)
C(9)	10917(3)	4310(2)	3516(2)	39(1)
C(10)	11257(4)	4605(2)	2793(2)	47(1)
C(11)	12078(4)	4511(3)	4228(2)	57(1)
C(12)	10711(4)	3410(2)	3462(2)	53(1)
C(13)	12212(4)	2502(3)	5677(3)	59(1)

C(14)	10761(4)	2308(3)	6486(2)	57(1)
C(15)	10497(4)	1498(2)	5331(2)	51(1)
C(16)	9035(4)	1291(2)	5196(2)	52(1)
C(17)	8135(5)	1788(3)	3891(3)	65(1)
C(18)	6756(4)	1771(3)	4751(3)	65(1)
C(19)	6489(5)	2096(3)	5449(3)	73(1)
C(20)	5502(5)	3417(3)	5069(3)	80(2)
C(21)	6730(5)	3141(3)	6359(3)	76(1)

Table 9.2.31. Crystal data and structure refinement for **2-(3',5'-Dimethylphenyl)-5,7-dimethylstibindolyl potassium-pmdeta (21)**

Identification code	mgh14i	
Empirical formula	$C_{27}H_{41}KN_3Sb$	
CCDC-Number	198210	
Formula weight	568.48	
Temperature	173(2) K	
Wavelenght	0.71073 Å	
Crystal system	monoclinic	
Space group	P2()/c	
Unit cell dimensions	a = 23.681(5) Å	α = 90°
	b = 9.641(2) Å	β= 105.79(3)°
	c = 13.243(3) Å	γ = 90°
Volume	2909.4(11) $Å^3$	
Z	4	
Diffractometer	Stoe IPDS	
Density (calculated)	1.298 Mg/m^3	
Absorption coefficient	1.109 mm^{-1}	
F(000)	1176	
Crystal size	0.4 x 0.3 x 0.3 mm^3	

Theta range for data collection	2.29 to 25.00°
Index ranges	-28<=h<=28, -11<=k<=11, -15<=l<=15
Reflections collected	35681
Independent reflections	5123 [R(int) = 0.1266]
Completeness to theta = 27.50°	99.8 %
Absorption correction	DIFABS
Refinement method	Full-matrix least-squares on F^2
Data / restraints / parameters	5123 / 0 / 301
Goodness-of-fit on F^2	0.923
Final R indices [I>2sigma(I)]	R1 = 0.0428, wR2 = 0.0908
R indices (all data)	R1 = 0.0738, wR2 = 0.0965
Largest diff. Peak and hole	0.747 and -0.929 e.Å^{-3}

Table 9.2.32. Atomic coordinates (x 10^4) and equivalent isotropic displacement parameters (pm^2 x 10^{-1}) for **2-(3',5'-Dimethylphenyl)-5,7-dimethylstibindolyl potassium-pmdeta (21)**. U(eq) is defined as one third of the trace of the orthogonalised Uij tensor.

	x	y	z	U(eq)
Sb(1)	2620(1)	6972(1)	3083(1)	52(1)
C(1)	2877(2)	8329(5)	4407(3)	49(1)
C(2)	2398(2)	8945(5)	4610(3)	46(1)
C(3)	1819(2)	8669(5)	3938(3)	42(1)
C(4)	1782(2)	7734(4)	3108(3)	43(1)
C(5)	1232(2)	7449(5)	2390(3)	48(1)
C(6)	741(2)	8117(5)	2527(3)	51(1)
C(7)	764(2)	9042(5)	3349(3)	49(1)
C(8)	1304(2)	9318(5)	4045(3)	44(1)
C(9)	211(2)	9724(7)	3481(4)	67(2)
C(10)	1188(2)	6472(6)	1492(4)	60(1)
C(11)	3479(2)	8535(5)	5036(4)	54(1)

C(12)	3607(2)	9094(6)	6053(4)	57(1)
C(13)	4182(2)	9273(6)	6672(4)	68(2)
C(14)	4633(3)	8871(7)	6258(5)	80(2)
C(15)	4533(2)	8312(7)	5273(5)	79(2)
C(16)	3959(2)	8155(6)	4666(5)	68(1)
C(17)	5043(3)	7856(8)	4849(7)	111(3)
C(18)	4303(3)	9913(8)	7747(5)	86(2)
K(1)	2349(1)	5965(1)	5597(1)	51(1)
N(1)	1253(2)	4494(5)	4919(3)	65(1)
N(2)	2256(2)	3300(4)	6540(3)	67(1)
N(3)	3365(2)	4264(6)	6095(5)	87(2)
C(19)	1336(3)	3928(8)	3945(4)	83(2)
C(20)	739(3)	5396(7)	4668(5)	77(2)
C(21)	1192(3)	3380(7)	5640(5)	84(2)
C(22)	1738(3)	2510(7)	6029(5)	84(2)
C(23)	2206(3)	3874(7)	7529(4)	91(2)
C(24)	2788(3)	2462(7)	6689(6)	92(2)
C(25)	3341(3)	3285(8)	6909(6)	102(2)
C(26)	3875(3)	5130(10)	6453(8)	140(4)
C(27)	3375(4)	3542(11)	5121(7)	134(4)

CURRICULUM VITAE

Personal data

Family name:	GHESNER
First name:	Mihaiela Emilia
Date of birth:	25th of April 1974
Place of birth:	Nasaud, Romania

Education:

- 1981 to 1993 primary and secondary school, in Nasaud, Romania
- 1994 to 1999 study of chemistry at the Babeş-Bolyai University, Cluj-Napoca, Romania
- June 2001, M.Sc. degree
- 2001 to 2003 Ph.D. student in the group of Prof. Dr. H. J. Breunig at the University of Bremen, Germany

Publications

1. Reactions of *cyclo*-(*t*-Bu_4Sb_4) with alkali metals; syntheses and crystal structures of [$M(L)_n$(*t*-Bu_4Sb_3)] (M = Na, K; *n* = 1, 2) and [K(L)(*t*-Bu_3Sb_2)] (L = $(Me_2NCH_2CH_2)_2NMe$)

Hans Joachim Breunig, Mihaiela E. Ghesner, Enno Lork

J. Organomet. Chem. **660** (2002) 167.

2. Syntheses and Coordination Chemistry of Di-, Tri-, and Tetrastibanes, $R_2Sb(SbR')_nSbR_2$ (n = 0, 1, 2)

Hans Joachim Breunig, Ioan Ghesner, Mihaiela E. Ghesner, Enno Lork

J. Organomet. Chem. **677** (2003) 15.

3. Syntheses, structures and dynamic behavior of chiral racemic organoantimony and -bismuth compounds, RR'SbCl, RR'BiCl, and RR'SbM; R = 2-$(Me_2NCH_2)C_6H_4$, R' = $CH(SiMe_3)_2$, M = H, Li, Na

Hans Joachim Breunig, Ioan Ghesner, Mihaiela E. Ghesner, Enno Lork

Inorg. Chem. **42** (2003) 1751.

4. Synthesis of a stibindolyl anion from trimesitylantimony and potassium

Hans Joachim Breunig, Mihaiela E. Ghesner, Enno Lork

Chem.Commun. (2003) 274.

Contribution to professional reports (presenter underlined)

1. Isolation and structural characterization of two solvated diorgano lithium antimonides $Li(thf)_3SbR_2$ (R = Ph, Mes), Hans Joachim Breunig, Mihaiela E. Ghesner, Tobias Borrmann,
at *4. Norddeutsches Doktoranden-Kolloquium*, Hamburg (Germany), Oktober 2001.

2. Reactions of *cyclo-(t-Bu_4Sb_4)* with alkali metals (Li, Na, K), Hans Joachim Breunig, Mihaiela E. Ghesner,
at *5. Norddeutsches Doktoranden-Kolloquium*, Osterholz Scharmbeck (Germany), Oktober 2002.

Acknowledgements

In particular I would like to express my gratitude to my supervisor Prof. Dr. Hans Joachim Breunig for his never-ending support, encourangement and guidance during this work.

General thanks are due to all other members of the group.

A special thank goes to Dr. Enno Lork for helping me with the solution of the X-ray crystal structures. Also, I want to thank to Mr. Peter Brackmann for his patience with the selection of suitable single crystals for the X-ray diffraction studies as well as for carrying out the X-ray crystallographic measurements.

Many thanks to Dr. Thomas Dülcks and Dipl. Ing. Heike Anders, who carried out the mass spectra measurements. Thanks also to Dipl. Ing. Johannes Stelten for the NMR measurements and for briefing me with the use of the DPX 200 device.

I would like to thank Prof. Dr. Cristian Silvestru and Conf. Dr. Ing. Anca Silvestru from Babeş-Bolyai University for their support.

Finally I wish to express my thanks to Deutsche Forschungsgemeinschaft for the financial support.